Thermally and Chemically Induced Changes in Interface Shear Behavior of Landfill Liners

Submitted by

Ling Li

A thesis submitted under the supervision of Dr.Mamadou.Fall

In partial fulfillment of the requirements for

the degree of Master of Applied Science

in

Civil Engineering

Department of Civil Engineering

University of Ottawa

Ottawa, Ontario, Canada

Abstract

Composite liners are used in landfills to isolate solid waste from the local environment. The combination of a high-density polyethylene (HDPE) geomembrane and compacted clay liner (CCL) is commonly used worldwide. In the Ontario region, bentonite sand mixtures (BSMs) and the local clay i.e. Leda clay, can be considered as appropriate CCL materials. However, the interface failure between smooth HDPE and CCL is a critical issue for landfill safety. The shear stress behavior and strength parameters at the interface between the HDPE and CCL can be affected by many factors, such as temperature and chemicals. The temperature difference between winter and summer in the Ontario region is approximately 50°C, which causes a freeze-thaw (F-T) phenomenon in local landfills. Leachate and heat are generated during the solid waste stabilization process. Landfill leachate usually contains a high concentration of cations, which can carry heat, thus affecting the landfill liner properties. As a result, the interface shear stress behavior and strength parameters are affected by the aforementioned conditions.

In this thesis, a series of experiments were conducted on the shear stress behavior at the interface of Leda clay / HDPE and bentonite sand mixture (BSM) / HDPE. In order to understand the influence of the F-T phenomenon, the samples were tested by varying the number of F-T cycles. Meanwhile, in order to understand the combined influence of cations and heat, the samples were saturated with different solutions, i.e. distilled water, potassium chloride and calcium chloride solutions. Then they were cured in an oven with different temperatures and room temperature, respectively. All of the laboratorial shear tests have been performed by using a direct shear machine. Results show that the BSM /HDPE and Leda clay/ HDPE interfaces are both influenced by the F-T cycles. The BSM/HDPE interface shear of the samples between 0 and 5 F-T cycles has more obvious differences, while the friction angle of compacted Leda clay/HDPE exhibits distinct reduction in the first 3 cycles, after which, the difference becomes hard to differentiate. The results also indicate that both high temperature and high concentration of cations from leachate can slight reduce the interface shear stress of BSM/HDPE. However, the combined influence of thermal-chemical conditions is not much more obvious compared to the effects of a single thermal or chemical condition. The BSM materials, which were saturated with different solutions, are also tested

by using X-ray diffraction to examine the mineral changes in the BSM. The calcium and potassium cations convert sodium-bentonite into calcium-rich bentonite and illite/semectie mixtures, respectively. Nevertheless, the changess of clay part caused by the combined effect of heat and leachate have limited influence on the BSM/HDPE interface shear behavior.

Acknowledgement

I would like to gratefully thank first and foremost, my supervisor, Prof. Mamadou. Fall, for his great guidance, support, understanding and patience throughout my graduate study. His experience and knowledge have helped me to find the right path for my research and obtain further understanding of the problems related to my research.

Besides my supervisor, my gratitude is also extended to the faculty and staff of the Engineering Department at the University of Ottawa. I would like to especially thank Jean Claude Célestin, the lab technician, and the technical officers in Mechanical Engineering, i.e. Léo Denner and Paul Burberry. Their immense help has overcome any laboratorial and technical issues during the experimental period of my research.

I would like to thank my colleagues and friends as their support has played a tremendous role in helping my study. Last but not at least, I would like to thank my family members, including my grandparents, parents and cousins, who have provided me with a large amount of support in so many ways throughout my study, research and writing period, and my life in general.

Table of Contents:

List of Figures:

List of Tables:

List of Abbreviations:

HDPE: High-density polyethylene

MDPE: Medium-density polyethylene

LDPE: Low-density polyethylene

VLDPE: Very low-density polyethylene

CCL: Compacted clay liner

BSM: Bentonite sand mixture

F-T: Freeze-thaw

GCL: Geosynthetic clay liner

LVDT: Linear variable differential transformer

DST: Direct shear tests

XRD: X-ray diffraction

R_L: The roughness in a two dimensional-profile.

Chapter 1 Introduction

1.1 Problem statement

Increasingly more natural resources are being consumed by modern society. Due to this reason, there is a growing demand on waste disposal at the same time. Statistical results have shown that landfill facilities are used as the primary means of solid waste disposal in the past decades. In doing so, landfill leachate has become the one of primary concerns of landfill operations. Application of reliable barriers underneath waste disposal sites (e.g. liner systems) is crucial for the protection of underground water resources. However, any defects in the liner systems can put the environment at risk due to possible leakage. A large number of factors could cause landfill liner failure for different reasons. One of the main factors is the insufficient interface shear strength of the composite liner.

Landfill liners are composed of various geosynthetic and/or soil components (Jogi, 2005). For domestic waste systems, the basic structure unit of landfill liners is normally a geosynthetic layer that is in contact with a compacted clay layer (CCL) for municipal solid waste (MSW) landfills. Several studies have shown that landfill lining failures on the slopes caused by liner system sliding take place at the interface between the CCL and geomembrane when the interface has low shear resistance (Ellithy & Gabr, 2000; Jogi, 2005). The shear strength is probably further reduced by the presence of water (Reddy, 1999).

Generally, local clays can be used as the CCL for economic considerations. For example, Leda clay is a typical type of sensitive marine clay which covers large areas of eastern Ontario and western Quebec. Leda clay has low hydraulic conductivity. Bentonite sand mixtures (BSMs) are another common option for use as a leachate barrier because they have an extremely low hydraulic conductivity (Olgun, 2013). BSMs are an ideal material for satisfying the requirements of a qualified barrier. The basic properties of BSMs are determined by different factors, such as the bentonite-sand ratio and water content of compaction.

According to landfill operation strategies, solid waste is normally separated into number of cells and lifts for the convenience of operation and monitoring. The buried solid waste of a working day can be accounted as one cell. Once the daily work is done, the daily cover can be used as a temporary shield (Bouazza et al., 2011). However, before the landfill is full, the

specific landfill organization as shown in Figure 1.1 shows that a part of the liner in the landfill is subjected to the climate effect.

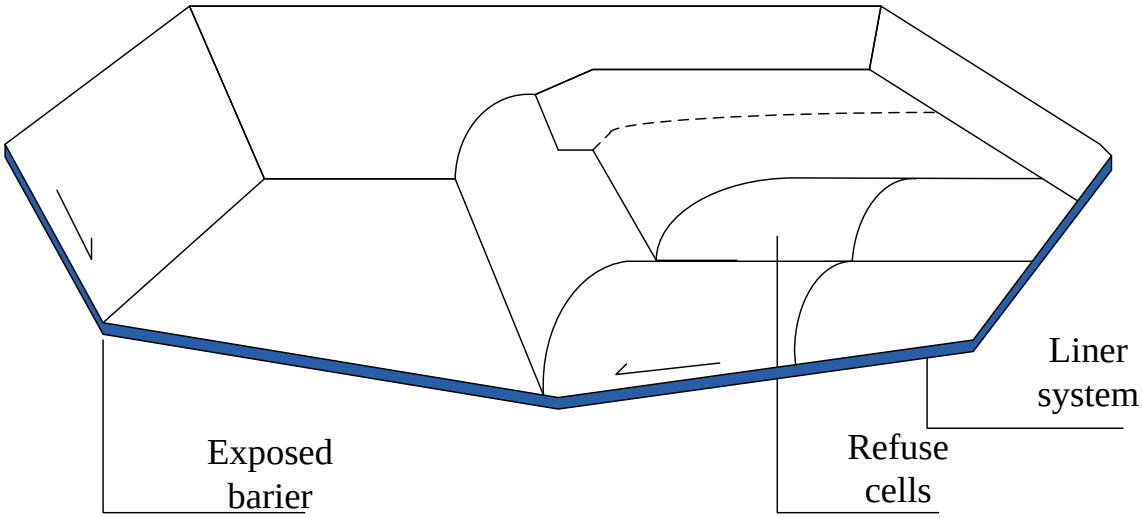

Figure 1.1 Sketch of design strategy for landfill cells (Modified after Bouazza et al., 2011)

In terms of the thermal conditions, Canada has distinctive seasons accompanied by significant fluctuations in temperature. The temperature in the summer can rise up to 35°C, while the temperature in the winter can be lower than -25°C (CEC Network, 2015). Before the landfill is filled and the final cover is completely built, parts of the liner system may be exposed to natural atmosphere for years (The District Municipality of Muskoka, 2014), and thus to several cycles of freezing and thawing. During the spring thaw, some liners show no obvious loss of bearing capacity while others show significant loss of bearing capacity which threatens the safety of landfills. Thus, F-T cycles should be considered as one of the crucial factors that influence soil engineering properties and increase the risk of landfill interface failures.

Moreover, waste degradation generates heat and leachate, which can also influence the properties of the liner as well. Precipitation (e.g. rainfall) can infiltrate into the daily cover and create a series of complex bio-chemical reactions with the waste, which form the landfill leachate. Leachate contains many chemical elements, including cations, which can affect bentonite properties and even change the properties of the clay of the liners. Furthermore,

when the leachate travels downward due to gravity, it carries landfill heat. The landfill temperature in the summer along with heat generated in the wastes can typically increase up to 50^{o}C or more. The combination of heat and leachate can contribute to a negative influence on landfill composite liners and then cause interface failure when the shear resistance decreases. The waste weight can reach high values sometime. The waste weight is determined by the unit weight and height of the waste. Normally the unit weight range changed from 3 to 20 kN/m^3 (Zekkos et al, 2005). The maximum waste height can reach 25m (Gartner Lee Limited, 2007).

Thus, it is important to understand the influences of i) the F-T cycles and ii) the combined effect of cations in the leachate and landfill heat on the interface shear behavior of composite liners to design landfill liners that meet safety requirements.

1.2 Research objectives

In the past decades, many studies have been performed to investigate the characteristics of various interfaces that exist in landfill composite layers under different saturation conditions. They have used direct shear or modified direct shear techniques. The results show that the geomembrane interface in CCLs are one of the most critical interfaces in stability analysis of the liner system (Masada et al., 1994). However, there is a paucity of information on the effect of F-T cycles on the interface shear behavior of landfill liners as well as the combined effect of temperature and leachate on the aforementioned interface.

The first objective of this research is therefore to experimentally study the shear strength parameters and behavior of landfill liner systems, especially those made of CCLs and geomembrane materials, under the influence of F-T cycles. In this thesis, a series of laboratory experimental tests are conducted to understand the influence of the F-T cycles on the shear strength parameters and behavior of compacted Leda clay, bentonite reinforced sand, and their interfaces with smooth high-density polyethylene (HDPE).

The second objective is to study the combined influence of heat generated by landfill and leachate on the interface shear behavior of a landfill liner (Bentonite sand mixture (BSM)/ smooth HDPE).

1.3 Research approach and methodology

In this study, all of the experiments are conducted under American Society for Testing

and Material (ASTM) standards. These following methods and approach are used in this study.

Leda clay is first dried and grounded into a powder, and then mixed with tap-water. Bentonite is mixed with sand. The weight of the bentonite is 10%, and the mixing is carried out for at least 10 minutes to ensure homogeneity. Standard dynamic compaction methods are used to prepare the samples into two different sizes: 60 mm × 60 mm × 25 mm for shear samples with only soil and 60 mm × 60 mm × 12 mm for the samples to test the interface shear strength. These samples are then subjected to a different number of F-T cycles. The number of F-T cycles are 0, 1, 2, 3, 5 and 10. The freezer is set to -30°C and the samples are thawed at room temperature.

Chemical cations can influence the properties of BSMs. In order to understand the interface mechanical behavior between the soil materials and geomembrane, the BSM is soaked in calcium and potassium chloride solutions which simulate the cation concentration of real landfill leachate. The soaking process of the BSM started at room temperature and then the temperature is increased up to 50^{o}C for 40 days through several steps. The BSM is also soaked in the same concentration solutions, but at room temperature for 40 days as the reference. All of the materials are made in different batches so that each sample can be tested after a similar saturation time. After that, the moisture content of the soil is reduced up to 15.3%, and the soil is made into samples for testing by using static compaction.

For BSM and BSM with a geomembrane interface, a direct shear apparatus is used as the primary tool to test the shear strength parameters. All of the direct shear tests (DSTs) are consolidated drained DSTs which conform to the situation of real landfills. Vertical stresses of 150, 250 and 350 kPa (waste weight) are applied during the shear testing, which is estimated from landfill waste density and the possible height.

X-ray diffraction (XRD) is used to determine the mineral changes in the BSM, which can provide a better understanding of the changes involved.

1.4 Thesis organization

Figure 1.2 depicts the schematic organization and structure of the thesis.

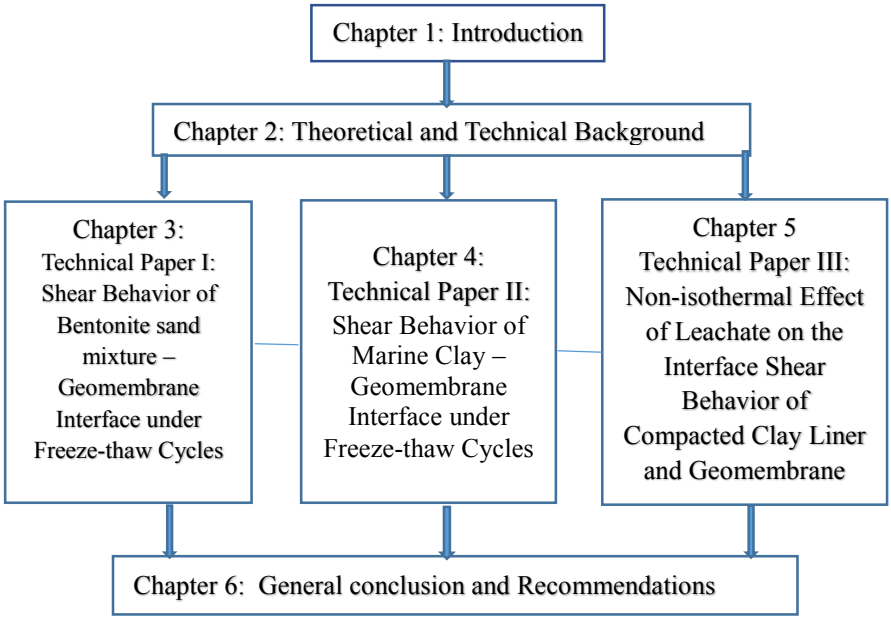

Figure 1.2 Structure and organization of thesis

This thesis is divided into six chapters as follows.

Chapter 1 includes: i) the problem statement which explains the primary problems addressed in this thesis; ii) the key research objectives of this thesis; and iii) the methodology and organization. **Chapter 2** provides the theoretical and technical background which is helpful for understanding landfills, specific materials of liners, thermal and chemical conditions in real landfill situations and their influences. **Chapter 3** presents the results of the experimental investigation of the effect of F-T cycles on the shear behavior of the interface between a compacted BSM and a geomembrane. **Chapter 4** presents the results of the experimental investigation of the effect of F-T cycles on the shear behavior of the interface between Leda clay and the geomembrane. **Chapter 5** provides the experimental results of the study of the combined effect of temperature and leachate on the interface shear behavior. **Chapter 6** provides the general conclusions and recommendations for further studies.

1.5 References

Bouazza, A., Nahlawi, H. & Aylward, M. (2011). In situ temperature monitoring in an organic-waste landfill cell. Journal of Geotechnical and Geoenvironmental Engineering, 137(12), 1286–1289.

CEC Network (2003). The Climate in Canada. Retrieved March 1, 2015, from http://www.studycanada.ca/english/climate.htm

Ellithy, G. S., & Gabr, M. A. (2000). Compaction Moisture Effect on Geomembrane/Clay Interface Shear Strength. In GeoDenver 2000 Congress (No. GSP No. 103).

Jogi, M (2005). A method for measuring smooth geomembrane/soil interface shear behavior under unsaturated conditions. Thesis of Degree of Master of applied Science, Department of Civil Engineering, University of Saskatchewan, Saskatoon, SK Canada

Masada, T., Mitchell, G., Sargand, S., & Shashikumar, B. (1994). Modified direct shear study of clay liner-geomembrane interfaces exposed to landfill leachate. Geotextiles and Geomembranes, 165-179.

Olgun, M. (2013). The effects and optimization of additives for expansive clays under freeze–thaw conditions. Cold Regions Science and Technology, P36-46.

Reddy, V. (1999). A comprehensive literature review of liner failures and longevity. Center for Marine Structures and Geotechnique, Department of Ocean Engineering, Florida Atlantic University

The District Municipality of Muskoka (2014). Long range solid waste management plan environmental assessment. Appendix H – Design and Operations Report of August 2007. Retrieved March, 13, 2015, from http://www.muskoka.on.ca/content/long-range-waste-plan

Zekkos, D. P., Bray, J. D., Riemer, M. F., Kavazanjian, E., and Matasovic, N. (2005). "Field investigation, characterization and unit weight of municipal solid waste." GeoEngineering Rep., Department of Civil and Environmental Engineering, Univ. of Calif., Berkeley, Berkeley, Calif. From: http://waste.geoengineer.org

Gartner Lee Limited (2007). Study of Stabilized Landfill Final Report. Prepared for Niagara Region, The City of Hamilton and The City of Toronto. Retrieved August, 25, 2015, from

http://www.durhamenvironmentwatch.org/Incinerator%20Files/FinalStabilizedLandfillGartnerLee.pdf

Chapter 2 Technical and theoretical background

In order to better understand the results presented in this thesis, or in other words, to better understand the interface shear behavior of a composite liner subjected to various chemical and thermal loading conditions, it is necessary to provide and discuss the background information on landfills (relevance, structure, operation, liners, leachate, and temperature), Leda clay, bentonite-sand mixtures (BSMs) and geomembranes, as well as the effect of temperature and leachate on bentonite material. Moreover, the interface shear behavior of landfills and previous studies conducted on the interface shear behavior of landfill liners will also be discussed in the present chapter. Common testing methods of the shear behavior of the liner interface will be presented and commented on in this chapter.

2.1 Landfills

In recent years, significant increases in the population, growth of the economy, living standards and industry can be seen in many countries. The result is that waste disposal rates are increasing at a rapid pace. Currently, there are many ways to dispose solid waste, among which landfills are used as the major means of disposal, particularly in Ontario (see Figure 2.1).

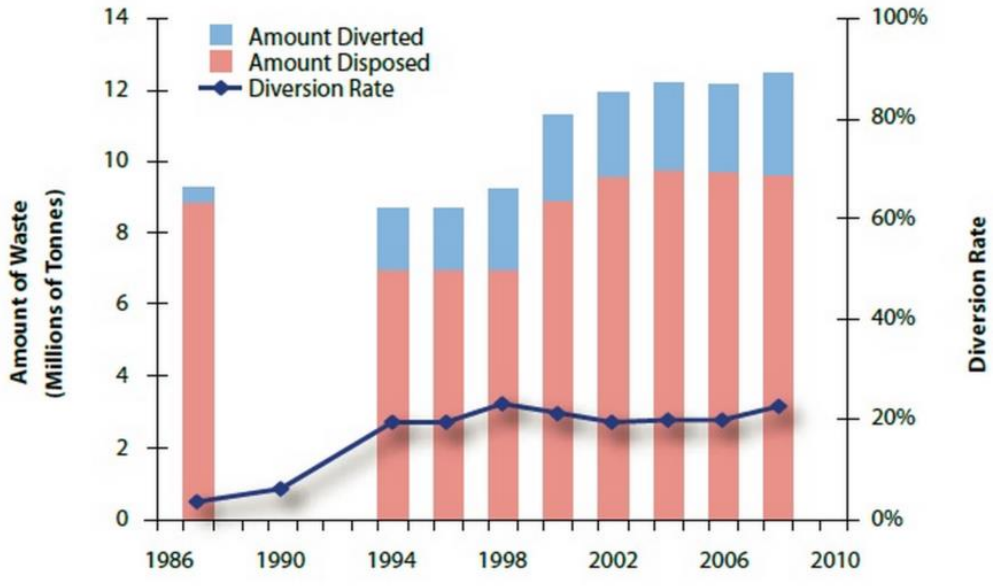

Figure 2.1 Amount of waste disposed in landfills and the diversion rate in Ontario. (Environmental Commissioner of Ontario, 2011)

2.1.1 Definition and the importance of landfill safety

Solid waste in modern landfills need to be safely stored. The American Heritage® Science Dictionary indicates that: "Modern landfills are often lined with layers of absorbent material and sheets of plastic to keep pollutants from leaking into the soil and water" (landfill, n.d.). Waste degradation generates leachate and landfill gas, which are both toxic to the environment. Normally, landfill leachate is a black liquid that contains many organic and inorganic materials as well as heavy metals. With the increase in environmental protection concerns and development of related techniques, more reliable barriers have been used in landfills to control the leaking of leachate (Environmental Protection Act, 2011).

2.1.2 Structure of landfills

Engineered and bioreactor landfills are the main types of modern landfills. The difference between these two types of landfills is that bio-methods are used in the latter to accelerate the speed of waste biodegradation, while leachate is collected and then transferred to other facilities in terms of the former. The main structures of these two types of landfills are similar. Normally, landfill structures can be divided into five components (see Figure 2.2) as follows:

1. Liner systems: used to isolate refuse and landfill leachate from the environment, especially from the ground and underground water. Commonly, compacted clay, geosynthetics and geosynthetic clay layers can be adopted,

2. Cover systems: used to restrict the infiltration of rainfall or water from snow-melt that can reduce leachate spillage, and at the same time, stop landfill gas emissions,

3. Leachate collection and treatment systems: use gravel/sand layers and pipes to collect and transfer leachate to leachate pools for toxic reduction treatments,

4. Landfill gas collection and treatment systems: use pipe networks to transfer landfill gas and recover energy from gas, and

5. Environmental monitoring: enables transitions of harmful components in the surrounding area to be monitored, which includes air quality (Government of Ontario, 2012).

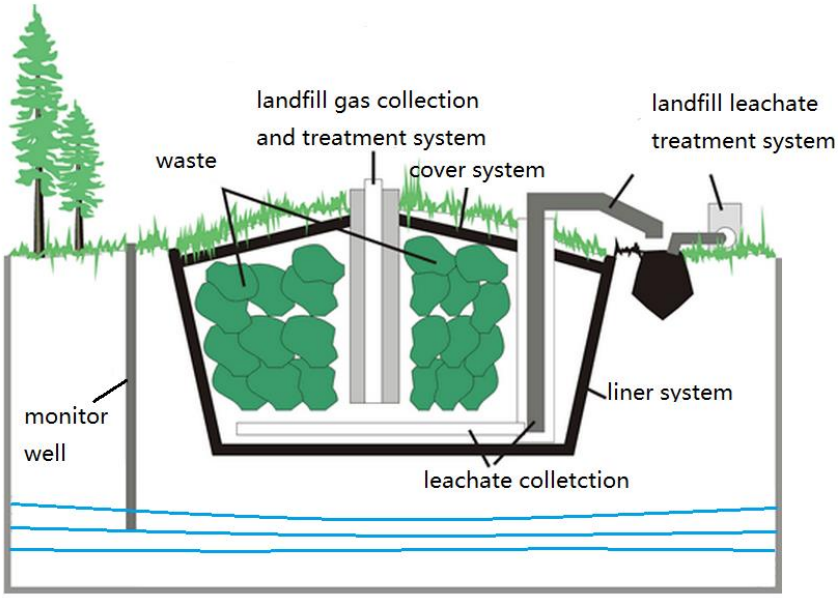

Figure 2.2 Common structure of landfill (Stewart, 2009).

2.1.3 Landfill operation strategies

On the one hand, it is important to maintain maximum capacity for landfill storage. On the other hand, it is necessary to ensure that a very minimum amount of waste is exposed to reduce cover material requirements for economic and environmental reasons. Thus, exposed wastes are to be placed in sites under specific orders. Wastes are disposed into landfills with an area method and a proper working face. Trash is deposited in layers, and compacted to reach the maximum density. Each working unit is called a cell, which contains one day of trash. Daily cells are normally less than 4 meters in height and the working face is inclined (Dillon Consulting, 2005). The compression of waste is done by heavy equipment (such as tractors, bulldozers and rollers). There are no steep slopes so that the operation of equipment does not encounter any issues and settlements are minimized. Once a cell is made, it is covered with a daily cover. As each lift is completed, the working face will be relocated to the next higher lift (Robinson, 1986). Waste cells are ordered in rows and layers of adjoining cells (lifts) (Dillon Consulting, 2005). This procedure means that the final cover will be gradually built from filled areas to the whole landfill. Thus, parts of the liner can be exposed to air for a long period of time.

2.2 Landfill liners

All liner materials have one common property: low hydraulic conductivity, which is 1 x 10^{-9} meter/second or less (Ryan, 2010).

2.2.1 Liner materials

Landfill liners consist of side slope and bottom liners. Compacted clay, geosynthetics and geosynthetic clay are commonly used as the materials.

Compacted clay liners (CCLs) are barriers that are stable and extremely low in hydraulic conductivity made of cohesive soil. Cohesive soils are compacted to be dense and homogeneous to reduce voids among particles as well as soil hydraulic conductivity (Government of Manitoba, 2007). CCLs are one of the most commonly used type of barrier in landfill sites. (Lake, 2000). They have a hydraulic conductivity of 10^{-9} m/s or even less with proper compaction. During lab experiments, they are often initially compacted with a moisture content of 2% to 4% wet of optimum to reach low hydraulic conductivity (Zhou, 1996). CCLs should be at least 1 m in thickness for municipal solid waste (MSW) landfills. CCLs are much more dependable due to fewer defects such as punctures and tears. Since landfill sites are often located in areas where clay materials are easy to find, construction costs may be dramatically reduced if natural clay soils can be directly used in CCLs. Local clay soils need to have low hydraulic conductivity and a percentage of fines (the percentage of fines higher than 30% and the percentage of clay higher than 15%). The plasticity index (PI) of the local clay should be greater than 7% and liquid limit (LL) should greater than 20% (Benson et al., 1994). If the local clay is not suitable, bentonite is a commonly used additive in CCLs (Cui et al., 2012).

Synthetic liners (geomembranes)

Synthetic liners or geomembranes, which are widely applied in many civil engineering works, are also used to prevent leachates (Fleming et al., 2006). In the past few decades, geomembranes have been increasingly used in landfills because they are easy to install and not as thick. Geomembranes are made of one or several kinds of plastic polymers combined with other materials, such as carbon black, plasticizers and anti-degradation agents (US Environmental Protection Agency, 2012). In landfills, geomembranes should be generally thicker than 80 mil (one mil is equal to 0.0254 mm). However, for HDPE, 60 mil is usually

acceptable (Fleming et al., 2006).

Geosynthetic clay liners

Geosynthetic clay liners (GCLs) have the properties of CCLs and partial advantages of geomembranes. Recently, geosynthetic clays have been widely utilized as a composite in both landfill liners and the final covers. GCLs are normally made up of a thin layer of bentonite, which is sandwiched between two geotextiles or bonded with a geomembrane (Mendes et al., 2010). Factory-manufactured bentonite is 5 to 10 mm in width (Koerner & Soong, 2000). Geotextiles are used for additional bonding to improve the stability of GCLs and incorporated by needling, stitching, or thermal bonding, or with chemical adhesives (Koerner & Soong, 2000), since it is difficult to avoid defects caused by construction and operations in landfills, such as punctures and tearing, or there might have been construction issues during the sewing of the GCLs. The combination of a geomembrane and a CCL is still commonly used in the composite liner system of landfills. The geomembrane/CCL can also be placed underneath the GCL as a back-up liner to further minimize seepage (Reddy, 1999).

2.2.2 Landfill liner structure

There are various standards and landfill requirements depending on the region. Different structures of landfill liners are adopted, such as single, double and single or double composite liners.

(1). Single liners

A single liner system has only one essential layer with low hydraulic conductivity. A leachate collection system will be placed above the single liner. Single liners have limited usage due to the high probability of leakage. They are only used at the base with good soil quality under relatively low landfill standard requirements (Reddy, 1999).

(2). Single composite liners

The composite layer is formed by numerous materials with low hydraulic conductivity that are directly in contact with each other; in this way, hydraulic conductivity of the composite layer is further reduced compared with each separate layer. A leachate collection system is also placed above single composite liners. GCLs are commonly a bentonite and geotextile sandwich (Jo, 2003). Therefore, GCLs are considered to be a single composite

liner.

(3). Double-layers

Double–layer systems are the combination of two liners with the same or different materials. These two layers are called the primary and the secondary layers. They also have two leachate collection layers. Above the primary liner, one drainage layer is required to reduce liquid accumulated above the primary layer and transfer the liquid to a leachate pool (US Environmental Protection Agency, 2012). Another leachate collection layer can be found between the primary and secondary layers. Its functions are to catch any leakage from the primary layer as well as giving warnings when there are other kinds of leakages.

(4). Double composite layers

Double composite layers are similar to double layers. The difference is that both the primary and secondary layers are composite liners. One leachate collection layer is placed above and the other between the primary and second layers. Obviously, this structure is the safest among all four kinds of liner structures as it takes advantage of various materials that have low hydraulic conductivity. Double composite liners with good qualities can attain the highest standard requirements (Reddy, 1999).

2.3 Landfill leachate

MSW landfills are designed with standards that try to minimize moisture penetration during their operation. Daily wastes are placed into separated lifts and cells. Daily covers are placed above the waste after working hours. A thin layer of soil or spray on slurries or foams which are not impervious are commonly used as daily covers. Thus, there could be some precipitation or other moisture that seeps through the daily covers and comes into contact with the waste. The infiltration go through a series of reactions with the waste, and form a toxic liquid. This kind of landfill liquid is called leachate (Taylor & Allen, 2006). Typically, leachate is black in color and leachate formation originates from the combination of various physical, chemical, and microbial processes from waste transfer pollutants, which range from waste materials to the water (Kjeldsen et al., 2010).

The most harmful environmental hazard of landfills is that leachates may contaminate underground waters. Commonly, landfill waste is a mix of municipal, commercial, and

industrial wastes. Such specific high concentrations of chemical compounds from waste are hardly found in everyday life (Kjeldsen et al., 2010). In landfills, the waste is located in different cells and lifts as they are buried at different times. Thus, the waste can be in different decomposition phases that correspond with the time and temperature. Nevertheless, enclosed layers and covers in landfills can form an anaerobic environment which eventually causes their compositions to be similar in different regions (Kjeldsen et al., 2010). Typically, landfill leachate can be categorized into four different groups of water-based polluting solutions, which include dissolved organic matters, inorganic components (common cations and anions including sodium, calcium, potassium, sulfate, chloride, iron, aluminum, zinc and ammonia), heavy metals, and xenobiotic organic compounds (Kjeldsen et al., 2010).

Landfill operations usually last for several decades, during which a series of complex chemical and biological reactions occur and result in waste degradation. It is therefore necessary to obtain a better understanding of the fundamental mechanisms of waste degradation. This long period of waste degradation of each landfill cell can be divided into phases that were first described by Farquhar and Rovers in 1973 (Kjeldsen et al., 2010). Now, they are more specifically divided into five phases: initial adjustment, transition, acid formation, methane fermentation and maturation (Adhikari et al., 2014). The leachate components change during these phases are shown in Figure 2.3.

In the first stage, the initial adjustment phase, oxygen found in the void spaces of newly buried refuse will be rapidly consumed and this leads to the highly concentrated production of carbon dioxide, and an increase in the chemical oxygen demand (COD) as well as landfill temperature. This phase only lasts for a few days. During the second phase or transition phase, there is the transition from aerobic to anaerobic conditions. The temperature increases at a constant rate and organic acids start to be produced, and there are high concentrations of cations. The second phase can last from one to six months. In the acid formation or third phase, the microbial activity is very much increased. Methane is generally produced, the pH is usually less than 5, and COD and biological oxygen demand (BOD) are reduced. In the fourth or methane fermentation phase, the methane production rate will reach the maximum and then remains stable. During this stage, significant solid decomposition can be observed, and the concentration of cations dramatically decreases. The pH value starts to reach a neutral level and this stage lasts from 8 to 40 years (Adhikari et al., 2014). The last stage is the

maturation phase, in which degradable solids are completely consumed. Methane production is significantly reduced in this phase (Kjeldsen et al., 2010).

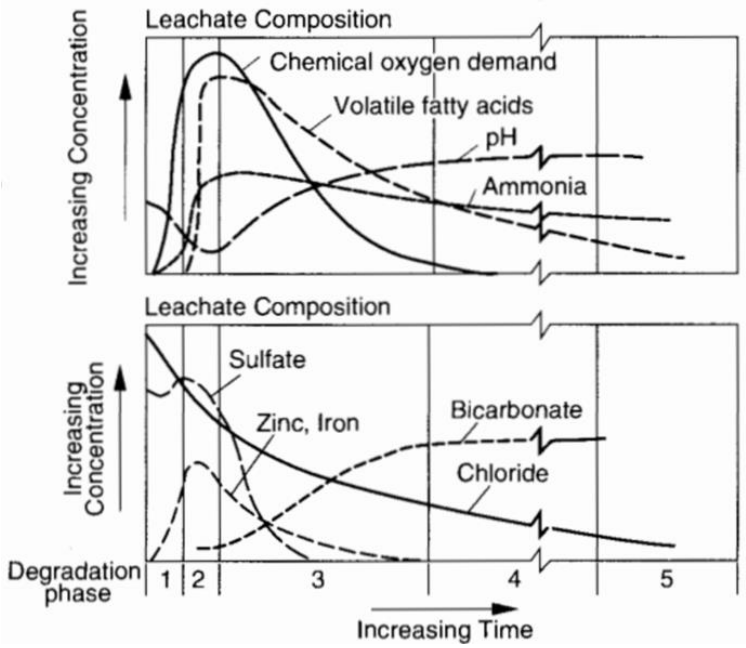

Figure 2.3 Changes in selected components of landfill leachate in different stages (Macpherson & Townsend, 1998).

As previously mentioned, the acid phase commonly entails high concentrations of cations, and some of the cation concentrations can significantly decline in this methanogenic stage. Based on work by Kruse (1994) who collected leachate data from 33 landfills, the composition concentrations of leachates in different operation phases are summarized in Table 2.1. This table provides clarity on the changing ranges and the average concentration of common existing elements in MSW landfill leachates.

Table 2.1 Common constituents in leachates from MSW landfills (Kruse, 1994)

	Parameter	Acid phase		Methanogenic phase	
		Average	Range	Average	Range
pH		7.4	6.2-7.8	7.6	7.0-8.3
Carbon	Biological oxygen demand (BOD)	9500	600-27000	230	20-700
Organic	Chemical oxygen demand (COD)	6300	950-40000	2500	460-8300
Nitrogen	Ammonia-N	740	17-1650	740	17-1650
Anion	Sulphate	200	35-925	240	25-2500
	Chloride	2150	315-12400	2150	315-12400
	Sodium	1150	1-6800	1150	1-6800
Cation	Potassium	880	170-1750	880	170-1750
	Magnesium	285	30-600	150	25-300
	Calcium	650	80-2300	200	50-1100
	Chromium	0.155	0.002-0.52	0.155	0.002-0.52
	Iron	135	3-500	25	4-125
Heavy	Nickel	0.19	0.01-1	0.19	0.01-1
Metal	Cobalt	0.09	0.005-0.56	0.09	0.005-0.56
	Zinc	2.2	0.05-16	0.6	0.09-3.5
	Cadmium	0.0375	0.0007-0.525	0.0375	0.0007-0.525
	Mercury	0.0015	0.000002-0.025	0.0015	0.000002-0.025
	Lead	0.16	0.008-0.4	0.16	0.008-0.4

2.4 Landfill temperature

Landfill heat can influence the physical, chemical, biological, and mechanical properties of wastes and liner materials in landfills (Yesiller & Hanson, 2003). At the same time, the local climate affects the ground base temperature. The temperature of landfill liners is determined by both the local ground temperatures and landfill heat generated by waste degradation (Yesiller et al., 2011).

2.4.1 Heat generated from waste degradation

Significant amounts of heat are generated in landfills due to the decomposition of organic

materials. After the refuse is buried, a series of biological and chemical reactions will then take place. Heat will be generated during this process and affected by the operating and climatic conditions. If the local temperature is low enough, decomposition can be inhibited due to reduced microbial activity in the refuse. Temperature increases under long-term anaerobic conditions are significant. The rate of heat generation is also affected by the rate of the waste placement, precipitation and waste density (Yesiller & Hanson, 2003). Fresh trash is added every day. The older waste maintains a temperature enough to accelerate the biodegradation of the fresh waste and its microbial reactions. The trend of the changes in the landfill temperature due to waste decomposition is provided in Figure 6. A common landfill temperature can be around 50-60℃ (see Figure 2.4). From previous records, the temperature of bioreactor landfills can increase up to 60℃ in Europe and 60-70℃ in Japan. In North America, the average temperature near the liners of the bottom of landfills can be higher than 50℃ (Cho et al., 1999). The temperature will influence the components of liner systems. The temperature of the leachate and waste will be transferred to the liner system. For clay materials, the properties will be impacted by thermal and chemical effects. Thus, these will affect the characteristics of CCLs.

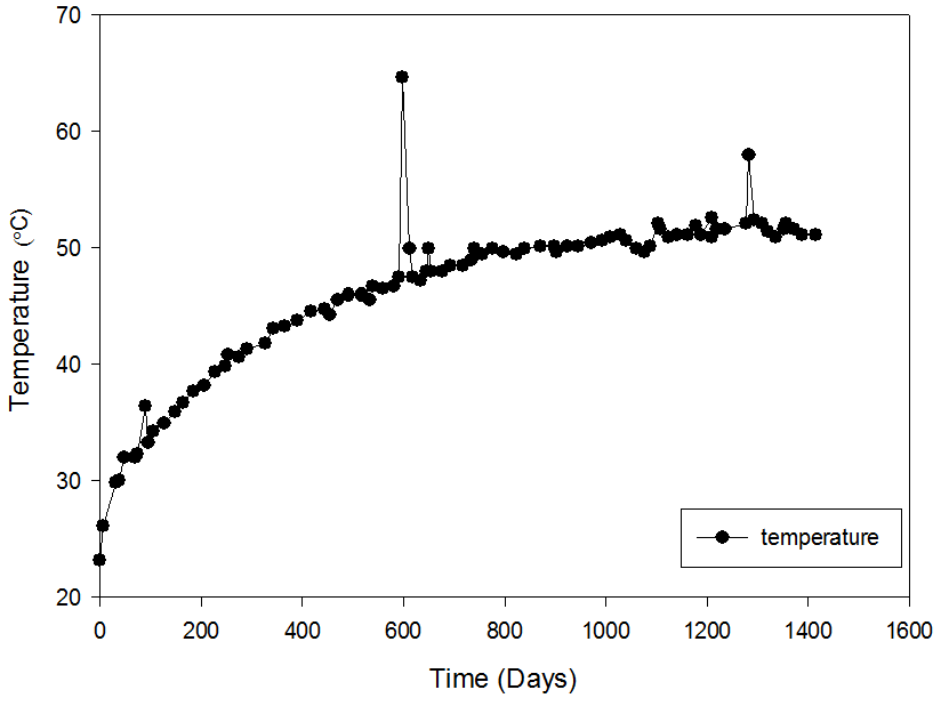

Figure 2.4 Temperature changes of landfill with time (revised from Yesiller & Hanson, 2003)

To sum up, for landfill liner systems, the temperature will change with the different operation stages and different climates. Before liners are fully filled with waste, parts of the liner system can be exposed to air. At this time, the temperature of the liner system will be equal to or slightly higher than the seasonal temperature (Yesiller & Hanson, 2003). Once the liners are buried by waste cells, the waste heat will add to the ground temperature. In Canada, the temperature of the liner system interface between the CCL and geomembrane will be far below 0℃ in the winter and around 50℃ in the summer (Karademir, 2011).

2.4.2 Climate effect of freeze-thaw cycles

In some regions of Canada, there is more than a 50℃ difference between summer and winter. Southern Ontario has a humid continental climate which presents four distinct seasons. From records of the previous decade (Figure 2.5), the daily average temperature in summer can rise up to 25°C. In winter, the temperature can drop to -15°C, and during cold snaps, below -30°C (Wikipedia, 2015). The temperature change can form a freeze-thaw (F-T) cycle during weather changes, and the F-T cycle changes the structure of the soils or liner materials and can influence the engineering properties of soil (Olgun, 2013).

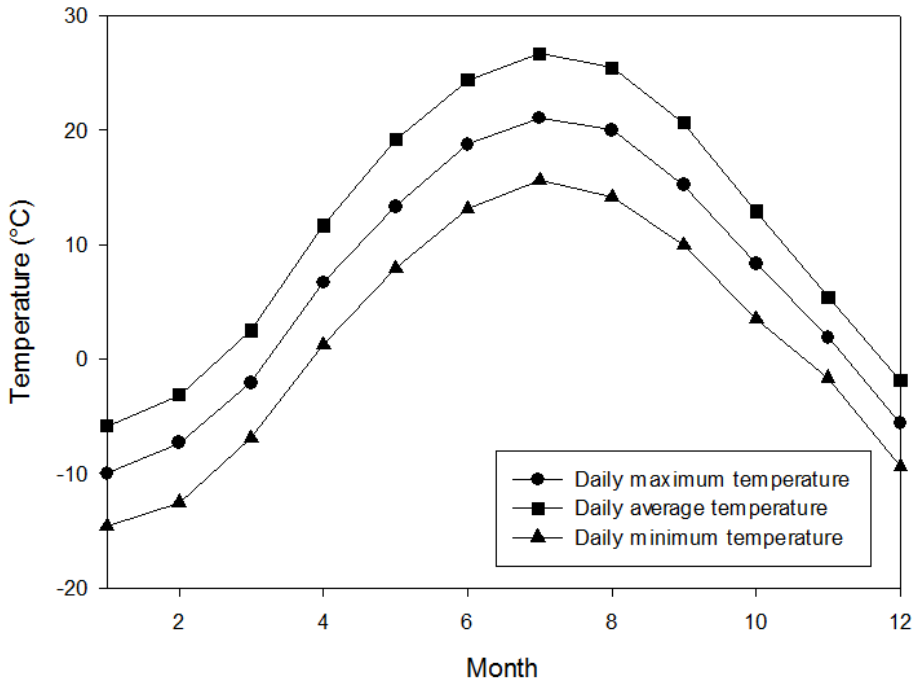

Figure 2.5 Average temperature chart from 1981 to 2010 in Ottawa (Government of Canada, 2015).

The freezing and thawing processes of soil can affect water migration. The capillary flow goes from higher to lower temperatures. When the soil freezes from the top side, the moisture turns to ice crystals, which are in a solid state, and thus the amount of wet moisture is reduced at the top. Higher water potential from the bottom layers will migrate towards the cold surface (Kahimba, 2008). Theoretically, the volume of water and ice are different, because ice will expand in volume by 9%. Hence, these pre-cracks and voids in soil are filled with water and then enlarged by ice after freezing.

The F-T phenomenon can change the physical properties of soil. When the soil is frozen, the bulk density is reduced since the water in the pores turn into ice which causes soil expansion. At this stage, the infiltration rate of the soil is reduced because the voids are blocked with ice lenses, which further impede the entry of water (Kahimba, 2008). However ice also forms cracks in frozen soil which will cause random macro pore changes. Thus, when the temperature increases, the surface moisture retreats to reach a balanced state, but soil cannot fully recover after void changes, and this is true for common types of soil, even rocks. The influence of the F-T phenomenon will depend on various factors, including the soil temperature and type, initial water content, dry density of the soil, etc. (Kahimba, 2008).

2.5 Background information on Leda clay and bentonite sand mixtures

With regard to the materials which can be used in CCLs in Ontario and Quebec, Leda clay, which is a local clay, and bentonite sand mixtures (BSMs) are commonly adopted. Therefore, it is necessary to have a basic understanding of these two types of materials.

2.5.1. Leda clay

Leda clay is also known as Champlain Sea clay. It is a type of sensitive marine clay in Canada (Crawford, 1968). Sensitive marine clays are usually proglacial and post glacial sedimentation products (Nader, 2014). There are thick deposits of Leda clays that cover large areas of the Quebec and Ontario provinces. In the primary depositing stage, sediment minerals were quartz, amphibole, mica, smectite, chlorite, feldspar, carbonates and glacial amorphous materials. With time, some original marine sediments were deposited (Nader, 2014). Leda clay has a high sensitivity. When the soil is disturbed, it can transform from a relatively brittle solid state to a liquid state (Crawford, 1968). The grains are so fine that

water cannot escape from the pores quickly. The clay particles of Leda clay are arranged in an open orientation similar to a card house structure. The formation of this open clay structure is the result of the deposition of the material in salty water which has a large number of cations that carry a positive charge. The positive charge of these cations leads to repulsive forces of the double layer absorbed water that push the platy particles apart, which results in an end-to-edge configuration. This end-to-edge configuration is stable in a salty environment. When the clay was uplifted from the bottom of the sea, the salinity of the pore water decreased due to the washing of the material by rainfall precipitation which changed the clay structure to a metastable state. A metastable structure is stable when it is not disturbed, similar to a card house. When the material is disturbed, collapse of the structure results in an increase in the pore water pressure since the water cannot escape from the pores quickly. This increase in pore pressure results in a decrease in effective stress, thus causing the material/Leda clay to liquefy. This also explains why remolded Leda clay commonly has much less strength than undisturbed Leda clay (Hyndman, 2010).

2.5.2 Bentonite-sand mixtures

Bentonite enhanced sand is a commonly used material to replace local clay as a composite liner material. Bentonite is a type of expansive soil which comes from glassy igneous material such as volcanic ash and tuff. It has high plasticity. The most significant advantages of bentonite are high swelling potential and low hydraulic conductivity, which make this material valuable in waste disposal facilities. Natural bentontite is generally rich in Na- and Ca-montmorillonite. The elementary unit of montmorillonite is made of an alumina octahedral sheet sandwiched between two silica tetrahedral sheets (see Figure 2-6). The alumina octahedral structure is composed of an aluminum atom and six hydroxyls. The silica tetrahedral is composed of a silicon atom and four oxygen atoms (Arifin, 2008). The layer charge is derived from the replacement of Mg^{2+} for Al^{3+} in the octahedral sheet and Al^{3+} for Si^{4+} in the tetrahedral sheet. Charge balance is maintained by exchangeable cations in the interlayer (Douglas, 1984).

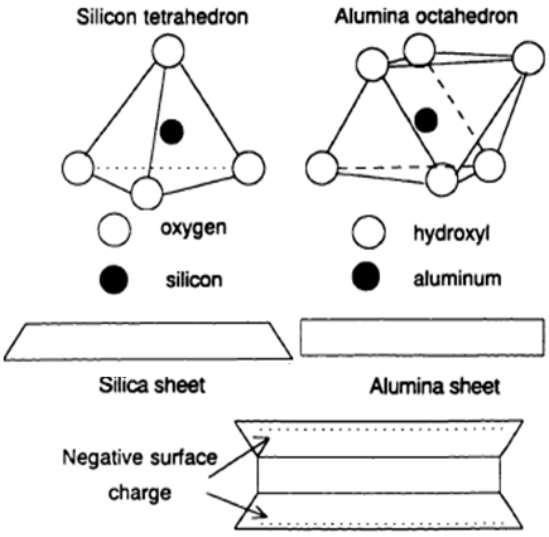

Figure 2.6 Sketch of montmorillonite structure. (Tang, 1999)

The elementary layers are stacked together to form particles. Under dry conditions, bonding between the elementary layers is provided by van der Waals force and exchangeable cations. In the hydration process, the water molecules are absorbed to develop water layers between the elementary clay layers, and the change in the physical state from a solid to a gel of bentonite clay is called swelling (Arifin, 2008). There are many factors that can influence the swelling capacity, such as the specific surface area, and cation type and concentration in the water (Cui et al., 2012). The type of exchangeable cation influences the number of elementary layers in a particle (Arifin, 2008). The relatively free expansion of the spacing between the layers of Na-montmorillonite can cause significant deviation from the original parallel arrangement of the layer and therefore the volume may increase many times. Ca-montmorillonite expansion maintains its original parallel arrangement of the layers and thus shows more limited swelling capacity. We can also observe similar results from potassium as a counter cation (Mesri & Olsen, 1971).

Bentonite can be mixed with other materials, and is frequently mixed with sand (Arifin, 2008). BSMs can incorporate two different sizes of particles. The coarse particles of sand generally form a skeleton, and the coarse voids are filled with fine bentonite clay to form clay matrices (Cui et al., 2012). BSMs have high structural integrity, thermal conductivity and stiffness. Therefore, the combined material makes them more effective and economical.

The ratio of bentonite and sand governs the properties of the mixture (Cui et al., 2012).

2.6 Background information on geomembranes

To protect water resources, geomembranes can be used as a hydraulic barrier to minimize the seepage of leachates. Geomembranes are made with one or more types of plastic polymers combined with other constituents, such as carbon black, plasticizers, processing aids and anti-degradants (US Environmental Protection Agency, 2012). A typical thermoplastic geomembrane will have a diffusion hydraulic conductivity range from 10^{-11} to 10^{-13} cm/s (Jogi, 2005). A wide range of plastic materials can be used in geomembranes, such as polyethylene (PE), polypropylene (PP), polyvinyl chloride (PVC), etc. PE is the most common geomembrane material. The density of PE is a major factor which can affect many of its key properties (Zhou, 1996). The materials for geomembranes can be subdivided into four main groups based on their density. These materials are high-density polyethylene (HDPE), medium-density polyethylene (MDPE), low-density polyethylene (LDPE) and very low-density polyethylene (VLDPE). HDPE is the most useful type of material in a landfill system (Zhou, 1996). The semi-crystalline microstructure of HDPE makes it more effective. (Zabielska-Adamska, 2006). HDPE has good stiffness, load bearing capacity, ultraviolet, thermal and tension resistance, as well as greater hardness (Jogi, 2005).

Various types of materials have different properties because of their different densities, hardness and roughness. Surface roughness is an important parameter that affects the frictional and shear behavior between soils and geomembranes. Geomembrane surface roughness is extremely varied (Karademir, 2011). Dove and Frost (1996) used optical profile microscopy to define the surface roughness of geomembranes. R_L (see Figure 2.7) is an abbreviation of roughness in a two dimensional-profile. A smooth geomembrane normally does not have significant topographic features in a cross-area profile.

The hardness of geomembranes can influence the HDPE properties. There is a critical stress of geomembranes that restricts normal loads; when the normal stress at the interface is greater than the critical stress, the soil particles and geomembrane interface will involve sliding and plowing behaviors. When plowing occurs, an increased force is required to displace the soil relative to the surface, thus resulting in increased interface friction (Jogi,

2005).

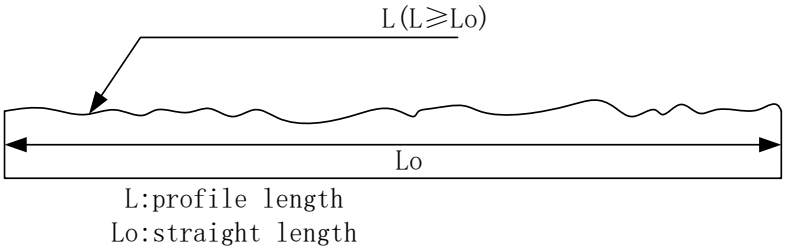

Figure 2.7 2D roughness profile of geomembrane (Nasir & Fall, 2008)

(R_L=L/Lo)

2.7 Landfill liner interface behavior

2.7.1 Interface failure

In terms of the static stability of landfills, side slopes are an important concern due to various interfaces that exist in the composite liner which may present low shear resistance. There is a high possibility of stability failure developed by the in-plane shearing of the waste mass within the composite liner. In order to maximize the fill volume, major landfills are designed with steeper side slopes. Nevertheless, once the side slope becomes steeper, there is a higher potential risk of sliding failure (Jogi, 2005). A simple composite liner system is shown in Figure 2-8.

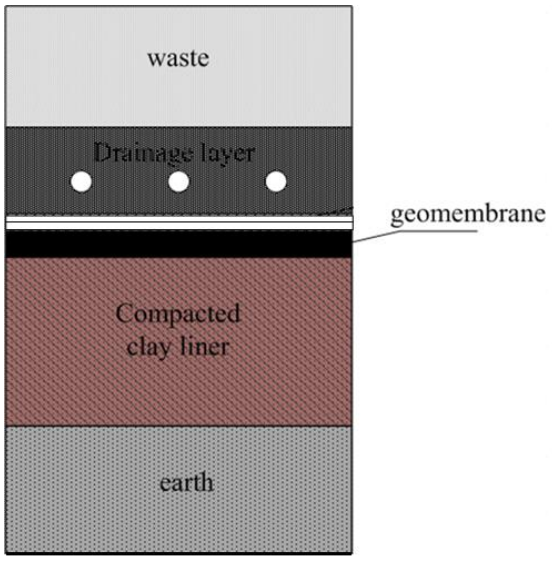

Figure 2.8 Geomembrane-CCL composite landfill liner

Aside from the interface between geomembranes and CCLs, others interfaces also have potential sliding risks. For geomembranes with GCLs, geotextiles and geonets, once shear behavior takes place in these interfaces, landfill stability will be lost. However, the main barrier capacity— hydraulic conductivity, has not been significantly affected, and toxic isolation continues to be mainly used. CCL and geomembrane combined materials act as the main protection barrier against leakage to minimize toxic leachate migration worldwide. Previous investigations have shown that there are a series of failures caused by movement within the composite liner, and the shear surface will probably pass through the clay-geomembrane interface (Jogi, 2005). Thus, the interface shear behavior of geomembranes and CCLs is the focus of this research.

2.7.2 Interface shear behavior mechanism

It is not easy to ensure the stability of side slopes at steeper angles because of the possibility of sliding at the geomembrane–soil interface (Fleming et al., 2006). There is relatively low interface frictional resistance between a smooth geomembrane and the contacting soil (Karademir, 2011). Normally, a geomembrane liner will be placed on the top and a low hydraulic conductivity soil liner will be placed beneath the geomembrane liner. The physical and mechanical properties of the two materials between the interfaces determine the shear behavior and the interaction between these two materials (Pando et al., 2002). The mechanisms of a geomembrane with a soil interface are a combination of several different mechanisms. Under saturated conditions, soil may undergo the following mechanisms: adhesion, sliding, rolling, plowing and interlocking with the geomembrane (see Figure 2.9) (Jogi, 2005; Lee, 1998)

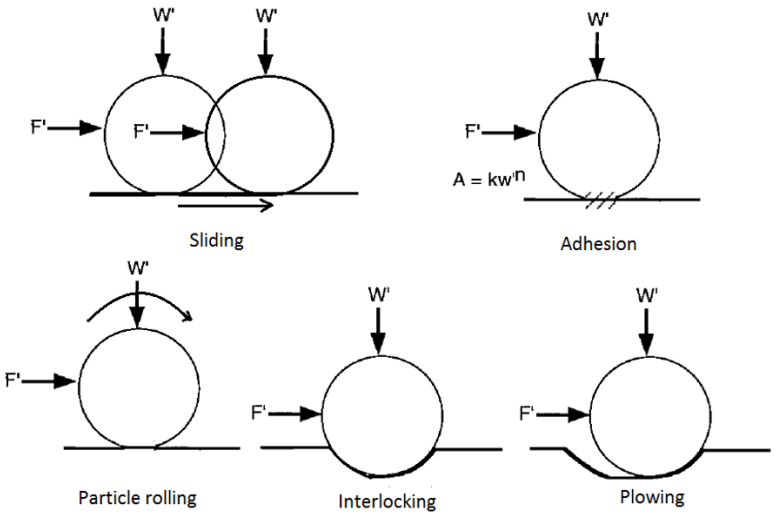

Figure 2.9 Several different mechanisms of interface shear behavior (Revised from Dove & Front, 1999)

2.8 Previous studies on interface shear behavior of landfill liners

There are many factors that can influence the interface shear behavior, and there has been much research work carried out on the interface shear behavior of landfill liner systems. In terms of the simple composite liner which combines a CCL and a geomembrane, researchers have previously focused mainly on the influences of several key factors, namely, materials for the CCL, roughness of the geomembrane, under saturated conditions, testing methods and shear rate changes.

A paper by Stark et al. (2011) provided a comparison between single- and multi-interface strength tests of landfill liners. In the paper, multiple liner combinations were favored, including a soil/geosynthetic interface. The work illustrated the influences of different types of geomembranes and soils. The authors compared the peak strengths between multi- and single-interfaces, and found that the shear strengths are similar. Kamon et al. (2008) studied the interface shear performance of landfill liner systems by using large-scale shear testing. In their work, various types of material interfaces were used. They tested CCL interfaces with geomembrane under different saturation conditions. Their results indicated that a saturated CCL-geomembrane interface has lower shear resistance compared with an unsaturated interface.

Swan et al. (2013) examined the interface shearing of soil-geomembrane under various compaction conditions, water contents and soil dry unit weights. This research showed that the cohesive soil compaction conditions strongly influence the interface shear strength. Fishman and Pal（1994）studied geomembrane interface shear with cohesive soil. This research used three types of clays and a smooth /textured HDPE geomembrane. The results were presented under both drained/undrained conditions by changing the shear rate. The authors found that the shear strength of clay-smooth HDPE interfaces is less than that of the clay for all of the cases studied. The textured geomembrane interface sheared with clay has a higher shear strength than that of the smooth geomembrane. Compared with the smooth HDPE, the shear behavior of clay /textured HDPE is more sensitive to the shear rate. Zabielska-Adamska (2006) also supported this, and indicated that textured geomembranes have greater shear strength than smooth geomembranes.

Lee (1998) reported the influence of surface topography on interface shear strength. The author presented a granular soil –geomembrane interface, which dramatically changed with the surface roughness of the geomembrane. The research by Lee also showed the interface failure mechanism changes. For a smooth geomembrane, shear strength is developed by the sliding and penetration of the sand particles and the shear strength of the textured geomembrane is developed by the interlocking and dilation of sand particles. Angularity sand has a higher plowing effect on the smooth geomembrane. Past studies (Zabielska-Adamska, 2006; Ali et al., 2012) have also presented results related to the geomembrane topography. Various ratios of BSMs as well as geomembranes with various surface roughness were used in the studies. Their results showed that bentonite content has little effect on the interface shear stress-displacement performance for different roughness of the geomembrane.

Koerner et al. (1986) found that the adhesion of soil to a geomembrane is significantly reduced when the sample is affected by leachate. Masada et al. (1994) investigated different geomembrane / CCL interfaces, which were affected by leachate. The results showed that the CCL-PVC interface is more susceptible to leachates. Karademir (2011) investigated the long term performance of temperature on the interface shear behavior between different geosynthetic and sand /geosynthetic materials. The temperature was changed from 20°C to 50°C. The results showed that for the geosynthetic materials, under higher temperatures, the hardness changes and plowing of sand would increase the interface shear behavior.

The literature review presented above shows that the effect of F-T cycles as well as the combined influence of temperature and leachate on the interface shear behavior of landfill liners have been neglected in previous studies. There is therefore the need to address these issues.

2.9 Overview of testing methods of liner interface shear strength

Many different testing methods have been proposed to test the stability of composite liners for side slopes. The most commonly used methods are direct shear and inclined plane testing.

2.9.1 Direct shear testing

Direct shear testing was originally carried out with a shear box. The shear box has an upper and a lower part, and horizontally split at the level of the center of the soil sample. The sample is installed inside the shear box, held with metal grilles, and porous stones may be placed for drainage purposes. A normal load (N) is applied on the top of shear box. It provides a vertical normal stress $\sigma = N/A$, in which, A is the area of the direct shear box (Jogi, 2005). Then, the horizontal load applied onto the lower half of the box is gradually increased to shear the sample until the sample fails. The upper half of the box is restrained and installed with a load measuring linear variable differential transformer (LVDT) device (Murthy, 2002). A modified direct shear test (DST) was proposed to test the strength of the surface between the soil and HDPE material, in accordance with ASTM standard D5321, which provides a way in the lab by which the shear strength of a geomembrane with a CCL interface can be measured. The clamping system for a geomembrane specimen should be able to afford the geomembrane with a uniform shear strength over the entire shearing process under applied normal stress. Normally, geomembrane samples are glued onto the top of a rigid substrate and then placed inside the lower shear box (Wasti & Özdüzgün, 2001). The structure of the direct shear device is shown in the Figure 2.10 below.

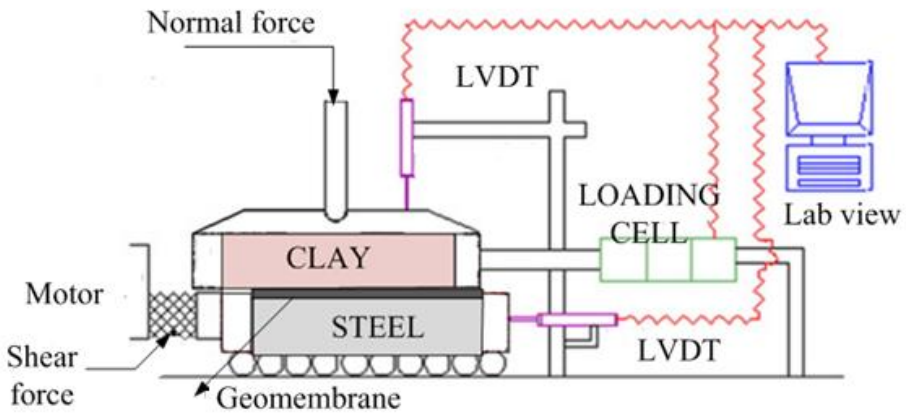

Figure 2.10 Principle of interface direct shear testing (Nasir and Fall, 2008; modified)

There are also consolidated drained (CD), unconsolidated drained (UD) and unconsolidated un-drained (UU) tests, which can simulate different conditions under various factors. These have been widely used for various projects. Direct shearing testing can also be modified with different dimensions and shapes, however, the principles of the testing are basically similar.

2.9.2 Inclined plane method

European standard ISO 12957-2 describes an inclined plane method which can be used to determine the friction angle of a geomembrane interface with soils at a low normal stress (see Figure 2.11) with two boxes. The initial normal stress is the summation of the weight of the soil and upper box. The soil sample is placed in the upper box. To avoid normal stress variation during testing, the front and rear side walls of the upper box are built with an inclination angle. The tested geosynthetic material must be bonded to the base plane in order to ensure that no relative movement occurs between the layer and the plane (Briançon et al., 2011). There are also parallel lateral guides beside the upper box to control the shear direction (Gourc & Ramirez, 2004). The base plane is inclined to provide a constant speed ($d\beta/dt = 3°/min$) and the upper box will start to slide. The displacement (δ), is measured at the same time. The interface friction angle (Φ) is therefore deduced from the inclined plane test which is calculated at a standard displacement, δ=50 mm (Pitanga et al., 2009).

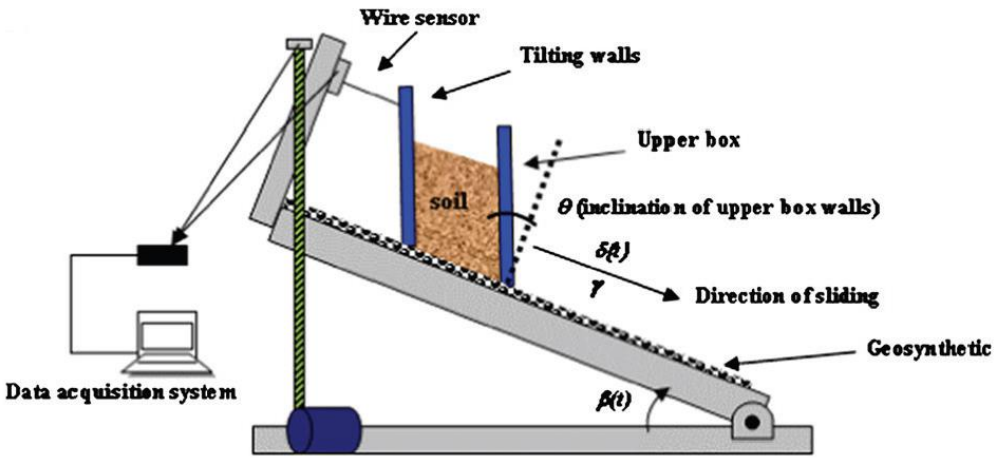

Figure 2.11 Inclined plane test set up (Pitanga et al., 2009)

However, in landfill systems, normal loads are higher than that supported by the inclined plane test. Thus, the DST is still the best means to study the interface shear behavior to consider the thermal and chemical influences.

2.10 Effect of temperature on bentonite

Thermal changes can impact bentonite properties, especially in terms of the hydraulic characteristics. The temperature influences the hydraulic conductivity of bentonite or bentonite mixtures. Pusch (1980) presented experimental results that show an increase in the hydraulic conductivity of compacted bentonite when heated up to 90℃. Cho et al. (1999) demonstrated the increasing hydraulic conductivity of a high density bentonite mixture when the temperature is increased from 20℃ to 100℃.

The impact of temperature on the water retention of bentonite was also studied by several researchers. Previous research also showed that the water retention decreases with temperature increases when the temperature is much higher than the natural climate temperature, especially when over 60°C for highly compacted bentonite (Villar et al., 2010). However, this change cannot be solely explained by thermal changes, and there are probably some chemical effects as well (Cho et al., 1999).

Pusch (1980) presented results that show that the swelling pressure of bentonite

specimens tested at 90°C is less than those tested at 20°C. The decrease of the swelling pressure is probably due to the unstable inter-layer and inter-particle water at high temperatures (Bag, 2011). In general, the swelling capacity of the bentonite will slightly decrease with an increasing temperature (Villar et al., 2010). When the temperature is higher than the threshold temperature, which is typically 100°C, the montmorillonite starts to convert into illite (Cui et al., 2012). This phenomenon will affect the properties of the bentonite, such as its swelling behavior.

2.11 Effect of leachate on bentonite

Leachate, which is generated in landfills, can gradually infiltrate into the liner during its service life. Therefore, the influence of leachate on liner materials must be considered. Chemical reactions are an essential factor since bentonite particles have high electrochemical activity. Thus, the cations of leachate can significantly impact the bentonite microstructure. This influence could cause changes in the shear behavior of the liner interface.

The ability to exchange cations is one of the basic properties of bentonites (Van Impe, 2003). Montmorillonite is the main component of bentonite, which accounts for 85% to 90% of the total mass. Natural bentontite is generally composed of both Na- and Ca-montmorillonite. Compared with Ca-montmorillonite, Na-montmorillonite has a much higher swelling capacity. Hydration of the exchangeable cations causes the bentonite to swell. The permanent negative charge caused by isomorphous substitution in the tetrahedral and octahedral sheets of montmorillonite clay layers is balanced by exchangeable cations (Muurinen, 2011). The occupying of bentonite exchanged cations depends on the cation type and concentration of the cations in the solution that are available for exchange (Egloffstein, 2001).

As previously mentioned, landfill leachate contains a high concentration of cations. Existing high concentrations of calcium cations in leachates mean that there is the tendency to exchange sodium cations into calcium in bentonite. When the clay particles adsorb highly charged cations, the total amount of electric charges on the surface of the clay particles is limited. With fewer cations in the dissipative layer, the dissipative layer and the hydration membrane of the clay surface will become thinner. The clay particles can be easily

consolidated (Ye et al., 2009). This phenomenon will reduce the sealing capacity if a large amount of Na-montmorillonites turn into Ca-montmorillonites. The reaction will continue for a long period of time until reaching an adsorption balance between the cation distribution in the bentonite material and the cation concentration of the leachate (Egloffstein, 2001).

Montmorillonite-to-illite transformation is the most frequently found alteration process in nature (Karnland & Birgersson, 2006). Potassium ions (K^+) may cause more significant changes to bentonite properties. In some situations, they will convert bentonite into illite or a smectite/ illite mixture. Charge deficiencies are partly balanced by the potassium cations between unit cell layers. The radius of K^+ is 1.33 Å. The size of the potassium cations means that they just fit into the molecular openings formed at the base of the silica tetrahedral, thus generating strong bonding between the layers (Mitchell, 1993). Also, K^+ is less hydrated compared to sodium ions (Na^+), and can easily migrate and bind to the clay surface to shield the negative charges on the surface (Liu & Neretnieks, 2006).

Therefore, the total illitization reaction may be expressed as:

K+/Ca2+/Na+-smectite + K+ + (Al3+) → illite + silica + Ca2+/Na+

(Karnland & Birgersson, 2006).

The illitization changes the distance of the expandable layers, thus leading to a change in the swelling pressure and hydraulic conductivity. The illitization rate will theoretically be higher when the temperature is increased with a constant potassium concentration (Karnland & Birgersson, 2006) (see Figure 2.12). When the cation concentration in leachate is high, the possibility that the cations will squeeze out into the adsorption layer is high. They will consume more particle charges, and consequently reduce the thickness of the diffusion and hydration layers (Ye et al., 2009).

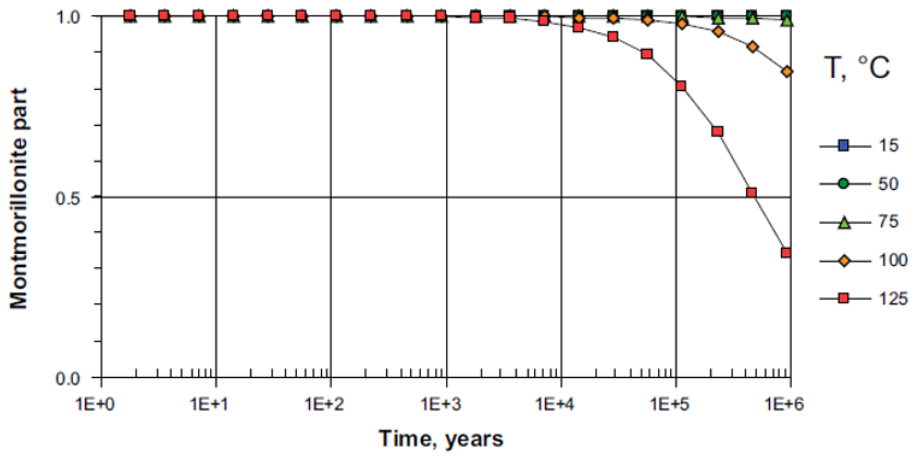

Figure 2.12 The temperature-montmorillonite amount-time changing relationship during illitization under same concentration of potassium cation (Karnland & Birgersson, 2006).

2.12 Conclusions

In this chapter, a background review of the various studies on the interface shear behavior of landfill liners has been presented, including the influence of the liner structure, materials, temperature, and leachate. This review also summarizes the influence of the properties of the materials that can be used in liners, specifically CCLs and geomembranes. One of the materials is Leda clay, which is a highly sensitive marine clay (Crawford, 1968). When the soil is disturbed, the trapped water in the pores can escape into the clay and the structure of the Leda clay particles collapse. This leads to an increase in the pore water pressure due to the low hydraulic conductivity of the material. The increase in pore water pressure results in lower effective stress between the clay particles, which leads to liquefaction of the clay material. Remolded Leda clay has much less strength than undisturbed Leda clay (Hyndman, 2010). Lost hydraulic cations can result in the repulsion and realignment of the clay particles. Bentonite is a type of expansive soil and also used in landfill liners. It has significant swelling capacity and low hydraulic conductivity. Bentonite can be used or mixed with other materials to minimize the anticipated transport of toxins (Arifin, 2008).

Once a composite liner is adopted, there is the potential risk of sliding failure at the interface. The influence of F-T, and the combined effect of high temperature and leachate on the interface shear behavior of the composite liner should be a concern. Previous studies have

only addressed the isolated effect of high temperature or leachate on CCLs but not the combined effect of temperature and leachate on the shear behavior of the liner interface. Moreover, the effects of F-T cycles on the behavior of the liner interface have been neglected in previous studies. F-T cycles change the soil structure, void ratio, density, resilient modulus and shear strength of soil samples. Cations from leachate have an effect on bentonite as well. Bentonite is a specific clay material, because it has high electrochemical activity which can change its properties. Both calcium and potassium cations exchange sodium cations from sodium-bentonite and this influences the swelling capacity. However, for BSMs, there is limited research related to the interface shear behavior and shear strength. In the following chapter, the effect of F-T phenomenon and influence of non-isothermal leachate on the interface shear behaviour and strength between CCL and smooth HDPE will be discussed.

2.13 References

Arifin, Y. F. (2008). Thermo-hydro-mechanical behavior of compacted bentonite-sand mixtures: An experimental study. Dissertation for doctor degree, Faculty of Civil Engineering, Bauhaus-University, Weimar. URL: http://e-pub.uni-weimar.de/opus4/files/852/Thermo_hydro_mechanical_behavior_of_compacted_bentonite_sand_mixture.pdf.

Adhikari, B., Dahal, K.R., & Khanal, S. N. (2014). A review of factors affecting the composition of municipal solid waste landfill leachate. International Journal of Engineering Science and Innovative Technology (IJESIT). Volume 3, Issue 5, September 2014.

Ali, F., Salman, F. A., & Subramaniam, S. (2012). Influence of surface texture on the interface shear capacity of landfill liner. Electronic Journal of Geotechnical Engineering, (17), 101-114.

Briançon, L., Girard, H., & Gourc, J. P. (2011). A new procedure for measuring geosynthetic friction with an inclined plane. Geotextiles and Geomembranes, 29(5), 472-482.

Bag, R. (2011). Coupled thermo-hydro-mechanical-chemical behavior of MX80 bentonite in geotechnical applications (Doctoral dissertation, Cardiff University).

Benson, C., Zhai, H., Wang, X. (1994). Estimating hydraulic conductivity of compacted clay liner. Journal of Geotechnical Engineering, Vol. 120. No. 2. Feb. P. 366 – 387.

Cho, W. J., Lee, J. O., & Chun, K. S. (1999). The temperature effects on hydraulic conductivity of compacted bentonite. Applied clay science, 14(1), 47-58

Cho, W. J., Lee, J. O., & Kang, C. H. (2000). Influence of temperature elevation on the sealing performance of a potential buffer material for a high-level radioactive waste repository. Annals of Nuclear Energy, 27(14), 1271-1284.

Cho, W.J., Lee, J.O. and Kwon, S. (2011). An analysis of the factors affecting the hydraulic conductivity and swelling pressure of Kyungju Ca-bentonite for use as a clay-based sealing material for a high –level waste repository. Nuclear Engineering and Technology, 44 (1), 89-102

Crawford, C. B. (1968). Quick clays of eastern Canada. Engineering Geology, 2(4), 239-265.

Cui, S. L., Zhang, H. Y. and Zhang, M.(2012). "Swelling characteristics of compacted GMZ bentonite–sand mixtures as a buffer/backfill material in China" Engineering Geology, 141: 65–73

Dillon Consulting (2005) Guysborough waste management facility draft operation plan. Municipality of the District of Guysborough.

Dove, J. E., & Frost, J. D. (1996). A method for measuring geomembrane surface roughness. Geosynthetics International, 3(3), 369-392.

Dove, J. E., & Frost, J. D. (1999). Peak friction behavior of smooth geomembrane-particle interfaces. Journal of Geotechnical and Geoenvironmental Engineering, 125(7), 544-555.

Douglas, S.W. (1984). The sealing performance and permeability of bentonite borehole plugs. Dissertation for doctor degree, University of Arizona

Environmental Protection Act. (2011). Ontario Regulation 232/98: Landfill sites. Retrieved August, 11, 2015, from http://www.ontario.ca/laws/regulation/980232

Egloffstein, T. A. (2001). Natural bentonites—influence of the ion exchange and partial desiccation on permeability and self-healing capacity of bentonites used in GCLs. Geotextiles and Geomembranes, 19(7), 427-444

Environmental Commissioner of Ontario. (2011). What a waste: Failing to engage waste reduction solutions. Engaging Solutions, ECO Annual Report, Toronto, The Queen's Printer for Ontario, 91-97.

Fleming, I., Sharma, J., & Jogi, M. (2006). Shear strength of geomembrane–soil interface under unsaturated conditions. Geotextiles and Geomembranes, 274-284.

Fishman, K. L., & Pal, S. (1994). Further study of geomembrane/cohesive soil interface shear behavior. Geotextiles and Geomembranes, 13(9), 571-590.

Gourc, J. P., & Ramirez, R. R. (2004). Dynamics-based interpretation of the interface friction test at the inclined plane. Geosynthetics International, 11(6), 439-454.

Government of Canada. (2015). Canadian Climate Normals. Accessed March 2, 2015 from http://climate.weather.gc.ca/climate_normals/index_e.html

Government of Ontario (2012). Landfill standards: A guideline on the regulatory and approval requirements for new or expanding landfilling sites. Toronto, Ontario, Queen's Printer for Ontario.

Hyndman, D. (2010). Natural hazards and disasters. Cengage Learning. p203

Jo, H.Y., (2003). Cation exchange and long-term hydraulic conductivity of geosynthetic clay liners (GCLs) permeated with inorganic salt solutions. Dissertation of Doctor of Philosophy. University of Wisconsin-Madison.

Jogi, M (2005). A method for measuring smooth geomembrane/soil interface shear behavior under unsaturated conditions. Thesis of Degree of Master's of Science, Department of Civil Engineering, University of Saskatchewan, Saskatoon, SK, Canada

Koerner, R. M., Soong, T. Y. (2000). Stability assessment of ten large landfill failures. Proceedings of GeoDenver 2000 Congress: Advances in transportation and geo-environmental systems using geosynthetics, ASCE Geotechnical Special Publication No. 103, 1–38.

Kruse, K. (1994). Langfristiges emissionsgeschehen von siedlungsabfalldeponien, veröffentlichungen des instituts für stadtbauwessen. Technische Universität Braunschweig, Heft 54.

Kahimba, F.C., (2008) Infiltration and soil moisture redistribution under Freeze-Thaw conditions. Dissertation of Doctor of Philosophy. Department of Biosystems Engineering, University of Manitoba, Winnipeg, Manitoba, Canada.

Karnland, O., & Birgersson, M. (2006). Montmorillonite stability. With special respect to KBS-3 conditions. Swedish Nuclear Fuel and Waste Management Co., Stockholm, Sweden.

Karademir, T. (2011). Elevated temperature effects on interface shear behavior. Doctoral dissertation, Georgia Institute of Technology.

Koerner, R. M., Martin, J. P., & Koerner, G. R. (1986). Shear strength parameters between geomembranes and cohesive soils. Geotextiles and Geomembranes, 4(1), 21-30.

Kamon, M., Mariappan, S., Katsumi, T., Inui, T., & Akai, T. (2009). Large-scale shear tests on interface shear performance of landfill liner systems. Geosynthetics in Civil and Environmental Engineering, 473-478. Springer Berlin Heidelberg.

Kjeldsen, P., Barlaz, M., Rooker, A., Baun, A., Ledin, A., & Christensen, T. (2010). Present and Long-Term Composition of MSW Landfill Leachate: A Review. Critical Reviews in Environmental Science and Technology, 297-336.

Lee S.W. (1998). Influence of surface topography on interface strength and counterface soil structure. Doctor of Philosophy in Civil and Environmental Engineering. Georgia Institute of Technology

Landfill. (n.d.). The American Heritage® Science Dictionary. Retrieved August 11, 2015, from Dictionary.com website: http://dictionary.reference.com/browse/landfill

Lake, C.B., (2000) Contaminant transport through geosynthetic clay liners and a composite liner system. Dissertation of Doctor of Philosophy. Department of Civil and Environmental Engineering. The University of Western Ontario

Liu,J.S. and Neretnieks, I. (2006). "Physical and chemical stability of the bentonite buffer" Technique Report of Chemical Engineering and Technology Royal Institute of Technolog, Swedish Nuclear Fuel and Waste Management Co

Macpherson, G. L., & Townsend, M. A. (1998). Water chemistry and sustainable yield.

Bulletin-Kansas Geological Survey, 117-158

Masada, T., Mitchell, G. F., Sargand, S. M., & Shashikumar, B. (1994). Modified direct shear study of clay liner-geomembrane interfaces exposed to landfill leachate. Geotextiles and Geomembranes, 13(3), 165-179.

Muurinen, A. (2011). Measurements on Cation Exchange Capacity of Bentonite in the Long-Term Test of Buffer Material (LOT). Working Report 2011-10. Posiva Oy.

Mitchell, J. K., (1993). Fundamentals of soil behavior. New York: Wiley.

Mendes, M. J. A., Touze-Foltz, N., Palmeira, E. M. and Pierson, P. (2010) Influence of structural and material properties of GCLs on interface flow in composite liners due to geomembrane defects. Geosynthetics International, 17, No. 1

Mesri, G., & Olson, R. E. (1971). Consolidation characteristics of montmorillonite. Geotechnique, 21(4), 341-352.

Moore, R. (1991). The chemical and mineralogical controls upon the residual strength of pure and natural clays. Geotechnique, 41(1), 35-47.

Murthy, V. N. S. (2002). Geotechnical engineering: principles and practices of soil mechanics and foundation engineering. Chapter 8. CRC Press, United States.

Nader, A. (2014). Engineering characteristics of sensitive marine clays-examples of clays in eastern Canada.

Nasir, O., & Fall, M. (2008). Shear behavior of cemented pastefill-rock interfaces. Engineering Geology, 101(3), 146-153.

Olgun, M. (2013). The effects and optimization of additives for expansive clays under freeze–thaw conditions. Cold Regions Science and Technology, 36-46.

Pando, M., Filz, G., Dove, J., & Hoppe, E. (2002). Interface shear tests on FRP composite piles. International Deep Foundations Congress, American Society of Civil Engineers, Orlando, Florida, 1486-1500.

Pitanga, H. N., Gourc, J. P., & Vilar, O. M. (2009). Interface shear strength of geosynthetics: Evaluation and analysis of inclined plane tests. Geotextiles and Geomembranes, 27(6), 435-446.

Pusch, R., (1980). Permeability of highly compacted bentonite. SKB Technical Report 80-16, Swedish Nuclear Fuel and Waste Management.

Reddy, D.V., (1999). A comprehensive literature review of liner failures and longevity. Center for Marine Structures and Geotechnique, Department of Ocean Engineering, Florida Atlantic University.

Robinson, W. (1986). The solid waste handbook: A practical guide. Appendix 11.4, 355. New York: Wiley.

Ryan, M (2010) Environmental standards for municipal solid waste landfill sites. Department of Environment and Conservation, Newfoundland and Labrador.

Stewart, R. (2009) Environmental Geoscience. Environmental Science in the 21st Century-An online textbook. Department of Geosciences, Texas A&M University. From, http://oceanworld.tamu.edu/resources/environment-book/groundwatercontamination.html

Stark, T. D., Niazi, F. S., & Keuscher, T. C. (2011). Comparison of single and multi geosynthetic and soil interface tests. Retrieved April, 13, 2015, from: http://tstark.net/wp-content/uploads/2012/10/JP87.pdf.

Swan Jr, R. H., Bonaparte, R., Bachus, R. C., Rivette, C. A., & Spikula, D. R. (2013). Effect of soil compaction conditions on geomembrane-soil interface strength. Landfill Closures: Geosynthetics, Interface Friction and New Developments, 10, 141-147.

Sunil, B. M., Shrihari, S., & Nayak, S. (2009). Shear strength characteristics and chemical characteristics of leachate-contaminated lateritic soil. Engineering Geology, 106(1), 20-25.

Taylor, R., & Allen, A. (2006). Waste disposal and landfill: information needs. Protecting Groundwater for Health: Managing the Quality of Drinking-water Sources. IWA: London. URI: http://discovery.ucl.ac.uk/id/eprint/40075

Tang, G.X. (1999). Suction characteristics and elastic-plastic modeling of unsaturated sand-bentonite mixture. Dissertation for doctor degree Department of civil and geological engineering University of Manitoba. URI: http://hdl.handle.net/1993/1580

Taha, A.M (2010). Interface Shear Behavior of Sensitive Marine Clays -Leda Clay.

Dissertation for Master Degree, University of Ottawa. ISBN: 978-0-494-73849-8

US Environmental Protection Agency (2012). Part IV Protecting Ground Water, Chapter 7. Guide for industrial waste management. Technical considerations for new surface impoundments, landfills, and waste piles. Accessed date April, 4, 2015 at http://www.epa.gov/waste/nonhaz/industrial/guide

Van Impe, P.O. (2003). Consolidation, contaminant transport and chemico-osmotic effects in liner materials. Dissertation for doctor degree, Department of Civil Engineering. Ancona University. Accessed date March, 21, 2015 from http://www.geotechnics.ugent.be/docs/phdpeter.pdf

Villar, M. V., Gomez-Espina, R., & Lloret Morancho, A. (2010). Experimental investigation into temperature effect on hydro-mechanical behaviors of bentonite.

Wasti, Y., & Özdüzgün, Z. B. (2001). Geomembrane–geotextile interface shear properties as determined by inclined board and direct shear box tests. Geotextiles and Geomembranes, 19(1), 45-57

Wikipedia. (2015). Southern Ontario. Accessed January 15, 2015 from http://en.wikipedia.org/wiki/Southern_Ontario

Ye, W.M., Huang, W., Chen, B., Yu, C. and Wang, J. (2009). Diffuse double layer theory and volume change behavior of densely compacted Gaomiaozi bentonite. Rock and Soil Mechanics, 30(7), 1900-1904

Yesiller, N., & Hanson, J. L. (2003). Analysis of temperatures at a municipal solid waste landfill

Yesiller, N., Hanson, J. L., & Yoshida, H. (2011). Landfill temperatures under variable decomposition conditions.

Zabielska-Adamska, K. (2006). Shear strength parameters of compacted fly ash–HDPE geomembrane interfaces. Geotextiles and Geomembranes, 24(2), 91-102.

Zhou, Y., (1996) Shear strength of geomembrane-cohesionless soil interface system. Dissertation of Doctor of Philosophy. University of Pittsburgh, UMI Number: 9728704

Chapter 3 Shear Behavior of Compacted Clay Liners – Geomembrane Interface under Freeze-Thaw Cycles

Abstract

There is a general consensus that bentonite sand mixtures (BSMs) can be used in compacted clay liners (CCLs) for waste disposal facilities when local clay is not suitable. In considering the drastic temperature variations in Canada, an understanding of the interface shear behavior of composite liners affected by freeze-thaw (F-T) cycles is necessary. This study is therefore an investigation on the influence of F-T cycles on the shear behavior of the interface between a BSM and a smooth high-density polyethylene (HDPE) geomembrane. An experimental program has been carried to assess the shear behavior and determine the shear strength parameters of the interface between the BSM and HDPE geomembrane. The studied BSM were subjected to various numbers of F-T cycles (i.e., 0, 1, 2, 3, 5 and 10 cycles). All of the tests are carried out with a direct shear testing apparatus by following an ASTM standard. The obtained results show that the interface shear strength is lower than the BSM. The shear strength of the interface between the BSM and smooth HDPE geomembrane decreases with increasing numbers of F-T cycles. The total reduction in the interface shear strength of the samples that did not undergo any F-T cycles in comparison to those that were subjected to 10 F-T cycles is 23%, 15.2% and 11.4% under 150, 250 and 350 kPa of vertical stress respectively. There is significant penetration of the sand particles into the geomembrane surface, and the extent of the damage is proportional to the level of normal stress.

3.1 Introduction

There are currently many different ways to dispose refuse. However, landfills have been the mainstream of solid waste disposal in the past decades. When waste degrades in landfills, leachate and landfill gases are generated which are toxic to the environment. Landfill leachate is a black color liquid; it contains many organic and inorganic materials as well as heavy metals that can pollute the groundwater (Kjeldsen et al., 2010). As awareness of environmental protection has increased, reliable engineered barriers are now used to ensure that leachate migration is controlled.

Several types of barriers are commonly used in landfill practices, such as compacted clay liners (CCLs), geosynthetic clay liners (GCLs) and geomembranes (Jogi, 2005). CCLs and geomembrane combinations are often considered to be good options for landfills. In order to maximize the capacity of landfills, the majority of landfills are designed with steep side slopes. However, the potential risk of shear sliding increases with the steepness of the side slopes. The sliding of the surface may take place between CCLs and geomembrane materials. A simple sketch illustrates this issue, see Figures 3.1a and 3.1b.

CCLs are a stable and low permeable type of barrier, which are made of densely and homogeneously compacted cohesive soils (Government of Manitoba, 2007). CCLs can have a saturated hydraulic conductivity equal to or less than 10^{-9} m/s. Bentonite is a highly expansive soil, which has high swelling capacity and extremely low hydraulic conductivity which is typically less than 10^{-9} m/s (Fall et al. 2009). Bentonite can be used or mixed with other materials as barrier material. The widely used material is bentonite sand mixtures (BSMs), which serve as an essential barrier to the natural flow of ground and underground water by minimizing the transport of toxins (Arifin, 2008). Bentonite combined with sand mixtures has a higher structural integrity, thermal conductivity and stiffness. Therefore, this combined material is more effective and economical (Cui et al., 2012).

Geomembranes are also a popular material for hydraulic barriers used to minimize the seepage of containment leachate. Thermoplastic geomembranes have a diffusion hydraulic conductivity that ranges from 10^{-13} to 10^{-15} m/s (Jogi, 2005). High density polyethylene (HDPE) is a type of polyethylene thermoplastic, which has high strength and excellent chemical resistance to various chemicals. It is also able to resist water, salt solutions, alkalis

and acids (Zhou, 1996). The semi-crystalline microstructure of HDPE makes it more effective (Zabielska-Adamska, 2006). Therefore, HDPE is used as a material for geomembranes.

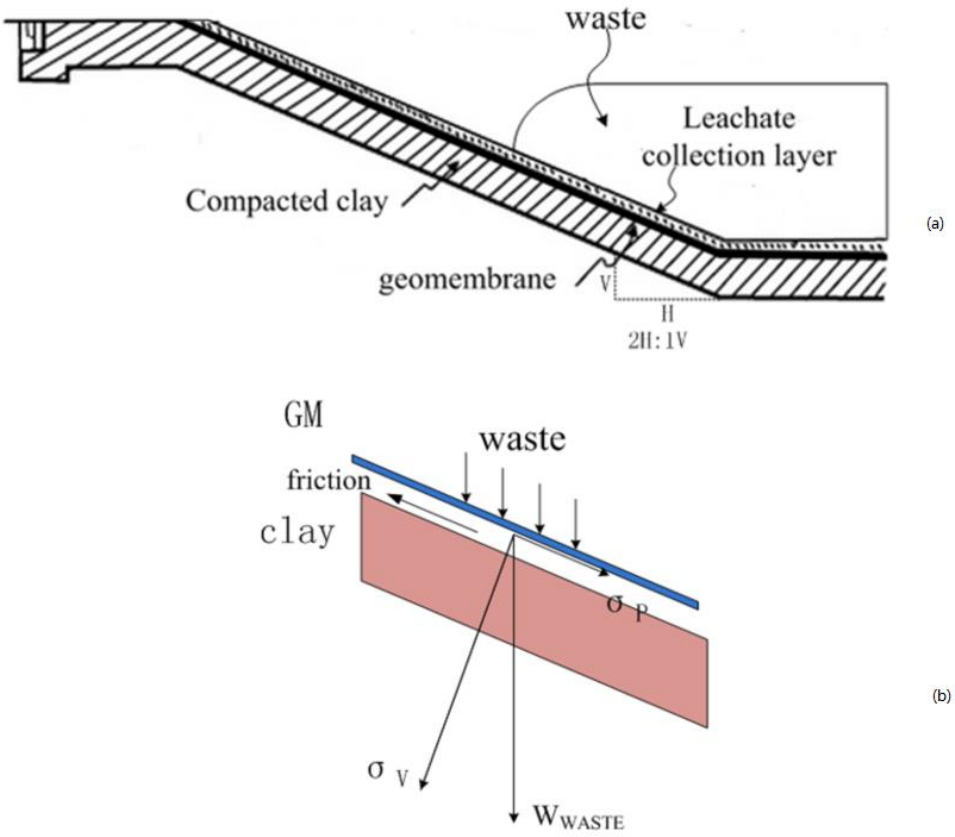

Figure 3.1 landfill side liner: (a) Simple Sketch of Landfill Side Liners. (b) Liner Force Analysis

Once CCLs and geomembrane materials are used as the composite liner, the interface shear behavior of the original geomembrane and CCLs will normally be taken into consideration in the case that there are risks of slipping failures. However, during landfill operations, the interface shear behavior can be influenced by changes in both the soil and geomembrane properties caused by various environmental effects. In Canada, temperature changes cannot be ignored as there is an approximate 50℃ difference between summer and winter (Wikipedia, 2015). These temperature changes result in freeze-thaw (F-T) cycles. Once a new landfill is in operation, wastes are placed into the landfill site in specific sequences, and the final cover is gradually built across the whole landfill. As a result, some parts of the slope liner of the landfill will be exposed to F-T cycles for years. There are several

previous studies on the influence of F-T cycles to soil materials (e.g. Benoit and Voorhess 1990, Othman and Benson 1993, Dagesse 2007, Fall et al. 2010). However, there is a paucity of research on the effect of F-T cycles on the shear behavior of the interface between a BSM and a smooth geomembrane. Therefore, this study has been conducted to experimentally investigate the effect of F-T cycles on the shear behavior and strength of a BSM, and the interface shear behavior and strength of BSM/smooth HDPE samples.

3.2 Materials and experimental program

3.2.1 Bentonite-Sand Mixture

Ottawa cube sand is used for this experiment. The sand is specially graded natural silica sand. The specific gravity of the sand is 2.65. The sand was mixed with manufactured sodium-bentonite at a ratio of 10:1 by weight. The liquid limit (LL) and plastic limit (PL) of the bentonite were determined to be 576% and 42.6%, respectively. The optimum water content of BSM was 13.2%. The specific gravity of sodium bentonite is 2.68. The grain size distribution curve of the BSM is shown in Figure 3.2. The result of the X-ray diffraction analysis of sodium bentonite showed that the bentonite has a high proportion of clay minerals of the smectite group (Figure 3.3).

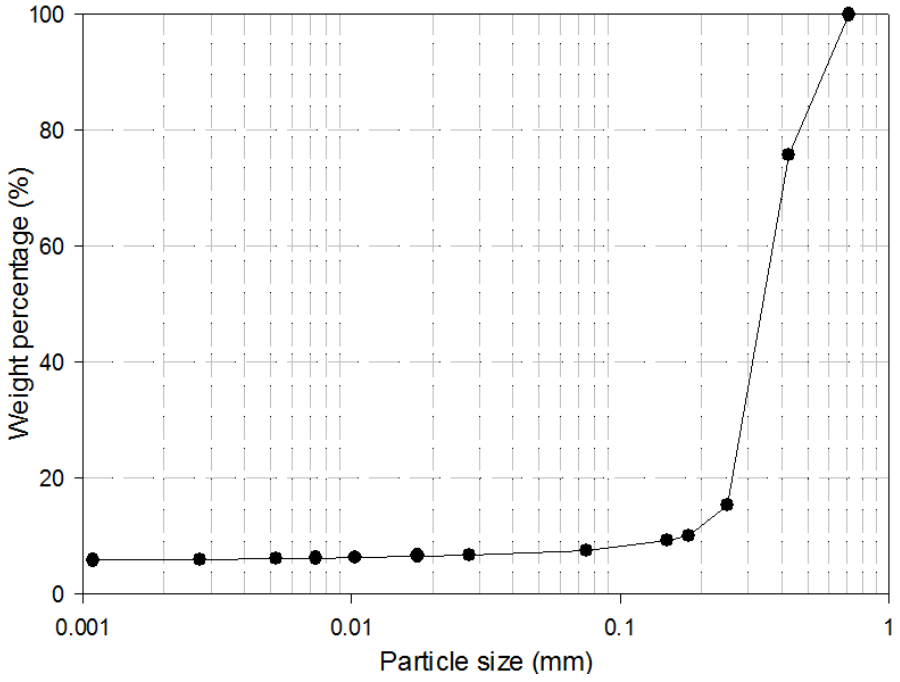

Figure 3.2 Grain size distribution curve of BSM material

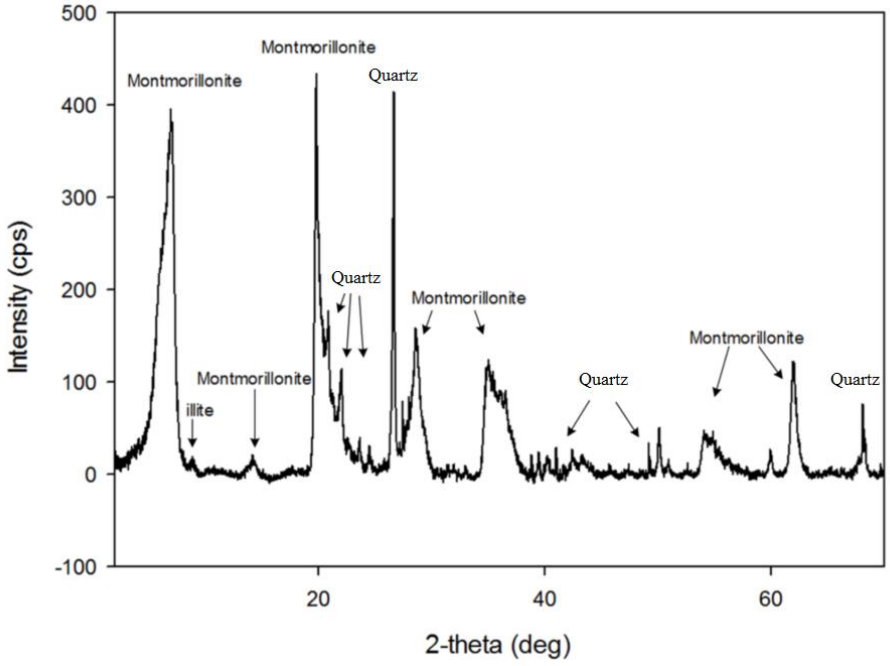

Figure 3.3 X-ray diffraction of the sodium bentonite used in the study

3.2.2 Geomembrane

Smooth HDPE with a thickness of 60 mil (1.5 mm) manufactured by GSE Lining Technology, Houston, USA, is used in this experiment as the geomembrane. The roughness of the geomembrane is 1.09 (Dove & Frost, 1996). HDPE has low hydraulic conductivity, which varies between 10^{-13} to 10^{-15} m/s (Jogi, 2005). HDPE also has satisfactory chemical and ultraviolet resistance properties which makes it suitable for use as geomembranes in landfill facilities. All of other properties of the HDPE used in this study are listed in Table 3.1.

Table 3.1 HDPE geomembrane properties which can be obtained from the GSE lining technology website (Geosynthetic Lining Systems, 2015).

Property of HDPE geomembrane	Minimum average value
Thickness, mm	1.5
Density, g/cm^3	9.94
Strength at break, N/mm	40
Strength at yield, N/mm	22
Elongation at break. %	700
Elongation at yield. %	12
Tear resistance, N	187
Puncture resistance, N	480

3.3 Specimen preparation and freeze-thaw procedures

As mentioned earlier, to create the BSM, 10% sodium bentonite by weight was added to the Ottawa test sand. It was then mixed with distilled water to a water content of 2% - 4% wet of optimum. The mixing procedure was carried out with a mixing machine for at least 10 minutes until the mixture became uniform. The mixed BSM was then sealed in bags to prevent evaporation and cured at room temperature for a minimum of 48 hours to achieve moisture balance. Then, the BSM was compacted via a dynamic compaction method in a 100mm diameter mould. The compacted mixture was then extracted and cut into cubes to be used as the samples. The sample dimensions were 60 x 60 x 25 mm for the pure soil samples, and 60 x 60 x 12 mm for shear testing of the interface. The actual water content range of the samples was 15.3% - 15.5%.

The pure BSM samples were directly wrapped with plastic film. In terms of the samples for the interface shear strength tests, the geomembrane was cut into pieces of 60 x 60 mm with smooth edges, and the smooth side was then placed in contact with the soil cubes. The entire sample was wrapped with plastic film. The volume sustained by landfill clay liners might change during the freezing process, and such changes are partially restricted. The

restrictions are caused by the surrounding clay and the weight from the gravity of the upper geomembrane and leachate collection layer. Thus, in order to simulate conditions close to the field situation, all of the samples were tightly wrapped with two layers of plastic film to restrict volume changes in the samples. All the wrapped samples were stored in zipper bags and placed in plastic boxes for storage.

The samples were subjected to various numbers of F-T cycles, which were 0, 1, 2, 3, 5 and 10 cycles, respectively. For the F-T process, the plastic boxes were placed into a freezer which was set at - 30℃, and then the frozen samples were thawed at room temperature. In order to measure the time required for the samples to reach a stable stage in the F-T cycle, the temperature gradients were tested. A thermal sensor was inserted into the pure BSM samples, then connected to a data acquisition system, which measured the core temperature changes of the samples. The curves of the freezing and thawing temperature changes with respect to time are presented below in Figure 3.4. BSM samples that are 60 x 60 x 25 mm require 4.25 hours to reach thermal stability. The 60 x 60 x 12 mm samples require less time compared with the former. In order to eliminate the potential influence of sample variability, all of the samples underwent cycles of 12-hours of freezing and 12-hours of thawing.

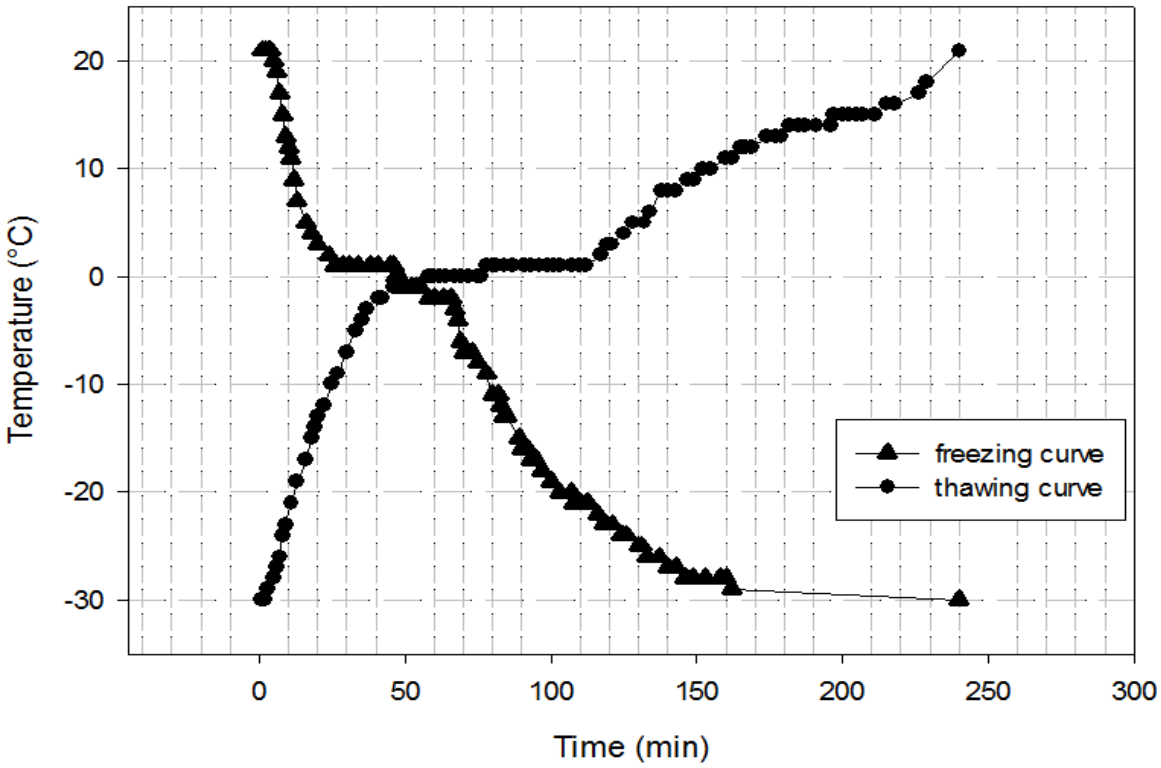

Figure 3.4 Freezing and thawing phases of bentonite sand mixture used in study plotted with time

3.4 Testing equipment and technique

3.4.1 Testing apparatus

A direct shear stress apparatus is commonly used to test the shear strength and determine the interface shear behavior. This apparatus has the advantage of simplicity and suitability for interface testing (Miller and Hamid, 2004; Taha and Fall 2013, 2014). ASTM standard D5321 was used to measure the shear strength of the interface between the geomembrane and CCL. Therefore, a standard direct shear testing machine was used for the shear strength testing of the BSM and the BSM/geomembrane interface. The schematic diagram of a standard direct shear testing machine, which was used in the interface shear tests, is shown in Figure 2.10 in Chapter 2.

The direct shear testing machine has a square shear box, and the devices on the upper half only have horizontal support. The direct shear testing machine also has a microprocessor controlled drive which is able to provide a designated shear speed. The normal stresses (N) are applied on the top of the shear box by adding weight to the weight hanger (Taha, 2010).

Then, the horizontal stress applied to the lower box is gradually increased until sample failure. The upper box is restrained and has a load cell device installed. The horizontal and vertical displacements are recorded by a linear variable differential transformer (LVDT) (Murthy, 2002). All of the data were collected by a computerized logger, and monitored and saved with LABVIEW software.

3.4.2Testing procedures and testing plans

The pure BSM and BSM/smooth HDPE interface were tested under consolidated-drained (CD) conditions and sheared under a low shear rate. This allowed the pore water pressure to dissipate. In previous studies carried out by Koerner et al. (1986) and Tsubakihara & Kisheda, (1993), a shearing rate of 0.06 mm/min and 0.03 mm/min were chosen respectively. Based on the results of the consolidation tests performed on the BSM in this study, the shearing rate for the direct shear testing is determined to be 0.025 mm/min. The consolidation tests are presented in the Appendix. For the pure soil samples, they were placed into the shear box and tightly screwed. The interface shear samples needed to be glued onto the geomembrane on top of a supporting steel piece and cured for at least 1 hour. When the soil/geomembrane sample and the steel block with the glued samples were loaded into the shear box, it was necessary to ensure that the interface of the soil/HDPE was exposed in the gap between the top and bottom of the shear box. Filter papers were used between two pervious metal plates and sample to prevent soil mass loss during saturation.

In order to achieve a relatively quick saturation of the sample, a well-sealed container with a strong vacuum resistance capacity was needed as an extra apparatus for the saturation. The bentonite-sand sample was placed into the shear box which was put into a vacuum container, which was filled with distilled water and then sealed by using vacuum grease. A negative pressure of 35 kPa was applied, which can help the BSM samples to reach 99% saturation after 24 hours.

Once the samples were saturated, they were placed in the sink of the direct shear machine. The sink was filled with distilled water and consolidation was carried out. The normal stresses were 150, 250, and 350 kPa, respectively. The consolidations under different vertical loads were processed by 3 or 4 load increments, and each was carried out for 1 hour to ensure that the primary consolidation was completed. After consolidation, the lower box with the

sink started to shear the samples at the speed of 0.025 mm/min.

3.5 Results and discussion

3.5.1 Shear behavior of samples not subjected to F-T cycles

Figures 3.5 to 3.8 illustrate the shear behaviors of the BSM/geomembrane interface and those of the BSM samples, which were not subjected to any F-T cycles.

Figure 3.5 shows a typical shear stress versus strain relationship for the interface shear behavior of BSM / smooth HDPE geomembrane samples that did not undergo any F-T cycles while Figure 3.6 depicts a typical shear stress versus strain relationship for the BSM samples for comparison purposes. From Figures 3.5 and 3.6, it can be observed that the BSM / smooth HDPE geomembrane interface presents a significant increase in initial shear stiffness with normal stress, in comparison to the BSM samples. This higher initial stiffness of the interface shear behavior can be explained by the fact that under normal stress, the BSM material is in close contact with the geomembrane. At the beginning of the shearing, the sand particles located at the interface were interlocked with the HDPE geomembrane surface, while the bentonite clay components that filled the sand voids were in contact with the geomembrane through adhesion. The shear stress had to significantly be increased to overcome the interface shear resistance and increase in shear displacement. The interface shear stress vs. relative displacement curves of the BSM / smooth HDPE geomembrane interface do not fit well with those of the BSM. This could suggest that the dominant shearing mechanism is taking place at the interface surface, but not in the BSM.

It can be seen that the BSM / smooth HDPE geomembrane interface does not exhibit distinctive peak and post-peak shear stress behaviors, which is also true when the curves of the BSM are examined. Since no other obvious peak stress can be observed, the shear stress at 15% of the shear strain is considered as the peak shear strength (in accordance with ASTM standard D5321). It should be mentioned that the residual state was not reached in any of these tests (interface residual shear strength could not be achieved with a conventional direct shear testing apparatus). Figures 3.5 and 3.6 also show that the peak shear stress and the shear displacement that corresponds to the peak shear stress both increase with an increase in the normal stress. For example, the peak shear stress for the BSM / HDPE geomembrane is

determined to be 70, 95 and 141 kPa at normal stresses of 150, 250 and 350 kPa, respectively. This is due to the fact that an increase in the normal stress on the plane of the shear failure leads to an increased contact area between the geomembrane and BSM particles. This causes increased frictional resistance between the soil and the geomembrane, and a corresponding higher peak shear stress (Fall and Nasir 2010, Nasir and Fall, 2008). Moreover, the peak shear stress of the interface is significantly lower (approximately 50%) than that of the BSM. This is due to the fact that the dominant shearing mechanism takes place at the interface (smooth) surface as mentioned above.

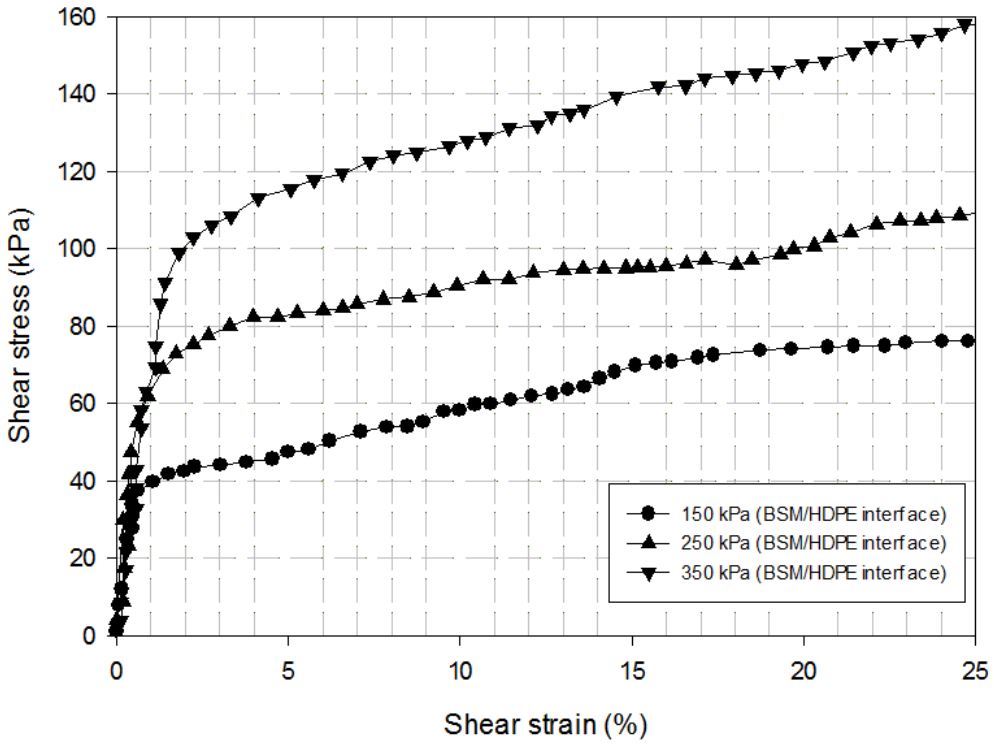

Figure 3.5 Shear stress vs. strain of BSM/smooth HDPE interface not subjected to an F-T cycle

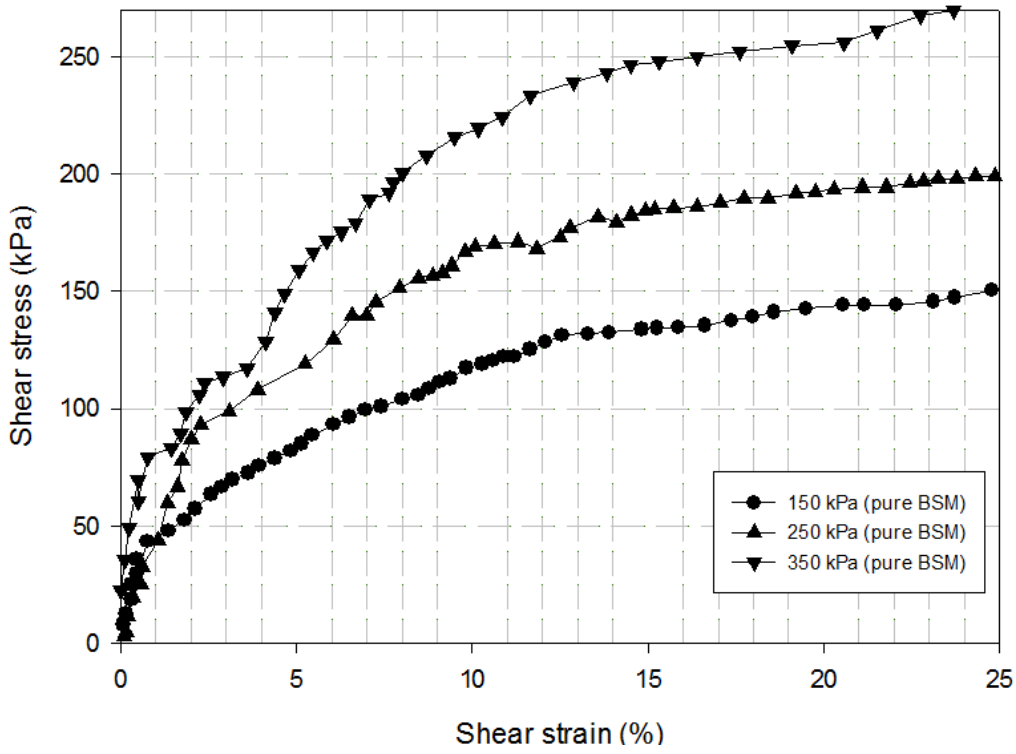

Figure 3.6 Shear stress vs. strain of BSM samples not subjected to an F-T cycle

Figures 3.7 and 3.8 show the curves of the typical results of vertical deformation versus shear deformation of the BSM/geomembrane interface and BSM samples, which did not undergo an F-T cycle. Figure 3.7 indicates that the vertical deformation of the BSM/smooth HDPE interface is characterized by contracting behavior. In the first stage (shear strain ≤ 4-5%), a high contraction rate and significant contraction are observed. This is explained by the fact that as soon as a normal stress is applied, the surface of the BSM and smooth HDPE geomembrane moves together. This is because at the beginning of the normal and shear loadings, more contact between the asperities on both the surfaces of the BSM and geomembrane is created, and the local voids become smaller (Fall and Nasir 2010). The penetratoin of the sand particles into the geomembrane surface is also an additional factor that contributes to the contraction. In the second stage, the vertical deformation of the interface tends to increase slowly compared to the first stage with increasing shear deformation. No dilation can be observed from the studied deformation range. For the BSM, the normal stress during shearing causes the vertical deformation of the samples, and the vertical dilation is due to the asperities of the sand particles. The sand particles override each

other at the point of contact during shearing, unless they are crushed. Figure 3.8 shows that the BSM samples undergo contractions up to 5% of the shear deformation. Between shear deformations of 5% and 15%, the BSM is characterized by a dilating behavior. The dilation is commonly observed in the direct shear testing of materials that contain sands (Al-Douri & Poulos, 1991; Simoni & Houlsby, 2006). A comparison of Figures 3.7 and 3.8 reveals that the percentage of vertical contraction of the BSM/geomembrane interface is larger than that of the BSM samples. This can be attributed to the contraction induced by the penetration of the sand particles into the geomembrane and the destruction of the asperities during shearing. However, it should be emphasized that the difference in the magnitude of the contraction between the interface and BSM is small. In fact, if the vertical deformation is presented in mm, the difference is only 0.1 mm. This small difference could also be caused by experimental errors and the measurement by the LVDT.

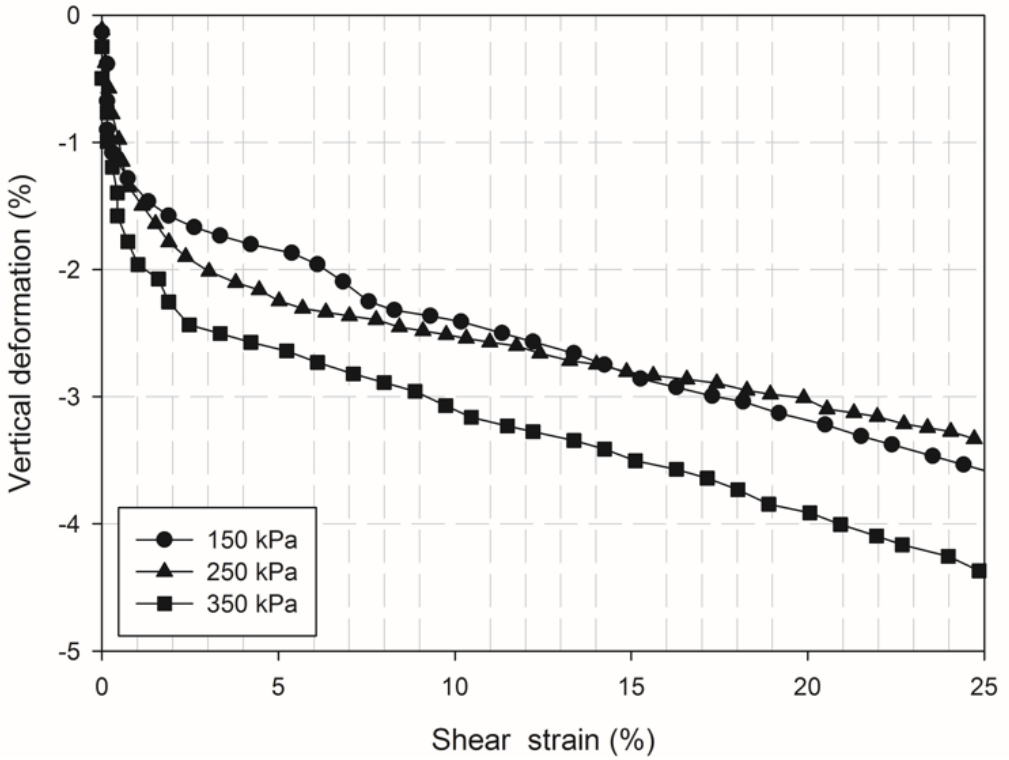

Figure 3.7 Vertical deformation versus horizontal deformation of BSM/geomembrane interface with no F-T cycle

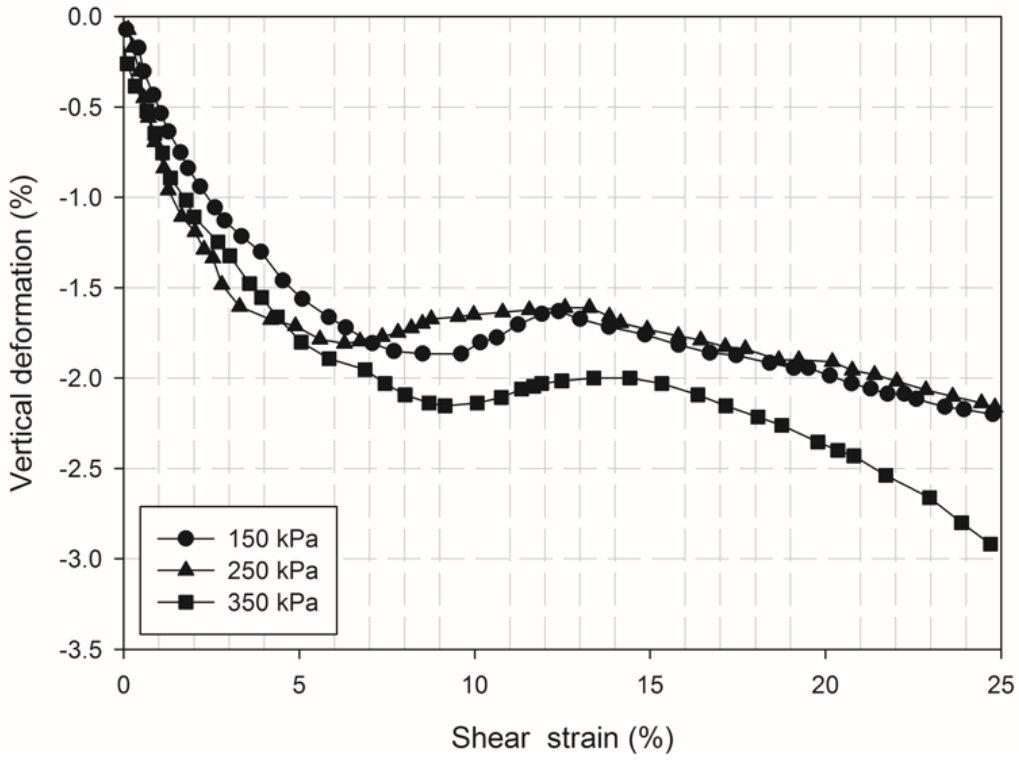

Figure 3.8 Vertical deformation versus horizontal deformation of BSM samples with no F-T cycle

3.5.2 Effect of F-T cycles on BSM/ geomembrane interface shear and BSM shear behaviors

Figures 3.9 to 3.11 show the results of the effect of F-T cycles on the shear stress versus shear strain of the BSM/geomembrane interface. Figures 3.9, 3.10 and 3.11 present the shear stress versus strain curves of the BSM /geomembrane interface subjected to various numbers of F-T cycles (0 to 10) and sheared at normal stresses of 150, 250 and 350 kPa, respectively. An analysis of Figures 3.5 and Figures 3.9 to 3.11 shows the F-T cycles have no significant impact on the shape of the stress-strain curves of the BSM/geomembrane interface. It can be observed that regardless of the number of F-T cycles, the stress-strain curves show a similar trend and shape. The stress–strain curves show no post-failure strain softening. The residual state is not achieved in any of these tests (residual shear condition could not be reached in these tests). However, Figures 3.9 to 3.11 depict that the F-T cycles significantly influence the interface shear strength. The interface shear strength decreases as the number of F-T cycles increase regardless of the normal stress applied. For example, for a normal stress of 150 kPa, the interface shear strength of the samples subjected to 0, 1, 2, 3, 5 and 10 F-T

cycles is 70, 66, 58, 57, 54 and 50 kPa, respectively. This F-T cycle induced reduction of the interface shear strength can be attributed to the weakening of the microstructure of the soil (BSM) by the pressure induced from the formation of ice lenses. The volume of the water in the pores increase with the growth of ice crystals, which result in the development of tensile stress in the soil (Dagesse, 2007). After thawing, the changes that have taken place in the voids will still partially remain. When the soil freezes again, the voids are further changed by the ice lenses. However, the most significant changes in the soil structure occur within the first few F-T cycles, and the effects decrease with increasing F-T cycles (Benoit and Voorhees, 1990; McConkey et al., 1990).

From Figures 3.9 to 3.11, it can be seen that the magnitude of the effect of the F-T cycles on the interface shear strength depends on the level of normal stress applied. These figures show that under different vertical stresses of 150, 250 and 350 kPa, the change in the shear strength of the BSM/geomembrane samples that did not undergo an F-T cycle compared to the samples subjected to 10 F-T cycles is 28.5%, 15.2% and 11.4%, respectively. From this result, it can be concluded that under higher vertical load restrictions, the difference in the stresses between the various samples is smaller. This is due to the fact that a higher vertical load makes the samples denser. Then, the deformation of the soil structure, which is caused by the F-T cycles, is reduced in the consolidation stages. The changes caused by the F-T phenomenon can be partially offset by the consolidation of higher normal stresses.

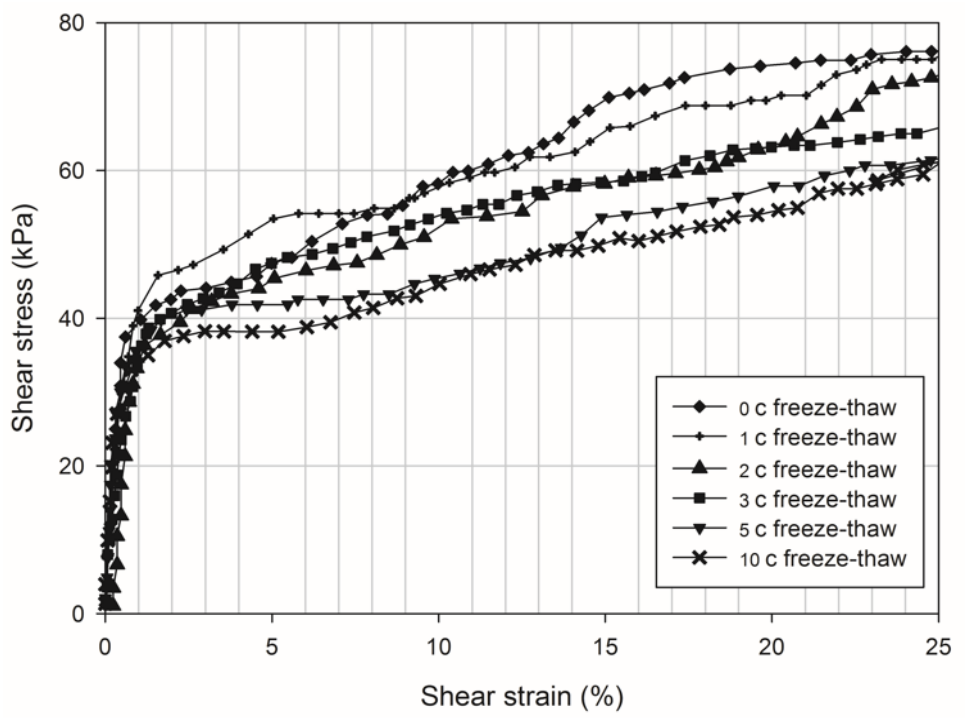

Figure 3.9 Shear stress versus strain curves of BSM/geomembrane interface under a normal stress of 150 kPa for various F-T cycles

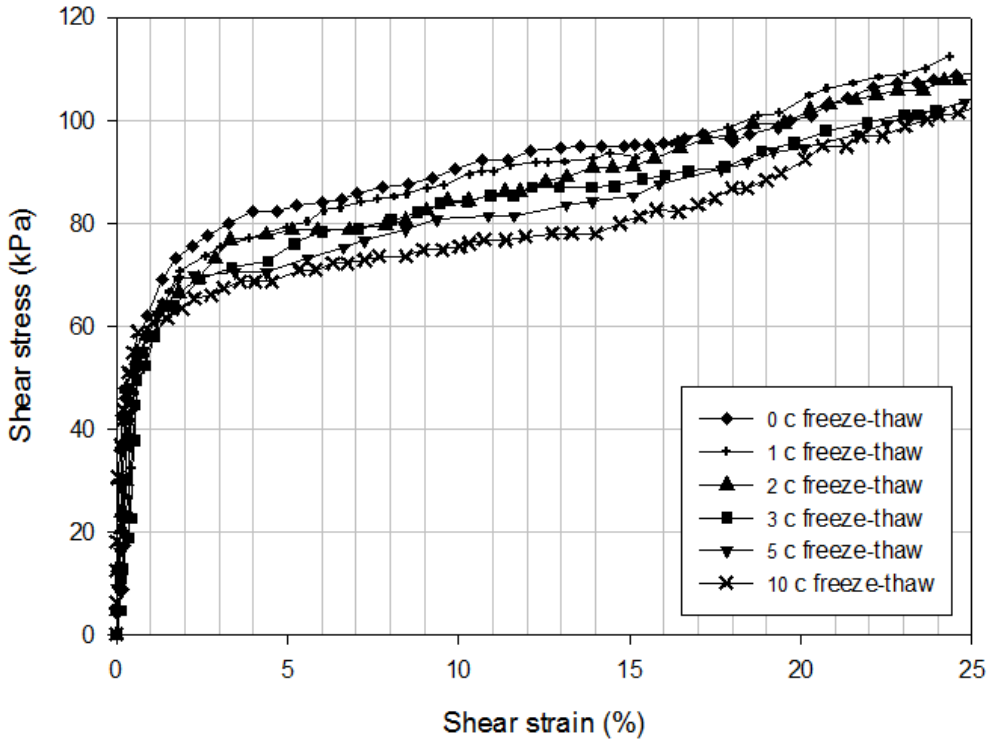

Figure 3.10 Shear stress versus stain curves of BSM/geomembrane interface under a normal stress of 250 kPa for various F-T cycles

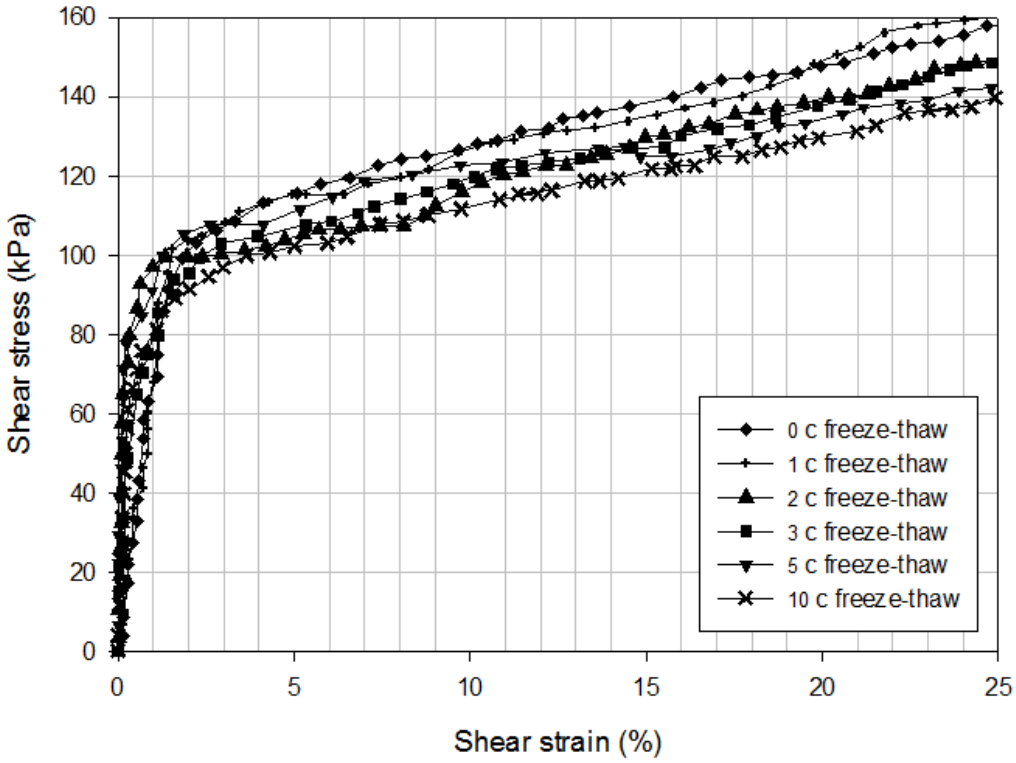

Figure 3.11 Shear stress versus stain curves of BSM/geomembrane interface under a normal stress of 350 kPa for various F-T cycles

The shear results of the BSM samples, which are influenced by the F-T cycles, are presented as a comparison. Figures 3.12, 3.13 and 3.14 present the shear stress-shear displacement curves of samples subjected to different numbers of F-T cycles and sheared at vertical loads of 150, 250 and 350 kPa, respectively. From the analysis of the curves in Figures 3.6 and Figures 3.12 to 3.14, it can be seen that the shape of the stress-strain curves of the BSM samples also have the same trend irrespective of the number of F-T cycles. Regardless of the applied normal stress, the highest stresses are all provided by samples that were not subjected to F-T cycles, and the shear strength starts to decrease when the samples were subjected to an increasing number of F-T cycles.

From Figures 3.12 to 3.14, it can be observed that the influence of the F-T cycles decreases with increasing vertical loads. These changes are similar to those observed in the results from the BSM/geomembrane interface. For instance, under a normal stress of 150 kPa, the shear strength of the samples subjected to 0, 1, 2, 3, 5 and 10 F-T cycles are 134, 131, 128, 125, 123 and 113 kPa, respectively. The total change in the shear strength of the

BSM samples from no F-T cycles to the samples that underwent 10 F-T cycles is 15.7%. When the samples were tested under 250 and 350 kPa, the total difference decreases to 7.3% and 7%, respectively.

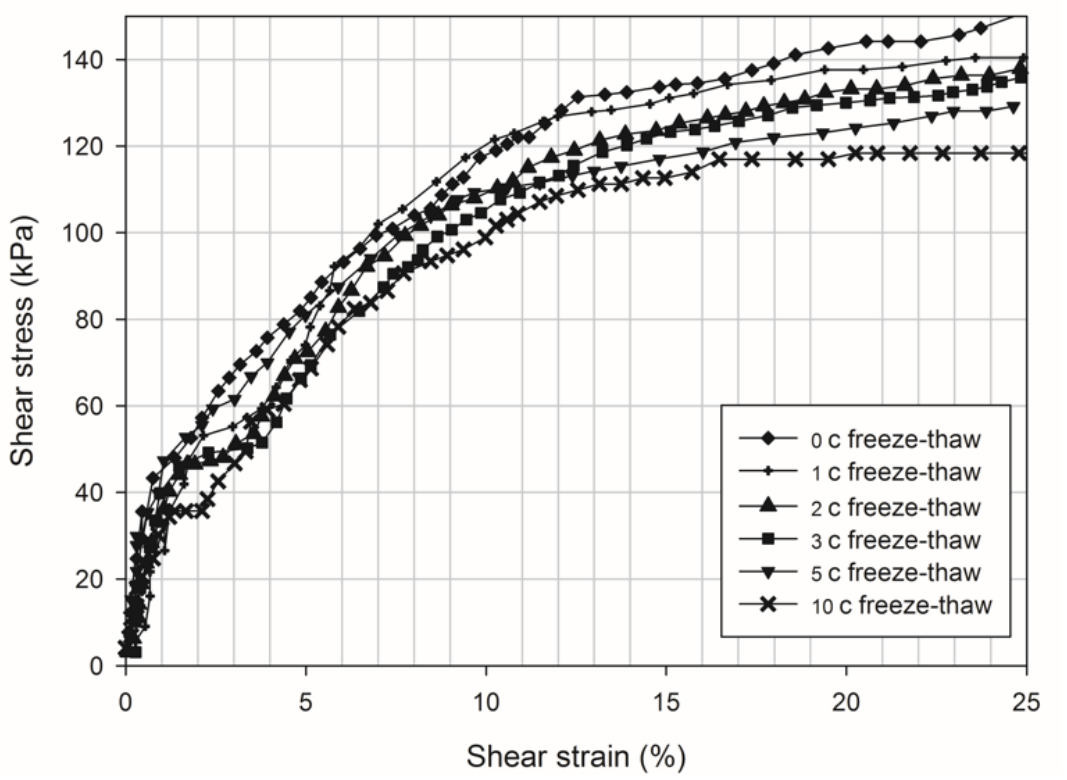

Figure 3.12 Shear stress versus strain curves of BSM samples under a normal stress of 150 kPa for various F-T cycles

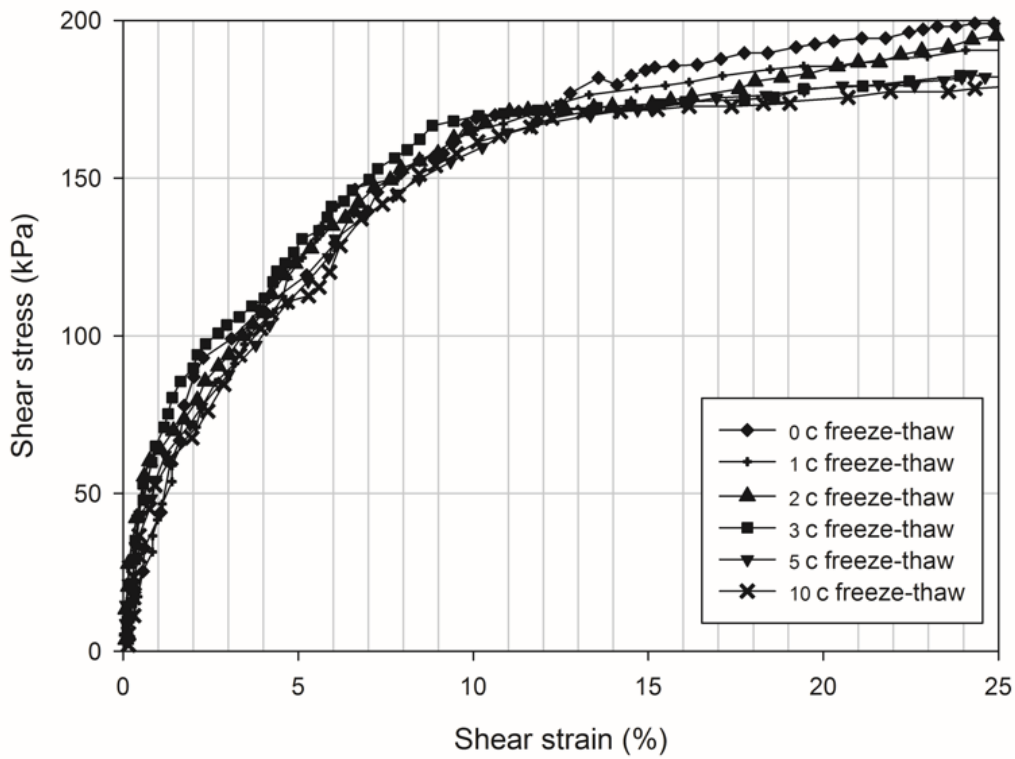

Figure 3.13 Shear stress versus strain curves of BSM samples under a normal stress of 250 kPa for various F-T cycles

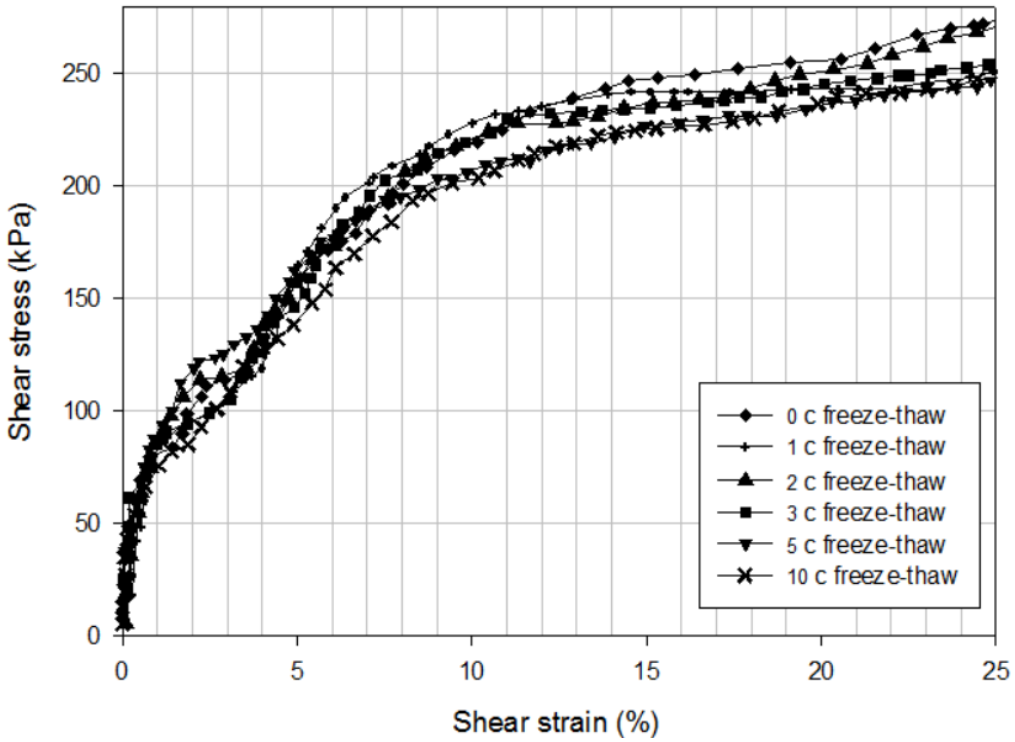

Figure 3.14 Shear stress versus strain curves of BSM samples under a normal stress of 350 kPa for various F-T cycles

3.5.3 Failure envelopes for BSM/geomembrane and BSM

Figures 3.15 and 3.16 illustrate the shear strength envelopes for the BSM/geomembrane interface (Figure 3.15) as well as the BSM shear (Figure 3.16) tests. The results of the BSM soil shear strength envelope are presented for comparison. These envelopes are the results of fitting regression lines through every set of data on the interface shear vs. normal stress. Since the shear tests were conducted under consolidation-drained condition, the cohesion is close to zero. For all of the regression lines, R^2 is approximately 0.9. A Mohr-Coulomb type equation is used to obtain the values of the interface friction angle for the range of normal stresses. From Figures 3.15 and 3.16, it can also be noticed that the F-T cycle significantly influences the internal friction angle for both the BSM-geomembrane interface and BSM samples. The friction angle decreases as the number of F-T cycles increase as illustrated in Figure 3.17. This figure is helpful for identifying the changes in shear resistance with thermal conditions for the two types of shear behaviors. The trends of the friction angle changes of the shear behavior of the BSM-geomembrane interface and BSM are similar. The maximum friction angle of BSM soil is 36.45°, and the friction angle is reduced with increasing F-T cycles, and decreases to 33.74° after the samples underwent 10 F-T cycles. When the BSM-geomembrane samples were not subjected to an F-T cycle, this resulted in the highest friction angle as well, which is 21.7°. After 10 F-T cycles, the value of the friction angles is reduced to 18.7°. These changes suggest that the effect of F-T cycles on the interface shear resistance cannot be ignored; F-T cycles should be considered in landfill design in cold regions. However, from Figure 3.17, it can be observed that after five cycles of freezing and thawing, the friction angle of the BSM- geomembrane interface is not significantly affected.

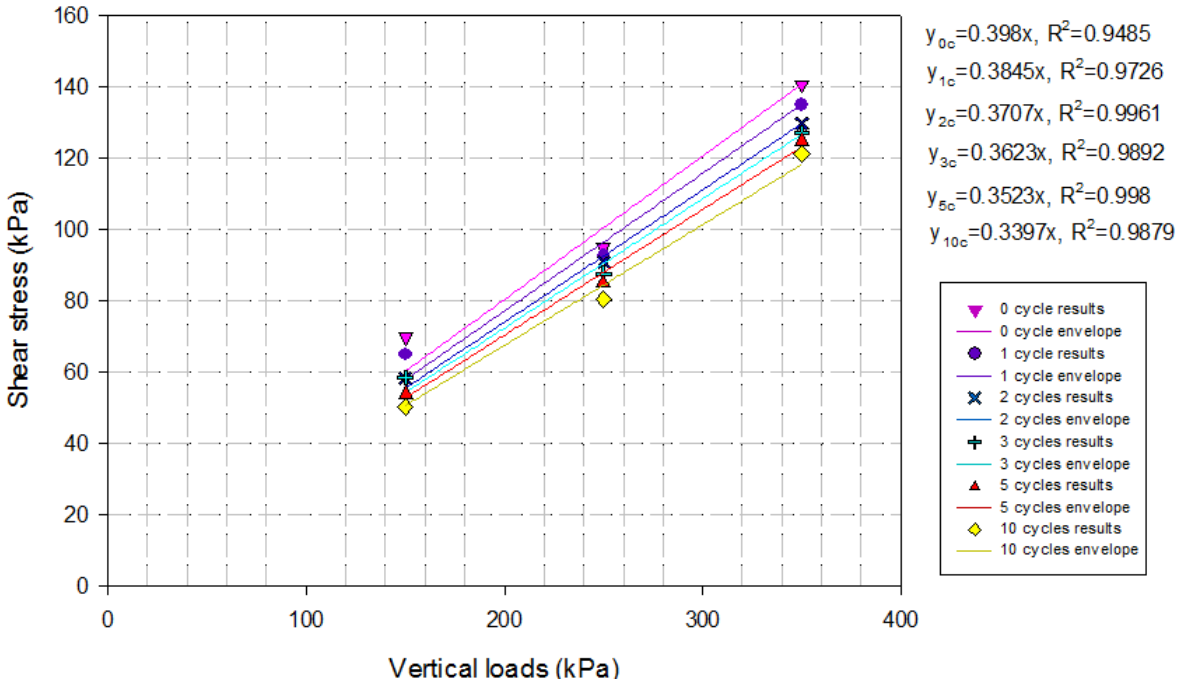

Figure 3.15 Shear envelopes of BSM-geomembrane interface vs. F-T cycles

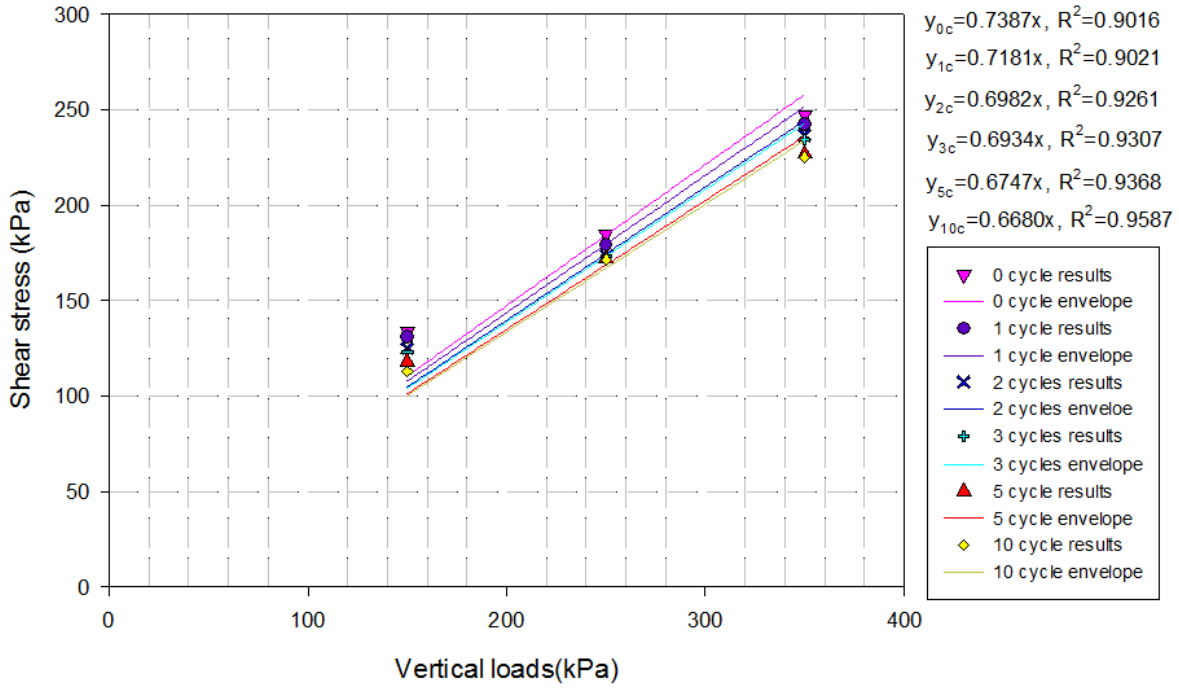

Figure 3.16 Shear envelopes of BSM vs. F-T cycles

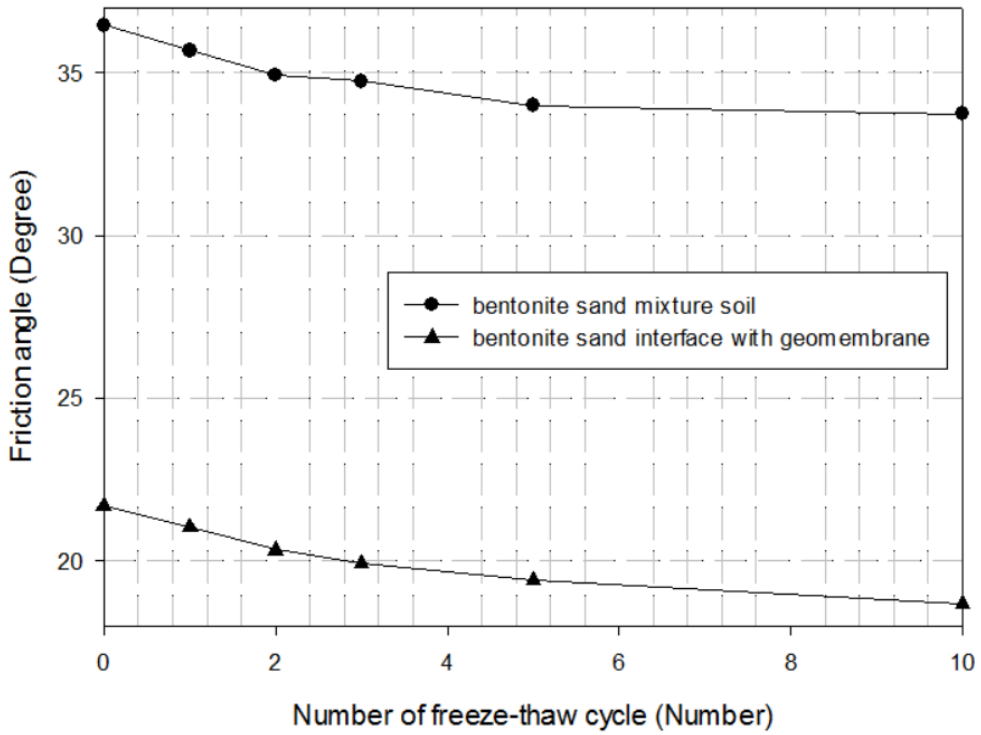

Figure 3.17 Effect of freeze-thaw cycles on the friction angle of BSM samples and BSM-geomembrane interface

3.6 Summary and conclusion

The objective of this study is to evaluate the interface shear behavior and strength of BSM-geomembrane samples subjected to F-T cycles. The shear behavior strength of the BSM samples that underwent F-T cycles is also evaluated for comparison purposes. Several results have been obtained. The shear strength of the BSM-geomembrane interface is much lower than that of the BSM samples for a given normal stress. The shear strength of the BSM/smooth HDPE interface that is not subjected to F-T cycles is 70, 95 and 138 kPa when the samples are tested under normal stresses of 150, 250 and 350 kPa, respectively. On the contrary, the BSM samples that are not subjected to F-T cycles show strength values of 134, 185 and 248kPa, under normal stresses of 150, 250 and 350 kPa, respectively. The shear failure envelope for the studied BSM-geomembrane interfaces obeys the Mohr–Coulomb failure criterion.

The shear behavior and resistance of the BSM-geomembrane and BSM are significantly affected by the F-T cycles, particularly the first 5 F-T cycles. The shear resistance and friction

angles of the BSM-geomembrane and BSM decrease as the number of F-T cycles increase. However, this reduction in shear resistance and decrease in friction angle are less obvious after 5 F-T cycles. This finding means that in cases where BSM-geomembrane liner systems are exposed to cycles of freezing and thawing, neglecting their effect on the shear resistance and the behavior of the liner systems will lead to a more unsafe design of the landfill liner.

3.7 References

Al-Douri, R. H., & Poulos, H. G. (1991). Static and cyclic direct shear tests on carbonate sands. Geotechnical Testing Journal, 15(2), 138-157.

Arifin, Y.F. (2008). Thermo-hydro-mechanical behavior of compacted bentonite-sand mixtures: An experimental study. Dissertation for doctor degree the Faculty of Civil Engineering, Bauhaus-University, Weimar. URL: http://e-pub.uni-weimar.de/opus4/files/852/Thermo_hydro_mechanical_behavior_of_compacted_bentonite_sand_mixture.pdf.

Benoit, G.R and Voorhees, W.B. (1990). Effect of freeze-thaw activity on water retention, hydraulic conductivity, density, and surface strength of two soils frozen at high water content. Proc. Intl. Symp. Frozen Soil Impacts on Agric., Range, and Forest Lands, Spokane, WA, Mar. 21-22, 1990. CRREL Spec. Rep. 90-1, 45-53.

Crawford, C. B. (1968). Quick clays of eastern Canada. Engineering Geology, 2(4), 239-265.

Cui, S. L., Zhang, H. Y. and Zhang, M. (2012). Swelling characteristics of compacted GMZ bentonite–sand mixtures as a buffer/backfill material in China. Engineering Geology, 141, 65–73

Dove, J. E., & Frost, J. D. (1996). A method for measuring geomembrane surface roughness. Geosynthetics International, 3(3), 369-392.

Dagesse, D. F. (2007). Effect of the Freeze/thaw Process on the Structural Stability of Soil Aggregates. ProQuest.

Fall, M., Célestin, J.C., Sen, H.F (2009). Suitability of bentonite-paste tailings mixtures as engineer barrier materials for mine waste containment facilities. Minerals Engineering 22

(9-10), 840-848

Fall, M., Nasir, O. (2010). Mechanical behavior of the interface between cemented tailings backfill and retaining structures under shear loads. Journal of Geotechnical and Geological Engineering 26(6), 779-790.

Government of Manitoba (2007).Technical reference document for liquid manure storage structures. Compacted Clay Liners. Accessed date, March, 7, 2015 at https://www.gov.mb.ca/conservation/envprograms/livestock/pdf/clay_liner_feb-2007.pdfGueddouda, M. K., Lamara, M., Aboubaker, N., & Taibi, S. (2008). Hydraulic conductivity and shear strength of dune sand-bentonite mixtures. Electronic Journal of Geotechnical Engineering, 13, 1-15.

Geosynthetic Lining Systems (2015). GSE HD Smooth Geomembrane. Retrieved 11 March, 2015, from:http://www.gseworld.com/content/documents/datasheets/membranes/North_America/HD_Smooth_Geomem_METRIC_DS.pdf

Jogi, M (2005). A method for measuring smooth geomembrane/soil interface shear behavior under unsaturated conditions. Thesis of Degree of Master's of Science, Department of Civil Engineering, University of Saskatchewan, Saskatoon, SK Canada. URI: http://hdl.handle.net/10388/etd-12122005-150824

Kjeldsen, P., Barlaz, M., Rooker, A., Baun, A., Ledin, A., & Christensen, T. (2010). Present and Long-Term Composition of MSW Landfill Leachate: A Review. Critical Reviews in Environmental Science and Technology, 297-336.

Koerner, R. M., Martin, J. P., & Koerner, G. R. (1986). Shear strength parameters between geomembranes and cohesive soils. Geotextiles and Geomembranes, 4(1), 21-30.

McConkey, B.G., Reimer, C.D and Nicholaichuk, W. (1990). Sealing earthen hydraulic structures with enhanced gleization and sodium carbonate. I. Laboratory study of the effect of a freeze-thaw cycle and a drying interval. Can. Agric. Eng. 32,163-170.

Miller, G. A., & Hamid, T. B. (2007). Interface direct shear testing of unsaturated soil. Geotechnical Testing Journal, 30(3), 182.

Murthy, V. N. S. (2002). Geotechnical engineering: principles and practices of soil mechanics

and foundation engineering. Chapter 8. CRC Press, United States.

Nasir, O., Fall, M. (2008). Shear behavior of cemented pastefill-rock interfaces. Engineering Geology 101(3-4): 146-143.

Othman M.A., Benson C.H. (1933).Effect of freeze–thaw on the hydraulic conductivity and morphology of compacted clay. Canadian Geotechnical Journal, 30 (2), 236–246

Simoni, A., & Houlsby, G. T. (2006). The direct shear strength and dilatancy of sand–gravel mixtures. Geotechnical & Geological Engineering, 24(3), 523-549.

Taha, A.M., (2010.). Interface shear behavior of sensitive marine clays-Leda clay. Thesis of M.A.Sc degree in Civil Engineering, University of Ottawa. ISBN: 978-0-494-73849-8

Taha, A., Fall, M., (2013). Shear behavior of the sensitive marine clay – concrete interface. ASCE Journal of Geotechnical and Engineering Geology, 139(4), 644-650.

Taha, A., Fall, M., (2014). Shear behavior of the sensitive marine clay – steel interface. Acta Geotechnica 9,969–980.

Tsubakihara, Y. & Kisheda, H. (1993). Frictional behavior between normally consolidated clay and steel by two direct shear type apparatus. Soils and Foundations, 33, 1-13.

Wikipedia (2015). Southern Ontario. Accessed January 15, 2015 from http://en.wikipedia.org/wiki/Southern_Ontario

Zabielska-Adamska, K. (2006). Shear strength parameters of compacted fly ash–HDPE geomembrane interfaces. Geotextiles and Geomembranes, 24(2), 91-102.

Zhou, Y. (1996) Shear strength of geomembrane-cohesionless soil interface system. Dissertation of Doctor of Philosophy. University of Pittsburgh, UMI Number: 9728704

Chapter 4 Technical Paper II: Shear Behavior of Marine Clay – Geomembrane Interface under Freeze-Thaw Cycles

Abstract

The influence of the number of freeze-thaw (F-T) cycles on the interface shear behavior of compacted Leda clay/ smooth high-density polyethylene (HDPE) geomembrane is investigated in this paper. Shear tests are performed on samples prior subjected to F-T cycles. All of the shear experiments are performed in a conventional direct shear box apparatus. Consolidated drained direct shear tests are conducted. The test results show that the interface shear strength of Leda clay/smooth HDPE geomembrane is lower than that of Leda clay. The interface shear strength of Leda clay/smooth HDPE geomembrane decreases with an increasing number of F-T cycles. Furthermore, the interface shear friction angles of the Leda clay/smooth HDPE geomembrane are significantly reduced within the first three F-T cycles.The reduction in shear strength beyond three F-T cycles is negligible. The total decrease in the shear strength of the samples that are not subjected to an F-T cycle compared to samples subjected to 10 F-T cycles is 18.3%, 17.6% and 13.6% under a vertical stress of 150, 250 and 350 kPa, respectively. There is no evidence of the penetration of the clay particles into the HDPE geomembrane surface. However, small sized gravel in the soil material can penetrate the geomembrane surface when they come into contact with the geomembrane.

4.1 Introduction

The waste disposal is a significant challenge since the quantity of solid waste has dramatically increased. During the past few decades, due to significant increase in population, landfills are widely used for the disposal of solid waste. Once a landfill is in operation, leachate and landfill gas are produced. Landfill leachate contains an abundance of toxic chemicals (Kjeldsen et al., 2010). The use of a reliable barrier is necessary to control the migration of contaminants. The combination of a compacted clay liner (CCL) and a geomembrane is a common option for composite liners of landfill facilities. In the design stage, the usage limit of a landfill has to be determined. In order to maximize the capacity of a landfill, steep side slopes are used; however, they contribute to a high risk of liner failure. There is also the possibility of sliding between the CCLs and geomembrane materials.

CCLs are a traditional barrier with low hydraulic conductivity. If the local clay is suitable for building CCLs, CCLs can have a hydraulic conductivity equal or less than 10^{-9} m/s after proper compaction (Zhou, 1996). In Canada, sensitive marine clays are widely distributed. For example, Leda clay is a common marine clay found in Ontario, and the major deposits of young glacial sedimentations. Leda clay has a high sensitivity. When the soil is disturbed, it can transform from a relatively brittle solid state to a liquid state (Crawford, 1968). The grains are so fine that water cannot escape from the pores quickly. The clay particles are arranged in an open orientation similar to a card house structure. The formation of this open clay structure is the result of the deposition of the material in salty water which has a large number of cations that carry a positive charge. The positive charge of these hydraulic cations leads to repulsive forces of the double layer absorbed water that push the platy particles apart, which results in an end-to-edge configuration. This end-to-edge configuration is stable in a salty environment. When the clay was uplifted from the bottom of the sea, the salinity of the pore water decreased due to the washing of the material by rainfall precipitation which changed the clay structure to a metastable state. A metastable structure is stable when it is not disturbed, similar to a card house. When the material is disturbed, collapse of the structure results in an increase in the pore water pressure since the water cannot escape from the pores quickly. This increase in pore pressure results in a decrease in effective stress, thus causing the material/Leda clay to liquefy. However, Leda clay and compacted Leda clay have low hydraulic conductivity, and water cannot easily escape from the pores. Therefore, they

are suitable for use in landfill barriers (liners or covers) because they meet the minimum hydraulic conductivity (10^{-9} m/s) required.

Geomembrane is one of the best materials for use as a hydraulic barrier. High-density polyethylene (HDPE) has high strength, stiffness, and good resistance to chemicals, ultraviolet rays and temperature, which makes HDPE an effective barrier material (Zabielska-Adamska, 2006) suitable to be made into geomembranes. The hydraulic conductivity of HDPE is also very low (from 10^{-11} to 10^{-13} cm/s) (Jogi, 2005).

In order to design composite liners, the interface shear behavior of HDPE and CCLs needs to be considered since it causes the risk of sliding failures. During landfill operations, the interface shear behavior can be influenced by many factors. Wastes are placed into landfill sites in specific sequences, and a landfill final cover is gradually built along with these sequences. As a result, parts of the slope liner can be exposed to freeze-thaw (F-T) cycles if the landfill is located in a cold region. Thus, temperature change is an important factor which cannot be neglected. In Canada, there is a difference of approximately 50℃ between the summer and the winter (Wikipedia, 2015). The drastic temperature difference particularly during spring season, can form F-T cycles. In short period of time, these F-T cycles can affect the interface shear behavior of the liner and thus jeopardize the safety of landfills.

Previous studies have been conducted on the influence of F-T cycles on soil materials ((Stark, 2011); Swan et al. (2013) and Fishman & Pal (1994)). However, there have been no investigations on the interface shear behavior of compacted Leda clay/HDPE material, and the influence of F-T cycles on its interface. Thus, in order to understand the behavior and interface resistance of composite liners in cold regions, particularly in Canada, a series of experiments have been conducted to study the effects of various numbers of F-T cycles on the interface shear behavior and strength of Leda clay/smooth HDPE. The objective of this paper is to present and discuss the obtained results.

4.2 Materials and experimental program

4.2.1 Leda clay

During the construction of landfills, the natural clay liner will normally be compacted. In Ontario and Quebec, Leda clay is usually utilized as the natural clay in liners. In this study,

Leda clay material is sampled from a construction site which is located on Bank Street in downtown Ottawa. During the sampling and storage stages, the soil was disturbed and the Leda clay experienced some degree of moisture loss. The Leda clay underwent compaction and treated in different ways in the lab; the clay was dried and grounded. In terms of the Leda clay that was grounded, the gravels which could not pass through a No.4 sieve were removed. The Atterberg limits of the remolded Leda clay were tested. The Leda clay passing the No.4 sieve had a plastic limit (PL) and liquid limit (LL) of 20.08% and 66.5%, respectively. The particle size analysis of the Leda clay was conducted in accordance with ASTM D422, using sieves and hydrometer methods. The particle size distribution curve of the remolded Leda clay is shown in Figure 4.1.

Figure 4.1 shows that there is an 82% fraction by weight of the Leda clay particles that are finer than 2 μm. The specific gravity was tested following ASTM standard D845, and it was found that the specific gravityof Leda clay is 2.78, which is within the acceptable range between 2.7 and 2.8 (Leroueil, 1999). A standard compaction method (ASTM D698) was used to obtain the optimum water content and maximum dry density of the compacted Leda clay. The compacted Leda clay should have a hydraulic conductivity of 1 $x10^{-9}$ m/s or even less (8.4 $x10^{-10}$ m/s) when properly compacted. The characteristics of the Leda clay used in this study is summarized in Table 4.1.

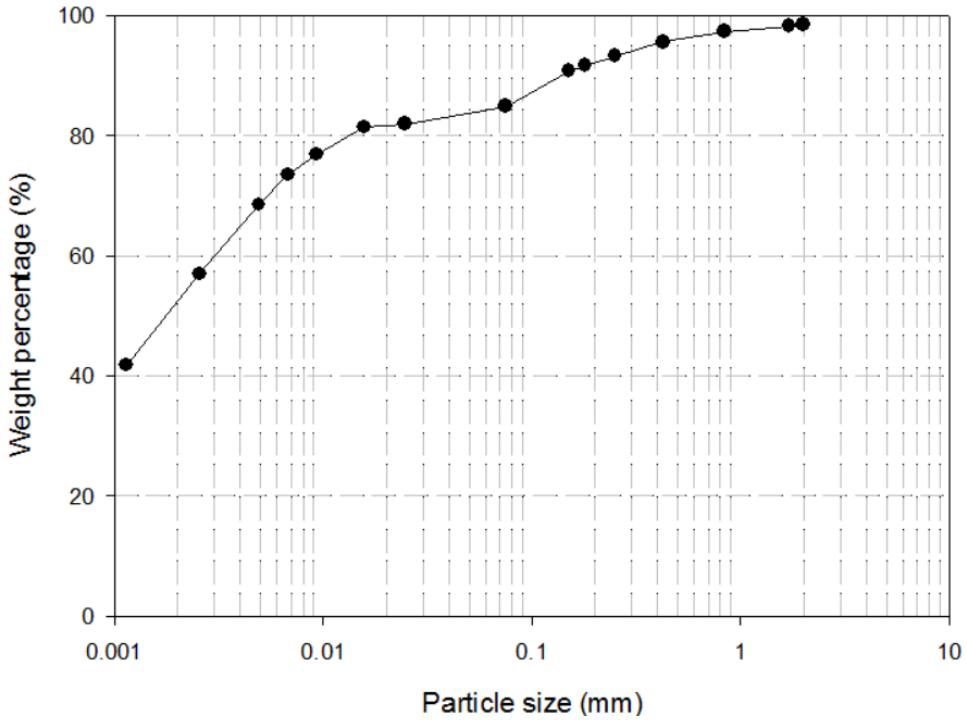

Figure 4.1 Particle size distribution of Leda clay

Table 4.1 Summary of the main characteristics of the remolded Leda clay

Property	**Value/classification**
Classification	CH (inorganic clay of high plasticity)
Liquid limit	66.5%
Plastic limit	22.1%
Plastic index	44.4%
Clay fraction	82%
Optimum water content	22.9%
Maximum dry density	1.647g/cm^3

4.2.2 Geomembrane

In this study, smooth HDPE (GSE Lining Technology, Houston, USA) with a thickness of 60 mil (1.5 mm) is used. The roughness of this product is 1.09, which has been tested by Dove

& Frost (1996). All of the other properties are obtained from the GSE website (Table 4.2).

Table 4.2 HDPE geomembrane properties which can be obtained from the GSE lining technology website (Geosynthetic Lining Systems, 2015).

Property of geomembrane	**Minimum average value**
Thickness, mm	1.5
Density, g/cm^3	9.940
Strength at break, N/mm	40
Strength at yield, N/mm	22
Elongation at break. %	700
Elongation at yield. %	12
Tear resistance, N	187
Puncture resistance, N	480

4.3 Specimen preparation

Leda clay clods were placed into an oven and dried at 35℃ for two weeks. A grounding machine was used to crush the clods into powder. In order to simulate the real situations of landfills, and in accordance with ASTM standard D698, oversized gravels were removed with the use of a No.4 sieve, and the smaller gravels were kept. Distilled water was added into the dry clay and they were mixed well. The mixed Leda clay had a water content of 2% - 4% wetter than optimum. Then, the mixed Leda clay was sealed in a bag for curing at room temperature for 24 hrs. The equilibration water content of the samples was 25.5%- 25.9%. The variations among the different batches may be attributed to manual errors. Following ASTM standard D698, the Proctor compaction method was used to carry out dynamic compaction in a cylinder, which uses a mould that is 100mm in diameter. Then, the compacted Leda clay were cut into two different sizes. The dimensions of the soil used for as direct shear samples (testing of only Leda clay) were 60 × 60 × 25 mm, and the Leda clay/smooth HDPE interface sample, 60 ×60×12 mm.

Theoretically, during the freezing of an exposed side liner, the volume of the landfill

CCL layer is subjected to changes when the water content turns into ice lens. However, such change is partially restricted by the surrounding clay and the weight of the upper liner material, including the geomembrane and leachate collection layer. Thus, the samples of Leda clay were directly wrapped with plastic film. The geomembrane pieces were then prepared for interface shearing. They were cut into pieces of 60 x 60 mm with smooth edges, and the smooth side was placed in contact with the Leda clay (60 × 60 × 12 mm cubes). Lastly, the interface samples were wrapped with plastic film. All of the wrapped samples were stored in zip lock bags and placed in plastic boxes to further minimize moisture loss.

Both the Leda clay and the interface shear samples were subjected to 0, 1, 2, 3, 5 and 10 F-T cycles. For the F-T process, the samples were placed in the freezer at a temperature of -30℃. When the freezing process was completed, they were placed at room temperature (20℃) to thaw circularly. In order to measure the required time of each F-T cycle, the temperature gradients were tested. A thermal sensor and a data acquisition system were used to test the core temperature changes of the samples with respect to time. The curves of the freezing and thawing temperature changes of the Leda clay versus the respective time are presented in Figure 4.2. Leda clay needs 5 hours to reach basic thermal stability. In order to reduce the potential influence of sample variability, all of the samples underwent cycles of 12-hours of freezing and 12-hours of thawing.

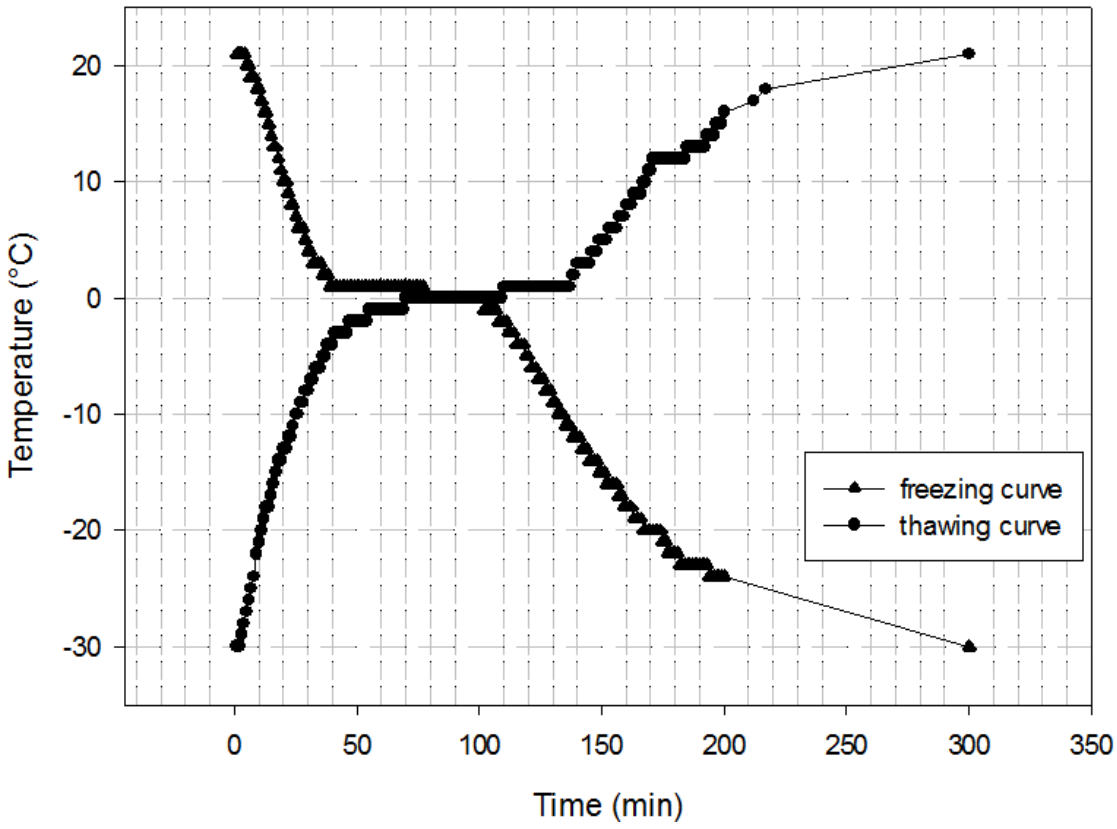

Figure 4.2 Curves of freezing and thawing temperature changes of the Leda clay versus time

4.4 Testing Technique

4.4.1 Testing apparatus

In the past decade, the direct shear stress apparatus has been one of the most commonly used apparatuses to test shear behavior. It is also a simple and practical means to carry out interface shear research (Miller & Hamid, 2007; Taha and Fall 2013, 2014). Thus, in this study, a standard direct shear testing machine is used (by following ASTM standard D5321), and the schematic diagram of this machine was provided in Figure 2.10 in Chapter 2. This apparatus has a square shear box. Normal stresses (N) are applied onto samples by adding weights to the weight hanger (Taha, 2010). This machine has a controlled drive system at a predetermined rate of shearing. Then, a shearing force is applied to the lower box, while the upper box only provides horizontal support, which is connected to a load cell to measure the shear stress changes. The horizontal and vertical displacements of the samples are measured by linear variable differential transformers (LVDTs) (Murthy, 2002).

4.4.2 Testing procedures and plans

The Leda clay and Leda clay/smooth HDPE interface shear samples were tested through consolidated-drained (CD) direct shear tests (DSTs). The samples were sheared at a low shearing rate, which allowed the pore water pressure to dissipate. A shearing speed of 0.03 mm/min was chosen in previous studies (Tognon et al., 1999; Tsubakihara & Kisheda, 1993. Here, the shear speed is set as 0.025 mm/min with respect to the results of the consolidation tests performed in this study. The samples were placed in the shear box and tightly screwed. For the interface sample, the smooth face of the HDPE was in contact with the clay material and the other side of the HDPE had to be glued onto a supporting steel cube beforehand. Then, the sample was placed into the shear box. It was necessary to ensure that the interface of the Leda clay/ smooth HDPE was exposed in the gap between the upper and lower shear boxes, and this was done so with the help of the steel cube which gave the sample more height. In all of the tests, filter paper was placed between two pervious metal plates and the sample, which can prevent soil loss during the consolidation stage.

Once the sample was loaded in the shear box, the shear box along with the sample were placed into a sink for saturation purposes. The Leda clay in the shear box required 1 day to reach full saturation. Then, the shear box was placed in the direct shear testing machine which has a moveable sink, and the sink was filled with distilled water. The sample underwent consolidation before shearing. The normal stresses chosen were 150, 250 and 350 kPa. Each normal stress of consolidation was completed with 3 or 4 load increments. Each increment was sustained for 1 hour to ensure that the primary consolidation was completed. After the consolidation stage, the lower box in the sink started to move at 0.025 mm/min.

4.5 Results and discussion

The DST results of the compacted Leda clay /smooth HDPE interface and Leda clay samples are presented in this section. All of the results are presented and discussed with four graphs, including those that show the shear stress-shear strain curves, shear strain-vertical deformation curves, shear strength envelopes and friction angles with respect to the number of F-T cycles.

4.5.1 Shear behavior of samples with no F-T cycle

Figures 4.3 to 4.6 illustrate the interface shear behavior of the Leda clay/smooth HDPE samples and shear behavior of the Leda clay samples, which were not subjected to F-T cycles. Figure 4.3 shows a typical shear stress versus strain relationship for the Leda clay/smooth HDPE with no F-T cycle, while Figure 4.4 presents that of the Leda clay samples as a comparison. From these two figures, it can be observed that the two shear behaviors demonstrate distinct trends and shapes with respect to the shear stress-strain curves. The Leda clay/smooth HDPE interface samples show a distinct peak shear stress. The peak shear stress is reached at a 5% horizontal displacement. This can be explained by the fact that the majority of Leda clay particles are smaller than 2 μm and cannot penetrate the geomembrane surface. Once the shear stress overcomes the shear resistance, the shear stress also decreases in correspondence to the reduction in shear resistance.

As a comparison, the Leda clay samples have no peak stress, and the residual shear stress cannot be reached due to the limitations of the direct shear apparatus. Thus, a shear stress at 15% of the shear strain is considered to be the peak shear strength (ASTM standard D5321). Figures 4.3 and 4.4 show that the interface shear strengths are lower than those of soil, and the shear stress versus strain curves do not fit. This suggests that the shearing took place at the interface plane, but not in the compacted Leda clay. It can also be seen from these two figures that the peak shear stress increases with an increase in the normal stress, regardless of the shear behavior. For instance, the peak shear stress for the remolded Leda clay / smooth HDPE is determined to be 46, 61 and 91 at a normal stress of 150, 250 and 350 kPa, respectively, while the clay samples can obtain a shear strength of 56, 87 and 107 kPa a normal stress of 150, 250 and 350 kPa, respectively. This is due to the fact that increasing normal stresses on the plane of the shear failure can lead to an increasing contact area between the clay particles and geomembrane. As a result, a higher peak shear stress is needed to overcome the increased frictional resistance (Fall and Nasir 2010, Nasir and Fall, 2008). The normal stress increased 67% and 191% when the normal stress is increased from 150 to 250 and 350 kPa, respectively. The corresponding interface shear strength of the Leda clay/smooth HDPE interface is increased 32% and 97% when the samples are sheared under a normal stress of 250 and 350 kPa respectively.

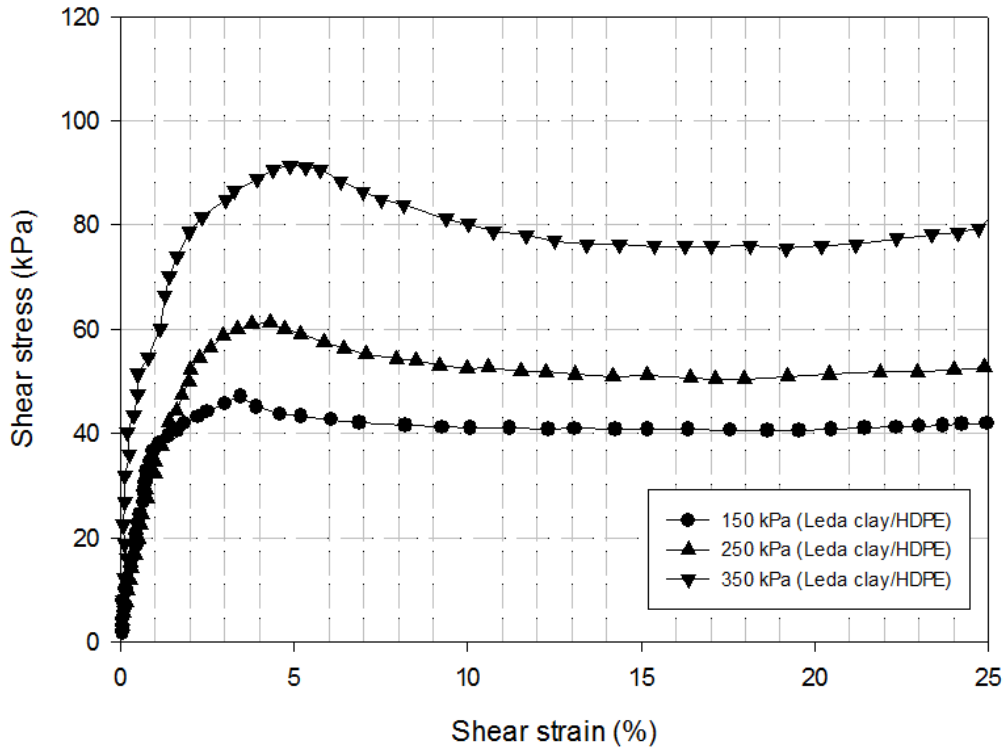

Figure 4.3 Interface shear stress versus strain curve of Leda clay/HDPE (no F-T cycle)

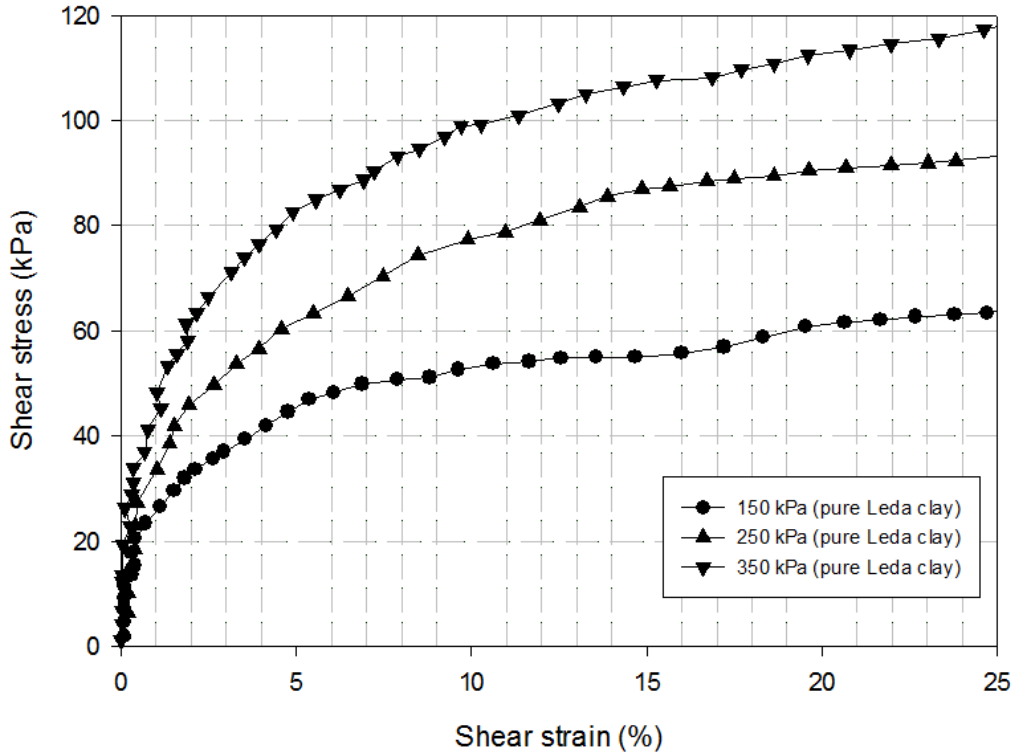

Figure 4.4 Shear stress versus strain curve of Leda clay (no F-T cycle)

Figures 4-5 and 4-6 illustrate that the vertical deformations of the Leda clay/HDPE interface and Leda clay samples are characterized by contraction behavior. No dilation is observed in the studied deformation range. The contraction rate gradually decreases with shear displacement. This phenomenon is the result of the normal stress and shear load at the beginning of shearing. The samples are therefore more firmly in contact at the shear plane (Fall and Nasir 2010).

Vertical deformation increases with increases in the normal stress, regardless of the type of shear behavior. From Figures 4.5 and 4.6, it can be observed that the interface shear behavior has a higher vertical deformation rate (%). This can be explained by the fact that during the interface shearing, there are some clay residuals on the geomembrane. The vertical deformation of the clay sample in upper half shear box is influenced by the reduced clay mass. However, if the vertical deformation is determined by using a unit of mm, the magnitude of the deformation is minimal. This is because the changes are only limited by 0.1 mm.

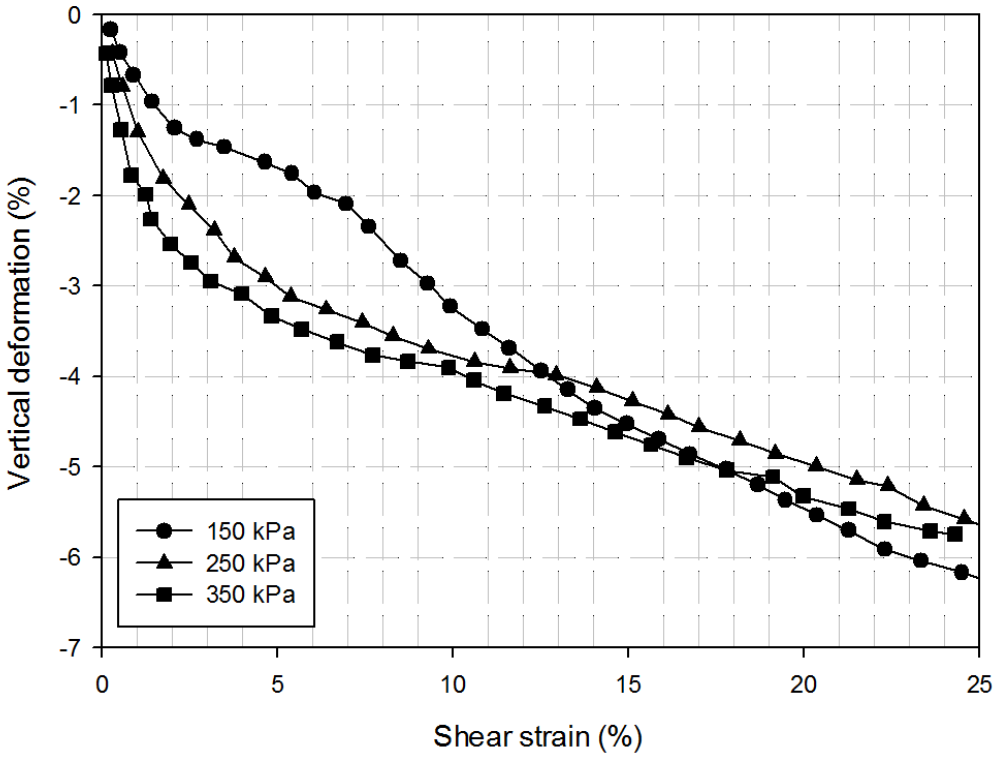

Figure 4.5 Vertical deformation versus shear strain of Leda clay/HDPE interface with no F-T cycle

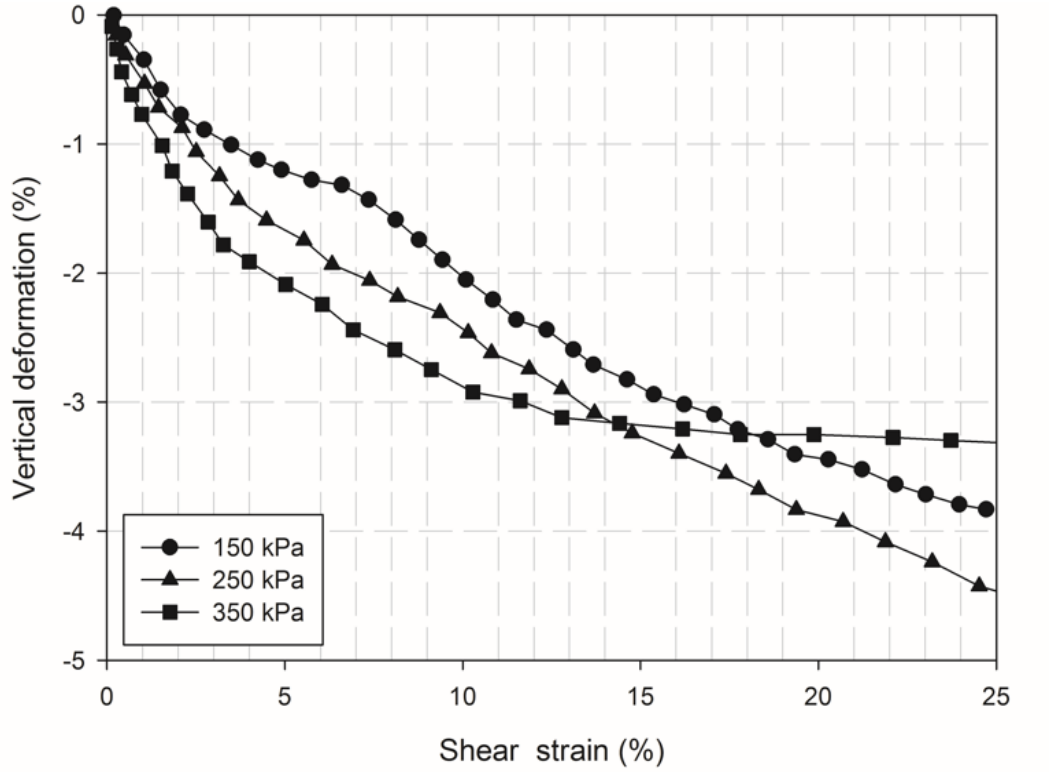

Figure 4.6 Vertical deformation versus shear strain of Leda clay with no F-T cycle

4.5.2 Effect of freeze-thaw cycles on interface shear behavior of Leda clay/HDPE and shear behavior of Leda clay

Figure 4.7 to 4.9 depict the shear stress versus shear strain results of remolded Leda clay/smooth HDPE interface samples. In these graphs, the Leda clay/smooth HDPE interface samples were subjected to 0 to 10 F-T cycles and sheared at normal stresses of 150 kPa, 250 and 350 kPa, respectively. Analysis of Figures 4.3, and Figures 4.7 to 4.9 shows that the F-T cycles have no obvious influence on the shape and the trend of the shear stress versus shear strain curves for the interface shear behavior. Under different normal stresses, all the interface shear curves can reach the peak shear stress. After the peak stress is reached, the curve of interface shear samples turns to the post-failure strain softening stage, and then reaches the residual stress when the horizontal displacement is approximately 25%.

From Figure 4-7 to 4-9, it can be observed that the peak shear stress and shear displacement that correspond to the peak shear stress both increase with increasing normal stress. The higher normal stress resulted in samples that are more firmly in contact with the geomembrane and lead to higher shear resistance.

The influence from the F-T cycles can be observed in Figures 4.7 to 4.9 as well. Regardless of the normal stress applied, the interface shear strength decreases as the number of F-T cycles increases. For instance, when the normal stress is 150 kPa, the interface shear strengths of the samples subjected to 0, 1, 2, 3, 5 and 10 F-T cycles are 46, 43, 41, 38, 38 and 37 kPa, respectively. The F-T cycles give rise to a reduction in the interface shear strength. This phenomenon is caused by the ice lenses, which induces the weakening of the microstructure or pore structure of clay. When freezing takes place, the pore water turns into ice and the volume of water is increased (Dagesse, 2007). The changes in the soil microstructure can be partially maintained after thawing. When the sample is placed in the freezer again, the voids can be further changed by the ice lenses. From the shear results, the most obvious shear strength changes occur in the first three F-T cycles, and afterwards, the effects are negligible. Some previous researchers (i.e. Benoit and Voorhees, 1990; McConkey et al., 1990) found similar results; the most significant changes in the soil structure occur within the first few F-T cycles, and then the changes are not so significant as the number of F-T cycles increase.

From Figure 4.7 to 4.9, it can be also observed that the magnitude of the influence of the F-T cycles on the interface shear strength depends on the level of normal stress. These figures show that when the samples are sheared under vertical stresses of 150, 250 and 350 kPa, the total influence from the F-T cycles is decreased. The difference in the shear strength between samples that were not subjected to F-T cycles compared to the samples subjected to 10 F-T cycles is 18.3%, 17.6% and 13.6%, respectively. These results indicate that a high normal stress can offset the influence of F-T cycles, due to the fact that the vertical stress causes the samples to become denser, and thus reduces the deformation caused by the F-T cycles during consolidation and shearing.

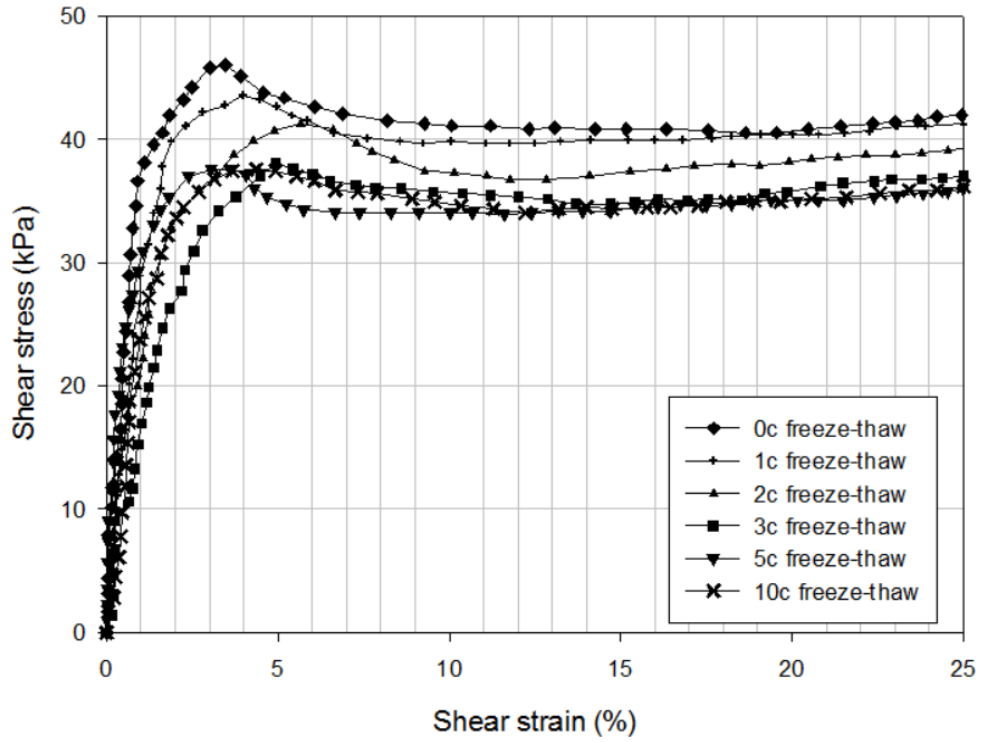

Figure 4.7 Leda clay/HDPE interface shear stress versus strain under normal stress of 150 kPa

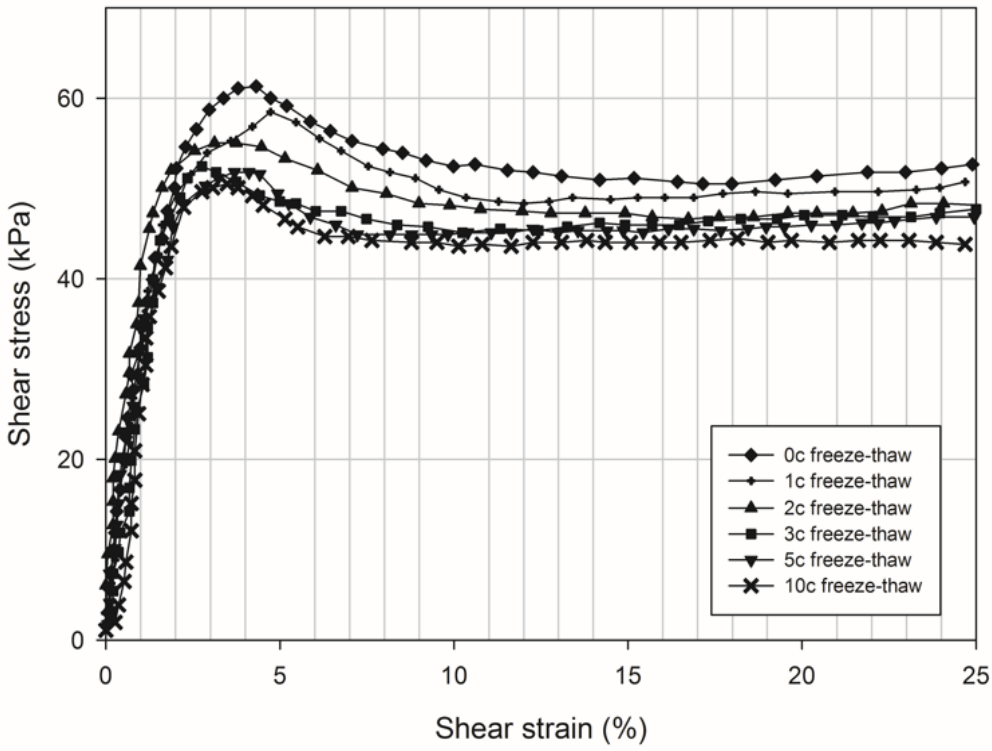

Figure 4.8 Leda clay/HDPE interface shear stress versus strain under normal stress of 250 kPa

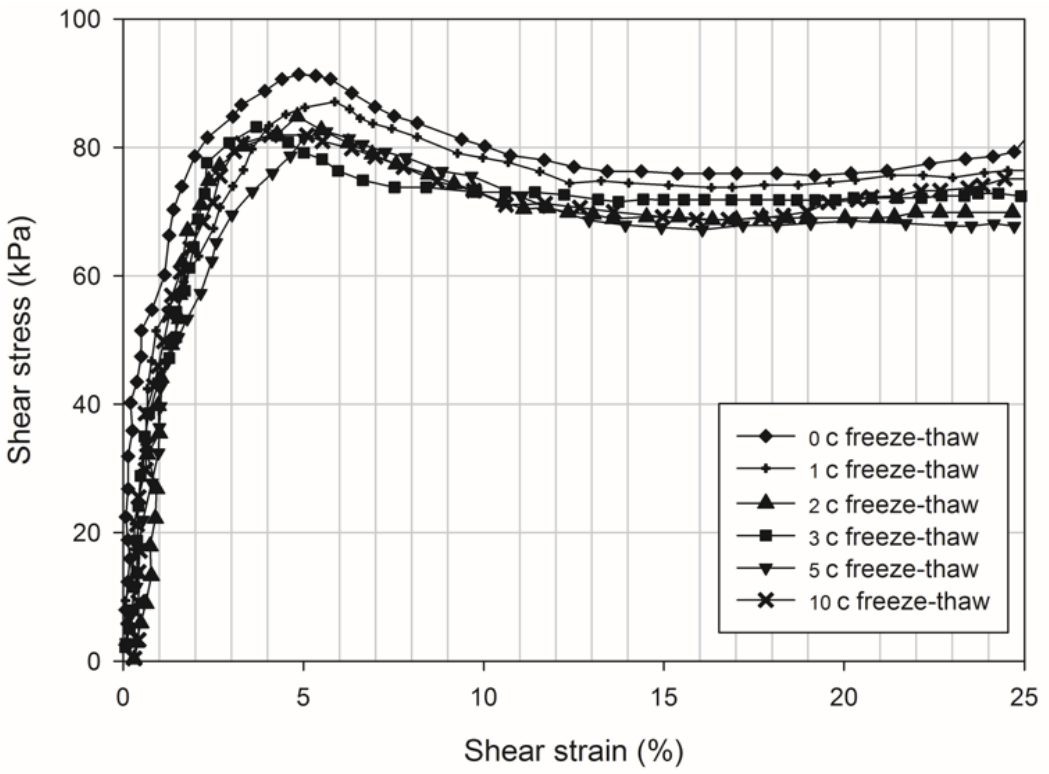

Figure 4.9 Leda clay/HDPE interface shear stress versus strain under normal stress of 350 kPa

As a comparison, Figures 4.10 to 4.12 present the shear results of the Leda clay. Analysis of Figures 4.4 and Figures 4.10 to 4.12 shows that the F-T cycles do not influence the trend and shape of the shear stress versus strain curves, irrespective of the applied normal stress. The interface shear results have curves that do not fit with those of the clay samples. However, the F-T cycles can reduce the shear strength in all of the samples. Regardless of the applied normal stress, the highest stresses are all provided by samples that did not undergo an F-T cycle, while the samples that underwent 10 F-T cycles provide the lowest shear strength.

In Figures 4.10 to 4.12, it can be seen that the magnitude of the influence of the F-T cycles decreases with increasing vertical stress. The total change in the shear strength of Leda clay samples that did not undergo an F-T cycle compared to the samples that underwent 10 F-T cycles is 21%, 20.9% and 15%, subjected to vertical stresses of 150, 250 and 350 kPa, respectively. These results are similar to the interface shear behavior. All of the shear results show that there is a more obvious influence for the first three F-T cycles, and this result can be further confirmed by the changes in the friction angles.

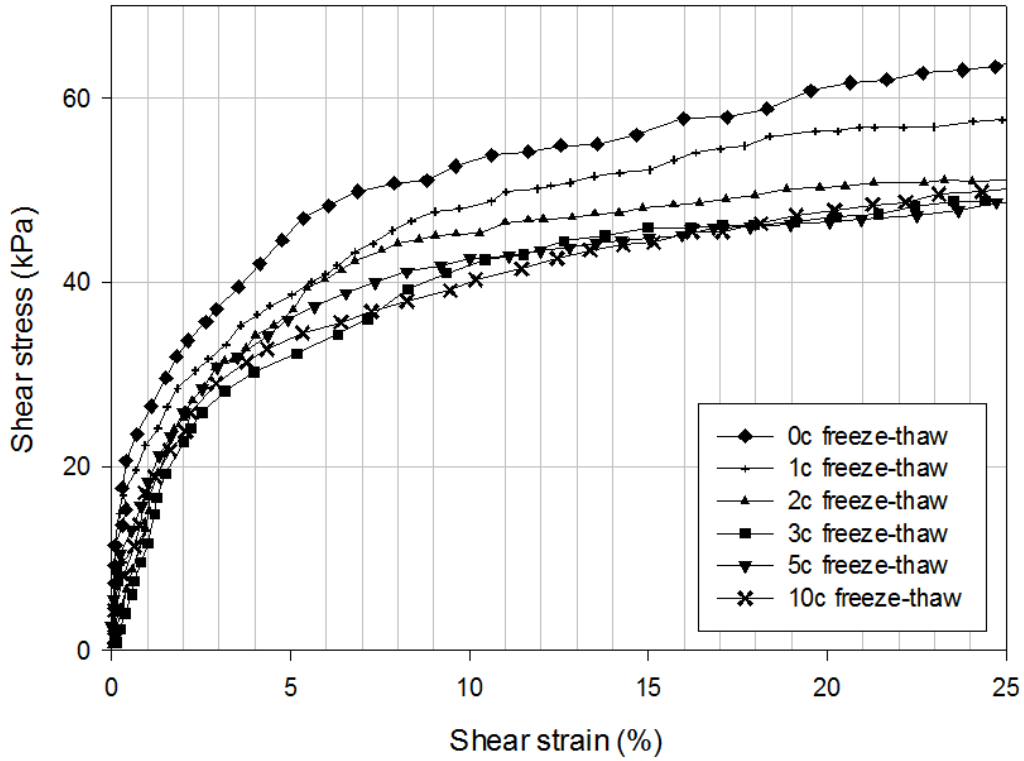

Figure 4.10 Shear stress versus strain of Leda clay under normal stress of 150 kPa

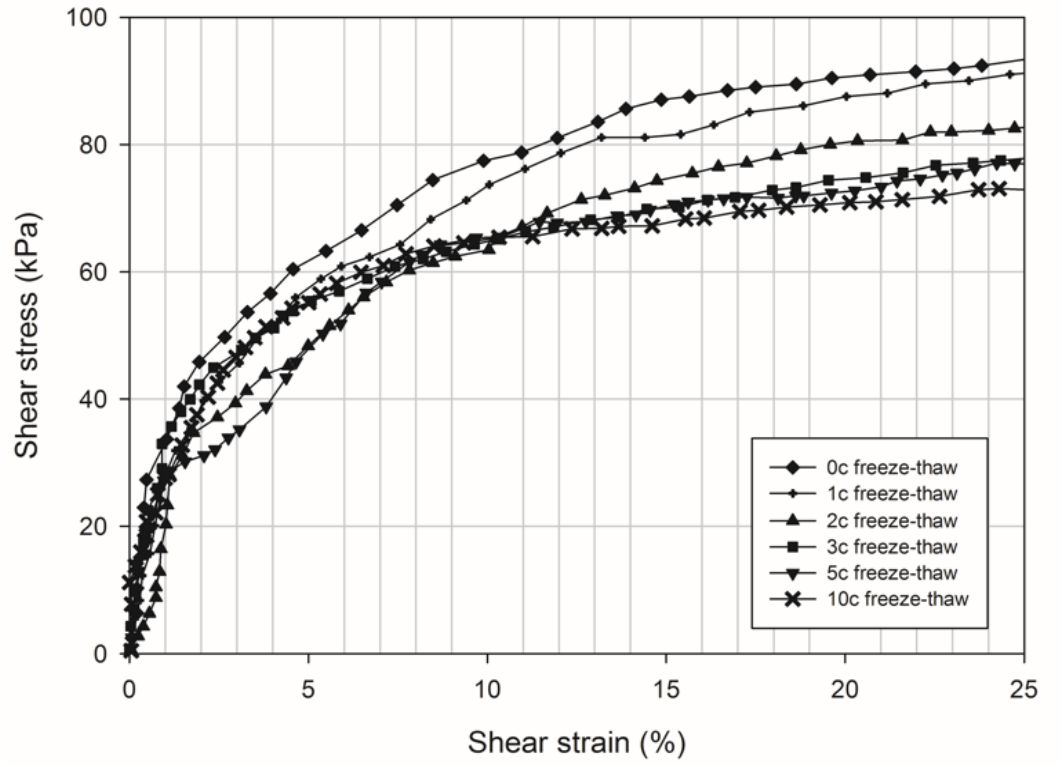

Figure 4.11 Shear stress versus strain of Leda clay under normal stress of 250 kPa

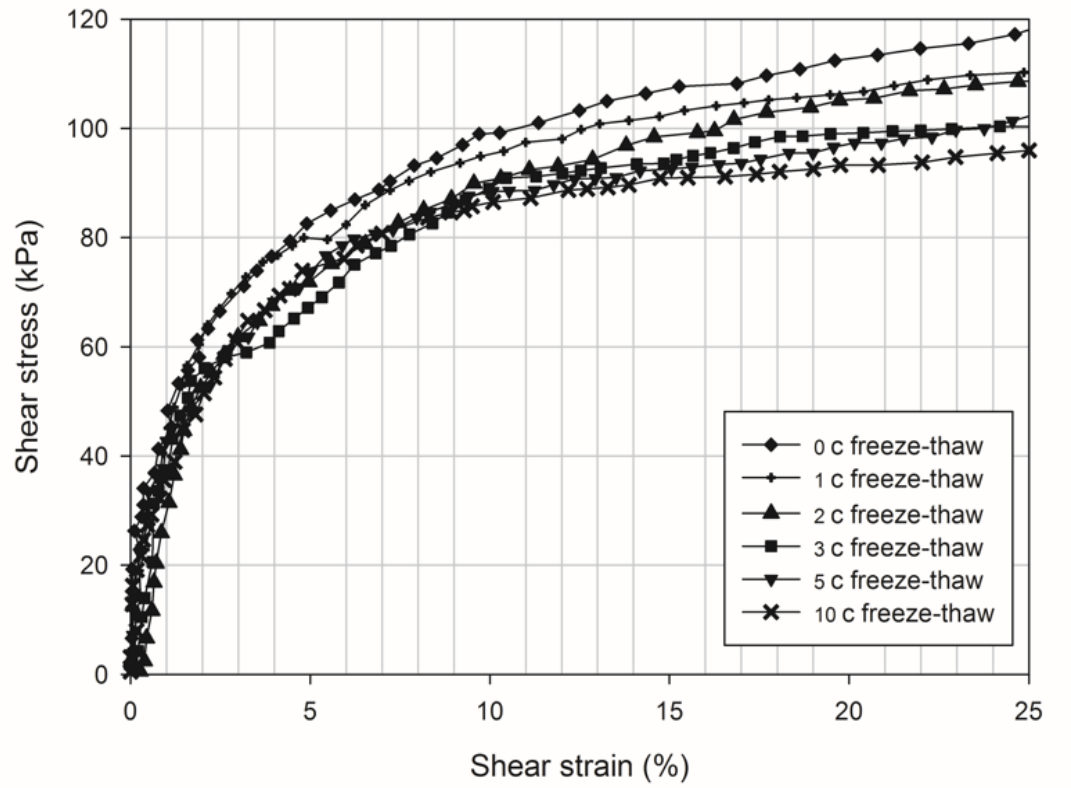

Figure 4.12 Shear stress versus strain of Leda clay under normal stress of 350 kPa

4.5.3 **Envelopes and friction angles of Leda clay / smooth HDPE and Leda clay samples**

Figures 4.13 and 4.14 present the shear strength envelopes for the Leda clay/HDPE interface (Figure 4.13) and the Leda clay shear (Figure 4.14) tests. All of the envelopes are the result of fitting regression lines through every data set of interface shear strength vs. normal stress. A Mohr-Coulomb equation was used to obtain the values of the interface friction angle for the range of normal stress. All the saturated Leda clay interface and pure soil samples were sheared by consolidation drained method. For all of the regression lines, the R^2 value is higher than 0.9. From Figures 4.13 and 4.14, it can be noticed that the slope of the envelope is significantly influenced by the F-T cycles.

The relationship between the friction angles versus the number of F-T cycles is illustrated in Figure 4.15. It can be seen that the friction angle decreases as the number of F-T cycles increase for both the interface shear and soil shear behaviors. The trends of the friction angle changes are very similar. The friction angles of the clay are larger than those of the interface shear behavior, thus this result confirms that the interface shear behavior

between Leda clay and geomembrane governs the failure of the CCL and geomembrane composite liner. The maximum friction angle of the clay samples is 18° with no F-T cycle, and the friction angle is reduced to 15.4° after 3 F-T cycles, and then, the changes are minimal. After 10 F-T cycles, the friction angle is 15°, and the total reduction is 3°. The interface shear strengths of the samples that did not undergo F-T have the highest friction angle, which is 14.6°. After 3 F-T cycles, the friction angle is 13°. The total change in the friction angle is 1.9°. Therefore, the changes caused by F-T cycles should be considered during the designing period if the landfill is to be located in a cold region. The first 3 F-T cycles have the most influence on the friction angles irrespective of the type of shear behavior.

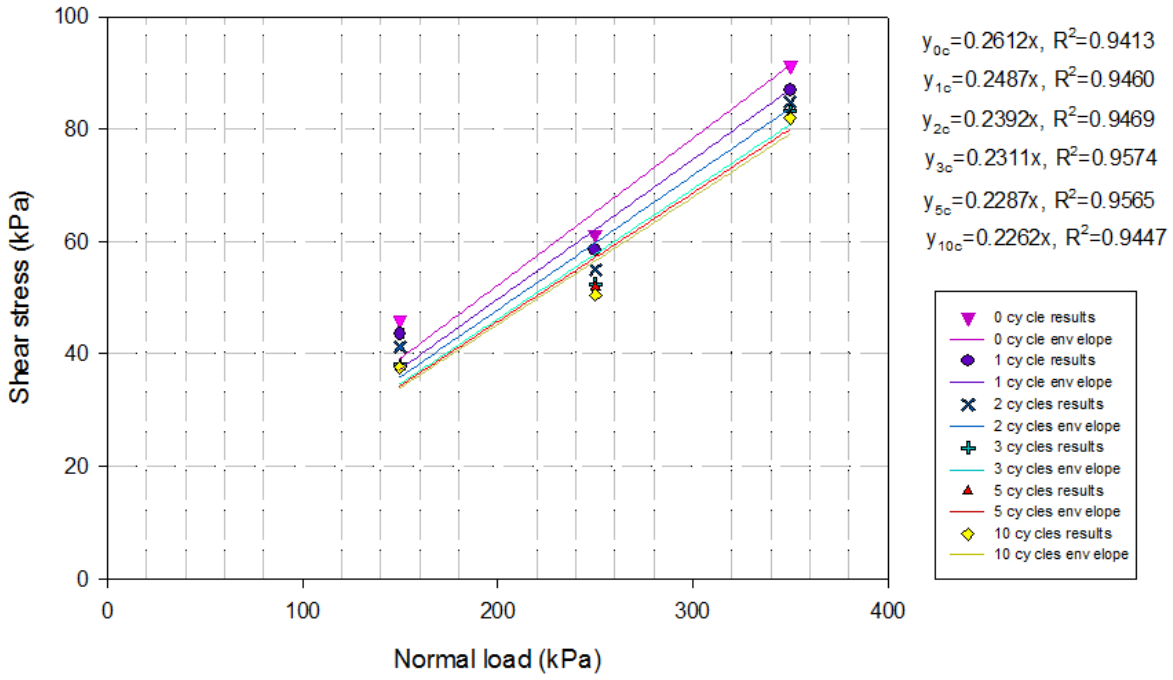

Figure 4.13 CD envelopes of Leda clay / HDPE samples that change with number of F-T cycles

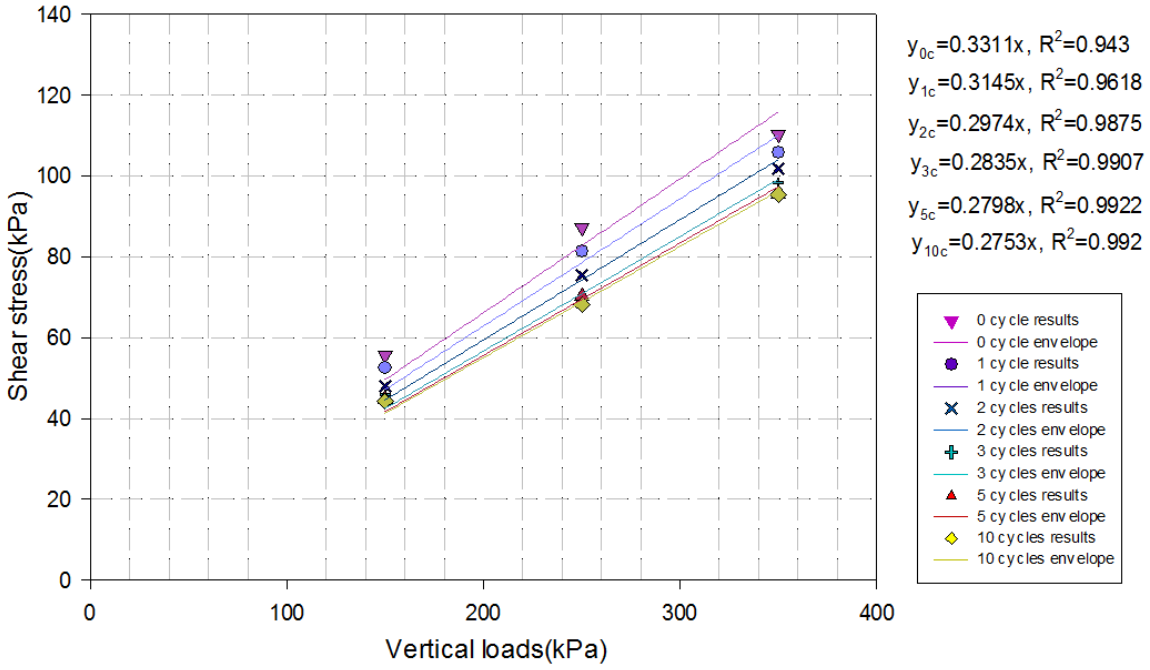

Figure 4.14 CD envelopes of remolded Leda clay samples with F-T cycles

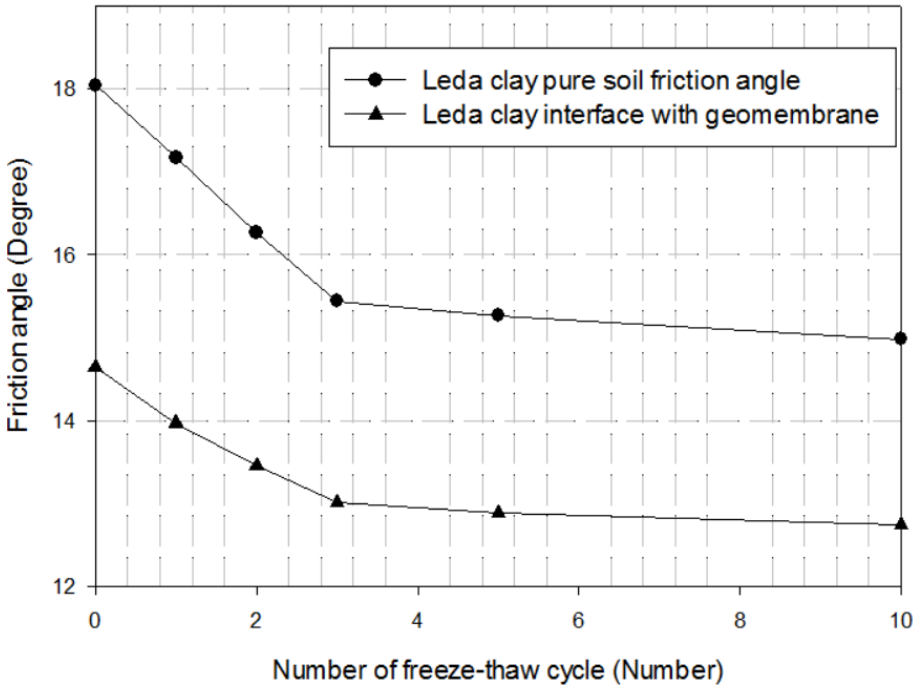

Figure 4.15 Friction angle changes with number of F-T cycles for shear behavior of Leda clay/HDPE interface and Leda clay samples

4.6 Summary and Conclusion

The objective of this research is to evaluate the interface shear behavior and shear strength of remolded Leda clay/ smooth HDPE samples that are subjected to different numbers of F-T cycles. The test apparatus is a direct shear testing machine. The shear behavior of Leda clay is used for comparison. The interface shear behavior has a higher sliding risk than shearing in soil materials. The highest shear strength can always be found with samples that are not subjected to F-T cycles and the shear strength decreases as the number of the F-T cycles increases. The maximum shear strength of the Leda clay/smooth HDPE interface is 46, 61 and 91 kPa when tested under a vertical load of 150, 250 and 350 kPa, respectively with no F-T. Meanwhile, the Leda clay samples that did not undergo an F-T cycle have a shear strength of 56, 87 and 107 kPa, which are measured under vertical loads of 150, 250 and 350 kPa, respectively.

When the shear behaviors of the two different materials are compared, the friction angles demonstrate a similar trend of change. The interface shear strengths have relatively low friction angles, and the sliding failure risk at the interface is higher than that in the CCL. When 10 F-T cycles have taken place, the total reduction in the friction angles is 3° and 1.9° for the Leda clay and Leda clay/geomembrane samples respectively.

Only some of the gravel which is located at the interface shear plane penetrates the geomembrane surface. The interface shear mechanism of Leda clay is dominated by adhesion and sliding. For the remolded Leda clay/geomembrane interface, the maximum change in friction angle can be obtained with the first 3 F-T cycles. Then, it becomes difficult to determine the thermal influences between the fifth and tenth F-T cycles regardless of the different shear behaviors.

4.7 References:

Andersson-Sköld, Y., Torrance, J. K., Lind, B., Odén, K., Stevens, R. L., & Rankka, K. (2005). Quick clay: A case study of chemical perspective in Southwest Sweden. Engineering Geology, 82(2), 107-118.

Arifin, Y.F. (2008). Thermo-hydro-mechanical behavior of compacted bentonite-sand mixtures: An experimental study. Dissertation for doctor degree the Faculty of Civil Engineering, Bauhaus-University, Weimar. URL: http://e-pub.uni-weimar.de/opus4/files/852/Thermo_hydro_mechanical_behavior_of_compacted_bentonite_sand_mixture.pdf.

Benoit, G.R and Voorhees, W.B. (1990). Effect of freeze-thaw activity on water retention, hydraulic conductivity, density, and surface strength of two soils frozen at high water content. Proc. Intl. Symp. Frozen Soil Impacts on Agric., Range, and Forest Lands, Spokane, WA, Mar. 21-22, 1990. CRREL Spec. Rep. 90-1, 45-53.

Crawford, C. B. (1968). Quick clays of eastern Canada. Engineering Geology, 2(4), 239-265.

Cui, S. L., Zhang, H. Y. and Zhang, M. (2012). Swelling characteristics of compacted GMZ bentonite–sand mixtures as a buffer/backfill material in China. Engineering Geology, 141, 65–73

Dove, J. E., & Frost, J. D. (1996). A method for measuring geomembrane surface roughness. Geosynthetics International, 3(3), 369-392.

Dagesse, D. F. (2007). Effect of the Freeze/thaw Process on the Structural Stability of Soil Aggregates. ProQuest.

Fall, M., Nasir, O. (2010). Mechanical behavior of the interface between cemented tailings backfill and retaining structures under shear loads. Journal of Geotechnical and Geological Engineering 26(6), 779-790.

Fishman, K. L., & Pal, S. (1994). Further study of geomembrane/cohesive soil interface shear behavior. Geotextiles and Geomembranes, 13(9), 571-590.Gourc, J. P., & Ramirez, R. R. (2004). Dynamics-based interpretation of the interface friction test at the inclined plane. Geosynthetics International, 11(6), 439-454

Geosynthetic Lining Systems (2015). GSE HD Smooth Geomembrane. Retrieved 11 March, 2015, from:http://www.gseworld.com/content/documents/datasheets/membranes/North_America/HD_Smooth_Geomem_METRIC_DS.pdf

Jogi, M. (2005). A method for measuring smooth geomembrane/soil interface shear behavior

under unsaturated conditions. Thesis of Degree of Master's of Science, Department of Civil Engineering, University of Saskatchewan, Saskatoon, SK Canada. URI: http://hdl.handle.net/10388/etd-12122005-150824

Kjeldsen, P., Barlaz, M., Rooker, A., Baun, A., Ledin, A., & Christensen, T. (2010). Present and Long-Term Composition of MSW Landfill Leachate: A Review. Critical Reviews in Environmental Science and Technology, 297-336.

Leroueil S. (1999). Geotechnical characteristics of eastern Canada clays. In Proceedings, of the International Symposium on The Characterization of soft Marine Clays; 1997 Feb. 26-28; Yokosuka, Japan. Rotterdam: A.ABalkema, 3-32.

Miller, G. A., & Hamid, T. B. (2007). Interface direct shear testing of unsaturated soil. Geotechnical Testing Journal, 30(3), 182.

Murthy, V. N. S. (2002). Geotechnical engineering: principles and practices of soil mechanics and foundation engineering. Chapter 8. CRC Press, United States.

McConkey, B.G., Reimer, C.D and Nicholaichuk, W. (1990). Sealing earthen hydraulic structures with enhanced gleization and sodium carbonate. I. Laboratory study of the effect of a freeze-thaw cycle and a drying interval. Can. Agric. Eng. 32,163-170.

Nasir, O., & Fall, M. (2008). Shear behavior of cemented pastefill-rock interfaces. Engineering Geology, 101(3), 146-153.

Stark, T. D., Niazi, F. S., & Keuscher, T. C. (2011). Comparison of single and multi geosynthetic and soil interface tests. Retrieved April, 13, 2015, from: http://tstark.net/wp-content/uploads/2012/10/JP87.pdf.

Swan Jr, R. H., Bonaparte, R., Bachus, R. C., Rivette, C. A., & Spikula, D. R. (2013). Effect of soil compaction conditions on geomembrane-soil interface strength. Landfill Closures: Geosynthetics, Interface Friction and New Developments, 10, 141-147.

Taha, A.M. (2010). Interface shear behavior of sensitive marine clays-Leda clay. Thesis of M.A.Sc degree in Civil Engineering, University of Ottawa

Taha, A., Fall, M., (2013). Shear behavior of the sensitive marine clay – concrete interface. ASCE Journal of Geotechnical and Engineering Geology 139(4), 644-650.

Taha, A., Fall, M., (2014). Shear behavior of the sensitive marine clay – steel interface. Acta Geotechnica 9, 969–980.

Tognon, A. R., Rowe, R. K., & Brachman, R. W. (1999). Evaluation of side wall friction for a buried pipe testing facility. Geotextiles and Geomembranes, 17(4), 193-212.

Tsubakihara Y., & Kisheda H. (1993). Frictional behavior between normally consolidated clay and steel by two direct shear type apparatus. Soils and Foundations, 33, 1-13.

Wikipedia (2015). Southern Ontario. Accessed January 15, 2015 from http://en.wikipedia.org/wiki/Southern_Ontario

Zabielska-Adamska, K. (2006). Shear strength parameters of compacted fly ash–HDPE geomembrane interfaces. Geotextiles and Geomembranes, 24(2), 91-102.

Zhou, Y. (1996) Shear strength of geomembrane-cohesionless soil interface system. Dissertation of Doctor of Philosophy. University of Pittsburgh, UMI Number: 9728704

Chapter 5 Technical Paper III: Non-isothermal effect of leachate on the interface shear behavior of compacted clay liner and geomembrane

Abstract

Bentonite, a highly expansive clay, which is usually mixed with sand to form barriers with high stiffness and low hydraulic conductivity in waste facilities with compacted clay liner. In considering the high concentrations of cations in leachate and the thermal variation inside landfills, it is considered necessary to study the non-isothermal effect of leachate on the interface shear behavior in composite liners. The main objective of this paper is therefore to investigate the interface shear behavior between a bentonite sand mixture (BSM) and a smooth high-density polyethylene (HDPE) geomembrane, which is impacted by the combined effect of high concentrations of potassium / calcium ions and varying temperatures. All of the shear tests are conducted with a direct shear testing apparatus. The results indicate that the interface shear behavior of BSM/smooth HDPE is affected by both thermal and chemical factors. The distilled water samples that are cured at room temperature always present the highest shear strength regardless of the shear behavior. However, the combined-effect of temperature and salinity on the interface shear behavior is limited compared with the impact from temperature or chemistry alone. X-ray diffraction (XRD) is used to investigate the mineral variations caused by the cations in non-isothermal conditions. Approximately, 60% of the sodium smectite components in the BSM samples are converted into illite with the presence of potassium chloride and different temperatures. On the other hand, the majority of the sodium smectite components of the BSM samples that are saturated with a calcium chloride solution and dried in an oven at temperatures of 20^{o}C to 50^{o}C are converted into calcium-rich montmorillonite instead. The XRD results of the samples that are saturated with distilled water and cured at various temperatures show that the mineral components remain the same on drying in an oven, and the hydration state of bentonite is somewhat affected.

5.1 Introduction

Landfills are widely used as the primary solution for solid waste disposal. Municipal solid waste (MSW) landfills are designed by following specific standards to minimize the amount of pollution that affects the environment. During landfill operations, degraded waste, leachate, landfill gas and heat are generated through various physical, chemical, and microbial processes. A thin layer soil or spray on slurries or foams that are not impervious are commonly used as the daily covers of solid waste. However, rainfall can infiltrate through daily covers and carry pollutants from waste material to water with a series of reactions (Kjeldsen et al., 2010). The final liquid resultant of these reactions which contain an abundance of organic and inorganic materials and heavy metals is called leachate (Taylor & Allen, 2006).

Composite liners are used to minimize the pollution from leachates. The combination of a compacted clay liner (CCL) and geomembrane is popular (Jogi, 2005). Bentonite sand mixtures (BSMs) are commonly used in CCLs, since they have good self-healing capacity and extremely low hydraulic conductivity, typically lower than 10^{-9} m/s. The properties of the sand in BSMs are stable. However, the bentonite properties can be affected by the cations in the leachate. Leachate components vary with respect to time that the landfill has been in operation and the territory itself, in spite of the main elements are similar. According to previous studies, the salinity elements and their average and range of cation concentration are summarized in Table 5.1.

Table 5.1 Leachate concentration of common cation elements in acidic and methanogenic stages of waste degradation (Kruse, 1994). (Values in mg/L)

	Parameter	Acid phase (mg/L)		Methanogenic phase(mg/L)	
		Average	Range	Average	Range
Cation	Sodium	1150	1-6800	1150	1-6800
	Potassium	880	170-1750	880	170-1750
	Magnesium	285	30-600	150	25-300
	Calcium	650	80-2300	200	50-1100

Chemical reactions are an essential problem for BSMs since bentonite particles have high electrochemical activity. This can change the bentonite properties and even the clay type. Theoretically, high concentrations of calcium cations that are available in leachate is contribute to exchange the sodium cations with calcium cations within bentonite. The electrovalence of sodium and calcium cations are different (Arifin, 2008). When the clay particles adsorb highly charged cations, fewer cations can be found in the dissipative layer, and therefore the dissipative layer and the hydration membrane of the clay surface will become thinner. Thus, the clay particles can be easily consolidated (Ye et al., 2009). A diagram of the exchange of sodium and calcium ions is shown as Figure 5.1. This phenomenon will diminish the sealing capacity of bentonite if large amounts of Na-montmorillonite turn into Ca-montmorillonite. The exchange reaction can continue for a long period of time until an adsorption balance is reached between the ion distribution in the bentonite material and the ion concentration of the leachate (Egloffstein, 2001).

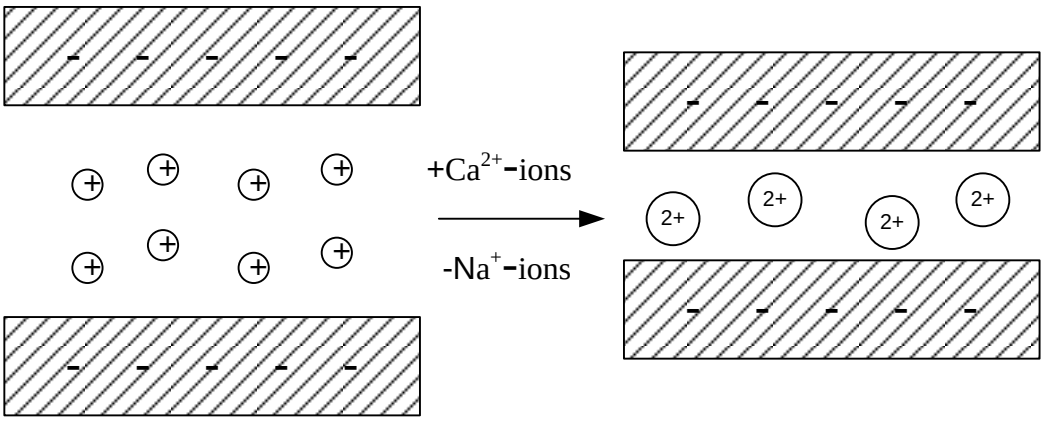

Figure 5.1 Exchange between sodium and calcium cations (Egloffstein, 2001).

Montmorillonite-to-illite transformation is another essential cation exchange phenomenon. It is a frequent alteration process found in nature (Karnland & Birgersson, 2006). Potassium ions can convert bentonite into illite or a smectite/ illite mixture. When the negative charges of clay are balanced by potassium cations, the size of the potassium ions just fits into the molecular openings formed by the base of the silica tetrahedral of bentonite, which creates strong bonds between the layers (Figure 5.2) (Mitchell, 1993). Moreover,

potassium ions have less hydration capacity compared to sodium ions. Thus, when sodium ions exchange with potassium ions, the repulsive forces are reduced and it is difficult for potassium ion-saturated clay to expand (Liu & Neretnieks 2006). This phenomenon is called illitization. The illitization rate will theoretically be higher when temperature is increased with a constant potassium concentration (Karnland & Birgersson, 2006).

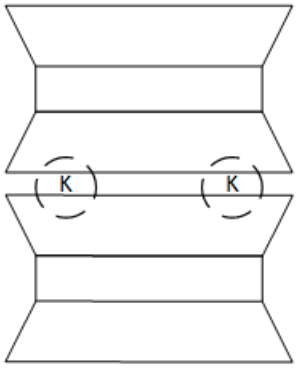

Figure 5.2 Schematic representation of structure of illite (Lal &Shukla, 2004)

Heat is typical generated during waste degradation; the impacts of thermal changes on bentonite properties should also be considered. In general, the swelling capacity of bentonite slightly decreases with an increasing temperature (Villar et al., 2010). Cho et al. (1999) determined that highly dense bentonite mixtures become increasingly permeable when the temperature is increased from 20℃ to 100℃ When the temperature is higher than the threshold temperature, the montmorillonite starts to convert into illite, which has a much lower expansion capacity (Cui et al., 2012).

However, research that examines the combined effect of a highly concentrated salinity solution and temperature on the interface shear behavior of BSM / smooth geomembrane is quite rare. Therefore, the influence of non-isothermal, cations of leachate on the shear behavior of a BSM/smooth HDPE interface is studied in this paper.

5.2 Materials and experimental program

5.2.1 Bentonite sand mixture

In this research, Ottawa cube sand is used. The specific gravity of the Ottawa test sand

is 2.65. This sand is mixed with manufactured sodium-bentonite, at a ratio of 10:1 by weight. The liquid limit (LL) and plasticity limit (PL) of the sodium bentonite are 576% and 42.6%, respectively. The plasticity index (PI) is 533.4%. The specific gravity of the sodium bentonite is 2.68. The particle size distribution of the BSM is presented in Figure 5.3. In the BSM, particles that are 99.96% by weight have a diameter finer than 0.71 mm, 75.6% finer than 0.425 mm, 15.3% less than 0.25 mm, 10% finer than 0.18 mm and 6.3% finer than 0.01 mm. The distribution curve slope significantly changes as the diameter becomes finer. An x-ray diffraction (XRD) analysis was conducted on the sodium bentonite and the XRD result is presented in Figure 5.4. It can be observed that the manufactured sodium-bentonite has a high concentration of montmorillonite.

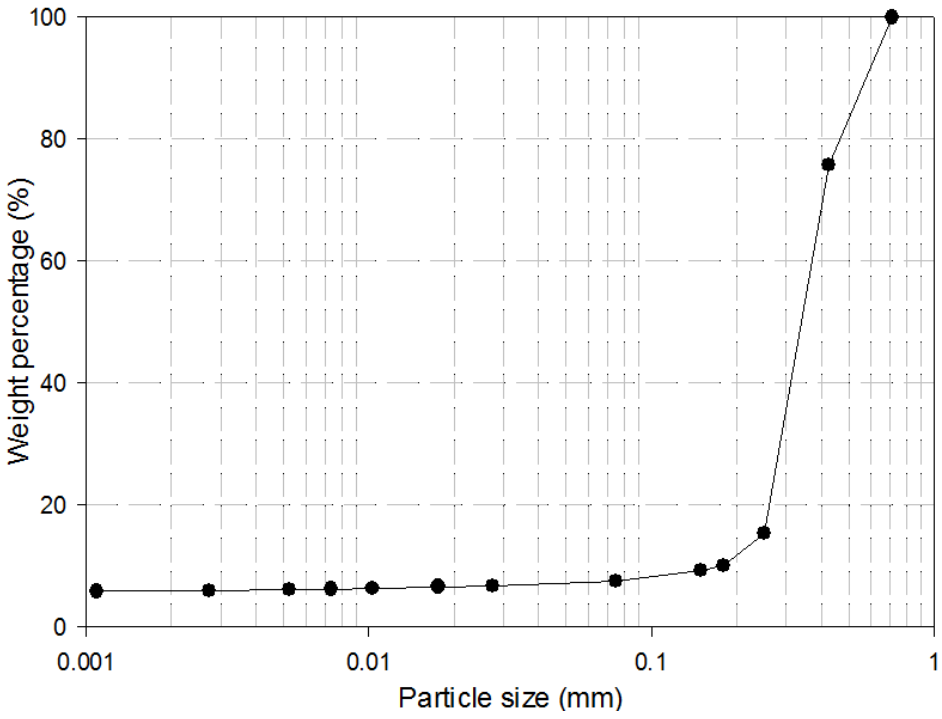

Figure 5.3 BSM grain size distribution curve

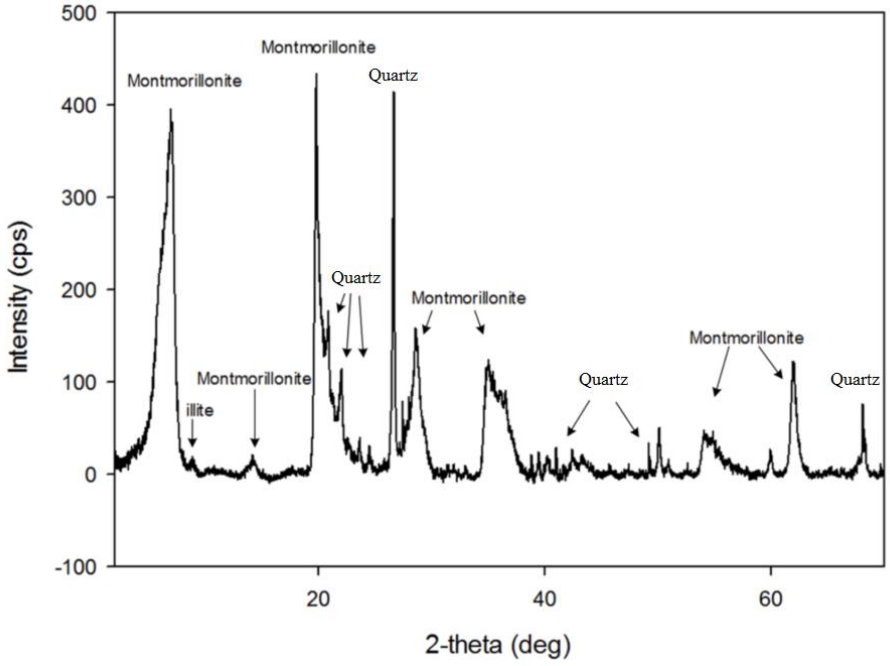

Figure 5.4 X-ray diffraction of the sodium bentonite used in this study

5.2.2 Geomembrane

Smooth HDPE with a thickness of 1.5 mm is used in this research, which was manufactured by GSE Lining Technology (Houston, USA). The roughness of the HDPE is 1.09 (Dove & Frost, 1996). The HDPE has low hydraulic conductivity, and excellent chemical and ultraviolet resistance capacities. All of the other properties of the smooth HDPE are listed in Table 5.2which were obtained from the GSE website (Geosynthetic Lining Systems, 2015).

Table 5.2 HDPE geomembrane properties which can be obtained from the GSE lining technology website (Geosynthetic Lining Systems, 2015).

Property of geomembrane	Minimum average value
Thickness, mm	1.5
Density, g/cm^3	9.94
Strength at break, N/mm	40
Strength at yield, N/mm	22
Elongation at break. %	700
Elongation at yield. %	12
Tear resistance, N	187
Puncture resistance, N	480

5.2.3 Solutions

In order to examine the influence of high salinity on the BSM /HDPE interface shear behavior and shear behavior of BSM, three different solutions were used to saturate the BSM. During the preparation of the BSM, potassium chloride and calcium chloride solutions were adopted to test the influence of the potassium and calcium cations, and distilled water was used as the control. The potassium chloride solution was prepared with a potassium cation concentration of 1750 mg/L, while the calcium chloride solution was prepared with a calcium cation concentration of 2300 mg/L.

5.3 Specimen preparation

For the BSM, 10% sodium-bentonite by weight was mixed into the Ottawa test sand. There were 6 batches of the BSM, which had been saturated with different solutions under two thermal conditions. Each batch of soil material was made of 1200 g BSM, mixed with 500 g distilled water, or solutions with different salinities.

For the purpose of creating a homogeneous clay matrix, the mix should last for at least

10 minutes. Temperature condition #1 denotes when the samples are cured in the oven temperature, which was increased from 20°C incrementally at 10°C intervals (i.e.30, 40 and 50°C). Each stage of the temperature increase was maintained for 10 days and the total treatment time was 40 days. BSM Batches 1 to 3 were prepared with distilled water, potassium chloride and calcium chloride solutions, respectively, and cured in the oven. Temperature condition #2 is room temperature, and the temperature was kept at 20°C for 40 days. BSM Batches 4 to 6 were prepared with distilled water, and potassium chloride and calcium chloride solutions and cured at room temperature.

However, in order to acquire the same curing time for each batch of BSM, the BSM was prepared at different times. After each batch had been cured for 40 days, the water content was reduced by using the oven or a fan. During this period of time, the soil slurry was stirred for 15 minutes each time until the weight of the soil and container reached the expected mass value which was calculated by using the BSM mass with a moisture content of 15.3%. This water content is 2% wetter than the optimum water content of BSM. After the BSM reached the expected water content, it was sealed and placed into a container to obtain water balance.

A static compaction method was used to prepare the samples. Theoretically, when the degree of static compaction is the same as that of dynamic compaction, it can be assumed that the samples have the similar structure and maintained properties. The density of BSM with a 15.3% moisture content is 2.04 g/cm^3. Static force was used to compact a pre-determined mass to the dimensions of 60 ×60 × 25 mm and 60 × 60 × 12 mm for the BSM and the BSM interface with geomembrane samples, respectively. The BSM samples were directly wrapped with plastic film, while the interface shear samples were placed so that they came in contact with the smooth side of the geomembrane (60× 60 mm), and then wrapped with plastic film.

In order to further understand the changes of the bentonite mineral in the mixtures after a non-isothermal chemical treatment, XRD was used to analyze the clay changes. The oven dried samples collected from different batches underwent a sieve analysis with a No.200 sieve. All of the sand could be separated, and 76% of the bentonite passed through the sieve. The parts of the clay that had passed through the sieve were then tested for mineral changes by using XRD.

5.4 Testing apparatus

5.4.1 Direct shear machine

The direct shear stress apparatus is commonly used to test shear strength, and also a widely used device to explore interface shear behavior. It has advantages such as simplicity and suitability for interface testing (Miller & Hamid, 2007; Taha & Fall 2013, 2014; Fishman & Pal, 1994). The measuring of the interface shear strength of BSM/smooth HDPE is carried in accordance with ASTM standard D5321. A schematic diagram of a standard direct shear testing machine, which was used in the interface shear tests, is provided in Figure 2.10. This apparatus has a square shear box. Normal loads (N) are applied on top of the shear box by adding weight to the weight hanger (Taha, 2010). The driver can provide the machine with a wide range of speeds and a horizontal load is applied onto the lower box. Meanwhile, the upper box is horizontally restrained, and a load cell is connected to the upper box to measure the shear stress. The horizontal and vertical displacements are measured by the linear variable differential transformers (LVDTs) (Murthy, 2002). All of the data were collected with a computerized logger, and monitored and saved by the LABVIEW program.

5.4.2 X-ray diffraction

X-ray analyses (XRD) were performed on the BSM samples to examine the mineralogical changes that were chemically and thermally induced. XRD was performed by using a Rigaku Ultima IV diffractometer with a fine focus copper x-ray source (0.15418 nm wavelength). The XRD patterns were measured at room temperature. The tube voltage and current were set to 40 kV, and 44 mA during the experiments, respectively. The scans were processed between 2-80 degrees of the 2theta range with a step width of 0.02 degree of 2theta, and the scan time was 0.6 s per step.

5.5 Testing procedures and testing plans

The BSM and BSM with smooth HDPE interface samples were tested by using consolidated-drained (CD) direct shear tests (DSTs) at a low shear rate (0.025 mm/min). Based on the results of the consolidation tests of the BSM performed in this study, the shear rate for the DSTs was determined. For the interface shear sample, the smooth face of the geomembrane was in contact with the BSM and another side of the geomembrane had to be glued onto the top of a supporting steel cube. When the interface shear sample was loaded

into the shear box, it was necessary to ensure that the interface of the BSM/HDPE was exposed in the gap of shear boxes.

BSM has low hydraulic conductivity (7.8×10^{-11}m/s), and in order to help the samples to quickly saturate, a well-sealed container was used, which has a strong vacuum resistance capacity. The samples were placed in the shear box and the shear box with the samples were placed into a vacuum container. This container was filled with distilled water and sealed with vacuum grease. A negative pressure of 35 kPa was applied, which helped the BSM samples reach a 99% degree of saturation after 24 hours.

The saturated samples in the shear box were placed into the direct shear machine. The sink of the machine was filled with distilled water and 3 or 4 normal stress increments were applied to consolidate the samples. The normal stresses used were 150, 250 and 350 kPa, respectively. Each increment of normal stress was sustained for 1 hour to ensure that the primary consolidation was completed. After the primary consolidation, the shear box and sample were sheared at a speed of 0.025 mm/min.

5.6 Results and discussion

Typical DST results of the BSM and the interface shear test results of the BSM/geomembrane are presented and discussed in this section. The results are analyzed in terms of the chemical and thermal influences, and the thermal-chemical combined effects on the interface shear behavior of BSM/smooth geomembrane, while the BSM samples are used as a comparison.

5.6.1 Salinity influence on shear strength for samples at room temperature

Figures 5.5 to 5.7 show the influence of the salinity solutions on the shear stress versus shear strain results of the BSM/ smooth HDPE interface, and on the BSM (presented for comparison purposes). All of the samples are made from Batches 4, 5 and 6 of the prepared BSM, which had been saturated under room temperature with distilled water, and potassium chloride and calcium chloride solutions. The samples were sheared at normal stresses of 150, 250 and 350 kPa, respectively.

An analysis of Figures 5.5 to 5.7 indicates that the different solutions have no significant

impact on the shape of the shear stress-strain curves for both the BSM/HDPE interface shear and the BSM samples. From the BSM/HDPE samples, it can be observed that regardless of the impact from the different solutions, the curves of all the interface samples have no peak shear stress values. Thus, the shear stress at 15% of the shear strain can be considered as the shear strength (in accordance with ASTM standards D3080 and D5321). All of the interface shear samples are not able to reach the residual state in any of these tests. At the early stages of the interface shear, there exists a significant high initial stiffness. This can be explained by the fact that the BSM material comes into contact with the geomembrane under the effect of normal stress. Before shear displacement happens, shear resistance comes from two factors: the sand particles at the interface are interlocked with the HDPE geomembrane surface, while the hydrated clay components are adhesively connected to the geomembrane. The shear stress has to overcome the interface shear resistance to increase shear displacement. Once shear displacement takes place, the sand particles can penetrate the geomembrane surface, clay particles slide onto the surface, and the increase of the shear stress becomes stable.

As a comparison, the shear results of the BSM samples are also presented in Figures 5.5 to 5.7. The curves of the BSM samples have different shapes, are smooth and the shear stress increases with increasing shear displacement, and the increasing rate gradually decreases. The BSM curves do not agree with the BSM/HDPE interface results. The shear strength values of the BSM/HDPE interface samples are approximately 50% of those of the BSM samples. This could suggest that the dominant shearing mechanism is shearing at the interface surface, instead of shearing in the BSM above.

Figures 5.5 to 5.7 also reveal that the peak shear strength increases with increasing normal stress, regardless of the type of shear behavior and the different solutions used. For example, the peak shear stress for the BSM / HDPE samples saturated with distilled water is determined to be 61, 95 and 137 kPa at a normal stress of 150, 250 and 350 kPa, respectively. This is due to the fact that an increase in the normal stress on the plane of shear failure can increase the contact area between the geomembrane and BSM particles. Hence, the frictional resistance between the BSM and geomembrane surface is increased, and a higher maximum shear strength is needed to overcome this shear resistance (Fall and Nasir 2010; Nasir and Fall, 2008). The BSM soil samples that were saturated with distilled water and cured at room temperature have a shear strength of 126, 194 and 250 kPa which are measured under vertical

stresses of 150, 250 and 350 kPa, respectively. The particles of the densely compacted BSM come into contact with each other under high vertical loads, which increase the sand shear resistance as well.

From Figures 5.5 to 5.7, it can also be observed that the value of the shear strength is influenced by the different solutions. The highest shear strength can always be found in the results of the samples that were saturated with distilled water, regardless of the normal stress and the type of shear behavior. This phenomenon can be explained by the fact that the shear resistance is provided by the two different particles in the BSM; sand is stable, while the clay shear resistance is changed by the different solutions. When the bentonite was saturated with other solutions, other exchangeable cations replaced the sodium cations, the swelling capacity of bentonite decreased, the hydrated clay volume in the sand voids was reduced and dissociated water molecules increased (as demonstrated and discussed in Section 5.6.4).

Compared with the BSM samples, the interface shear behavior has relatively small differences. This can be explained by the fact that at the shear surface, the BSM properties are only slightly changed, and the HDPE properties are constant. For the samples that were saturated with the potassium and calcium solutions respectively, the shear strengths obtained at 15% of the shear displacement are commonly similar, and it is difficult to pinpoint exactly which solution has a more significant influence. Under 150, 250 and 350 kPa, the maximum difference in the shear strengths of the BSM/smooth HDPE interface samples that were saturated with the various solutions is 9.8%, 7.2% and 10.9%, respectively.

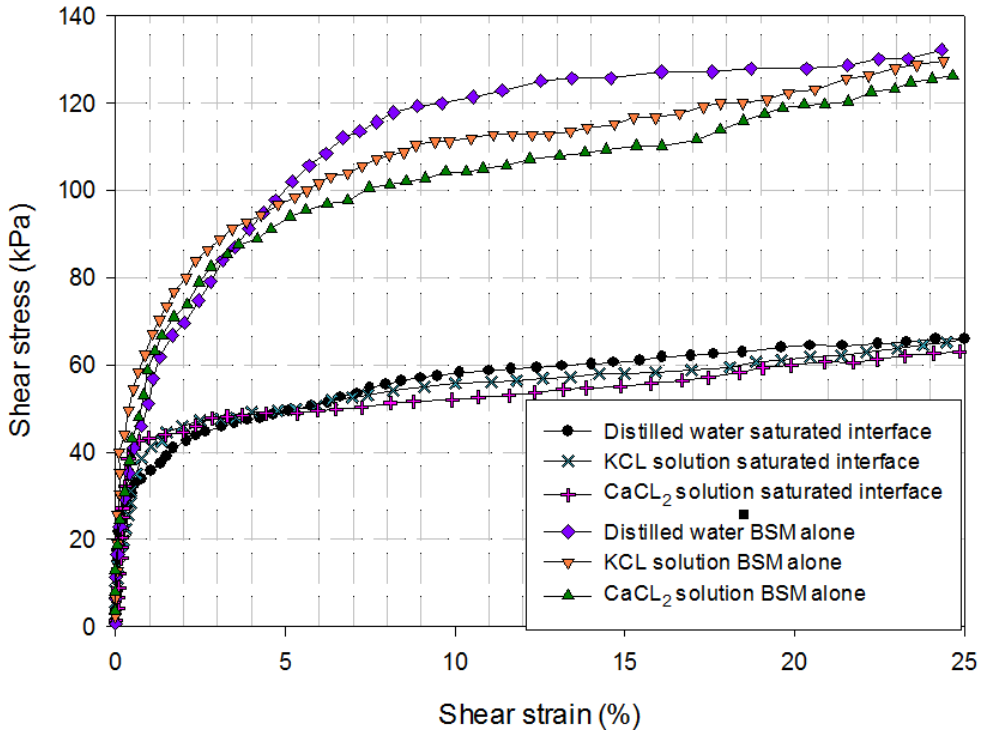

Figure 5.5 Influence of salinity on the stress-strain of BSM/ smooth HDPE interface for a normal stress of 150 kPa

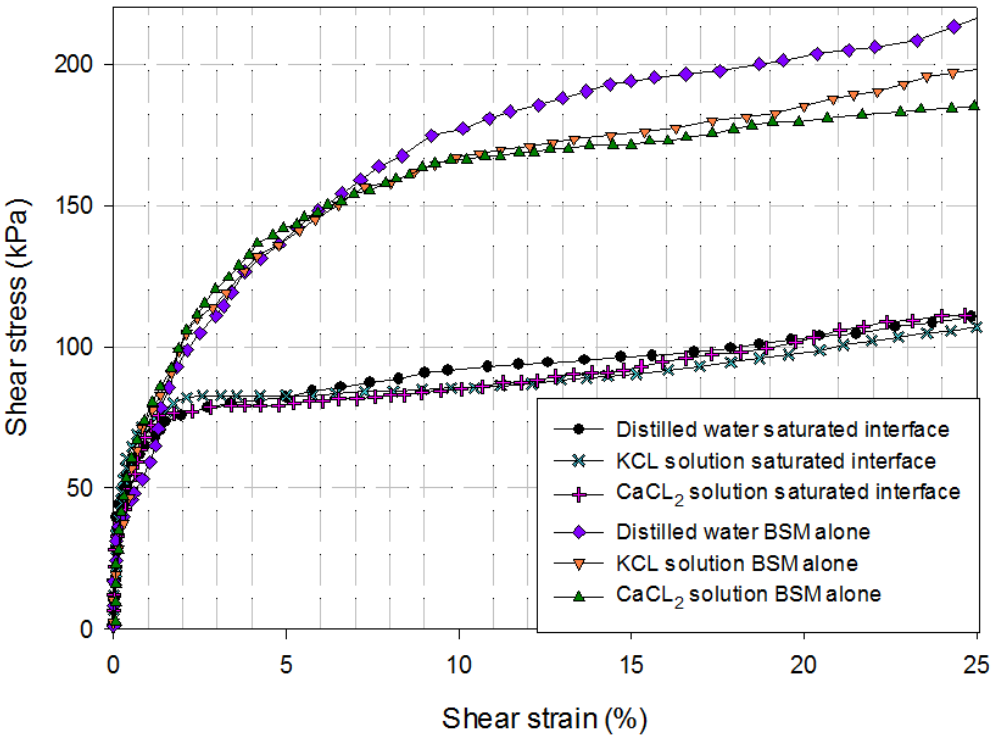

Figure 5.6 Influence of salinity on the stress-strain curve of BSM/ smooth HDPE interface for a normal stress of 250 kPa

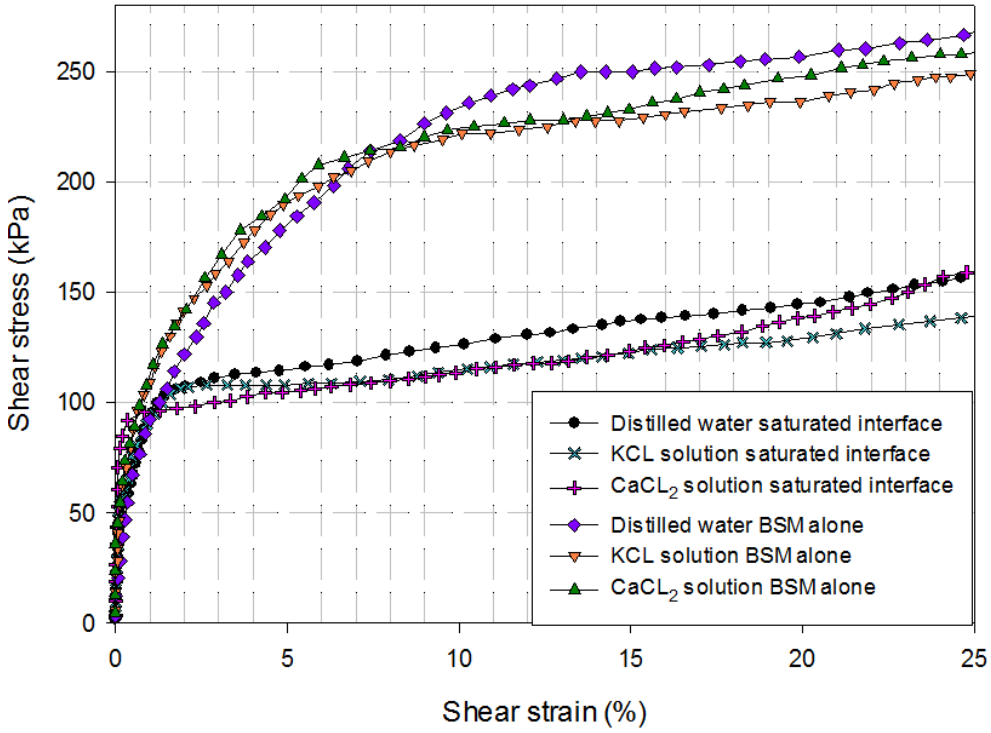

Figure 5.7 Influence of salinity on the stress-strain of BSM/ smooth HDPE interface for a normal stress of 350 kPa

The influence of the solution salinity on the vertical deformation of the samples which were sheared under a normal stress of 150 kPa is also presented in Figures 5.8 and 5.9. From these two figures, it can be noticed that the samples that used the calcium chloride solution have the highest vertical deformation when the horizontal displacement reaches around 25%. The LL of the sodium bentonite can be significantly reduced by the calcium chloride solution (Ahonen et al., 2008; Bouazza et al., 2007); the LL is reduced from 576% to 157%. Compared with the LL, the PL has only minimal changes, with a slight decrease from 42.6% to 41.5%. Thus, the plasticity index (PI) of the BSM changed from 533.4% to 115.5% after using the calcium chloride solution. This result indicates that after the samples that used the calcium chloride solution were sheared, the edges of some of the samples dissolved while in the sink of the direct shear machine. Therefore, the mass of the BSM decreased, and the normal load plane was inclined at the end of the shearing.

Figure 5.8 illustrates the vertical deformation versus shear displacement curves of the BSM/HDPE interface. Since all of the samples were subjected to the completion of primary consolidation under vertical loads, once the shearing started, the variation of the vertical deformations for the different samples under the same vertical stress is limited, which is

around 0.1 mm. All of the samples show mainly contractive behavior. The deformations at 15% of the lateral displacement are determined to be -2.1%, -2.3% and -2.6% for the samples that are saturated with the potassium chloride solution, distilled water and calcium chloride solution, respectively.

Figure 5.9 depicts the vertical deformation versus shear horizontal strain curves of BSM under a vertical stress of 150 kPa for comparison purposes. In this figure, it can be noticed that thet curves mainly show contraction. However, the curves also show a transition between the contracting and dilating behaviors. The dilation is commonly seen in the DSTs of material that has sand (Al-Douri & Poulos, 1991; Simoni & Houlsby, 2006). A normal load of 150 kPa causes the samples to experience vertical deformation, and the vertical dilation is due to the asperities of the sands. They need to override each other at the points of contact, unless the sand particles are crushed. The vertical deformations of the samples that are saturated with different salinity solutions changed from -1% to -1.25%.

To sum up, the manual influences and experimental errors which cause minor differences in the vertical deformation in both the BSM/HDPE interface shearing and BSM shearing are difficult to avoid. The differences in the vertical deformation of the samples that were saturated with various salinity solutions under normal stresses of 250 and 350 kPa, and the effects of temperature on the vertical deformation are omitted, since the changes are also minimal.

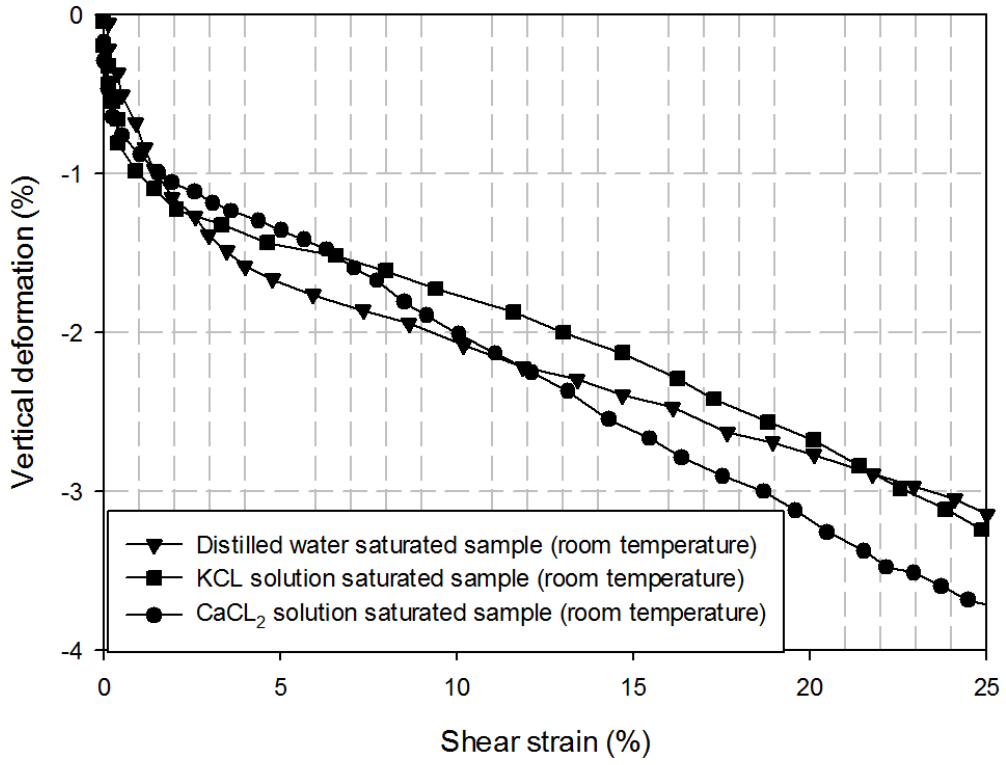

Figure 5.8 Influence of solution salinity on the vertical deformation versus shear strain of BSM/HDPE for a normal stress of 150 kPa

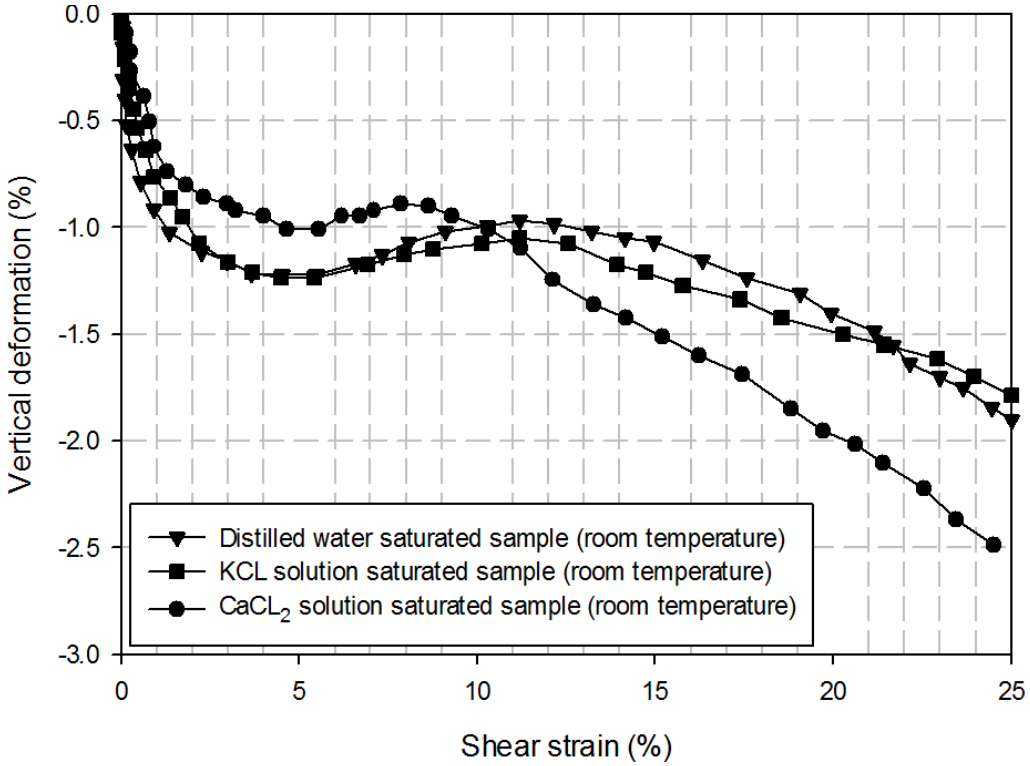

Figure 5.9 Influence of solution salinity on the vertical deformation versus shear strain of BSM for a normal stress of 150 kPa

5.6.2 Temperature influence on shear strength of samples that used distilled water

In order to understand the influence of temperature on the shear behavior of BSM and BSM/HDPE interface, the shear results of samples which were saturated with distilled water and cured at different temperatures are discussed. It can be seen from Figures 5.10 and 5.11 that the samples cured at room temperature always have a slightly higher shear strength compared with those cured in an oven. This phenomenon can be explained by the variations of the hydration state in the bentonite. In the BSM, the sand voids are filled with hydrated bentonite particles. At room temperature, the clay is usually hydrated. On the contrary, higher temperatures can influence the bentonite swelling behavior. When dried in the oven from 20^{o}C to 50^{o}C, the swelling strain decreases with a reduction in the hydration between the elementary layers, and the temperature also causes instability between the inter-aggregate water and intra-aggregate water. This phenomenon causes less hydrated clay and more dissociated water molecules to fill the sand voids (Arifin, 2008; Villar and Lloret, 2004).

Figure 5.10 depicts the interface shear behavior of BSM/smooth HDPE samples that were saturated with distilled water and subjected to vertical stresses of 150, 250 and 350 kPa. It can be seen from this figure that under normal stresses of 150, 250 and 350 kPa, the difference in the shear stress between the samples that were cured in the oven and at room temperature is 6.1% 8.1% and 8.7%, respectively. Theoretically, the influence of the temperature on the shear behavior should less significant than the vertical stress. However, the shear results of the BSM/HDPE interface show similar magnitudes of the shear strength changes between the samples cured at room temperature and in the oven.

As a comparison, Figure 5.11 presents the results for the influence of the temperature on the shear behavior of BSM. When subjected to vertical loads of 150, 250 and 350 kPa, the difference between the samples that underwent thermal treatment and those that did not, is 15.9%, 6.2%, and 7.6%, respectively. This result reveals that the influence from the vertical load is more significant than that of the temperature, since the sand voids on a shear plane can become more densely compacted under a high vertical load, which can partially offset the effects from the temperature.

The results from the comparison reveal that the contraction at the interface of the

BSM/HDPE sample caused by vertical stresses are smaller than that of the BSM samples at the shear plane. Furthermore, most of the interface shear strength of BSM/HPDE is provided by sand that penetrates the geomembrane. When the vertical load is increased, the load level, geomembrane stiffness, sand shape and other properties define the magnitude of the penetration. Although the BSM was cured in an oven, the properties of the sand and geomembrane are all constant since the samples are sheared at room temperature. Thus, the interface samples cured at room temperature and in an oven have similar magnitudes of change in terms of the shear strength, which are sheared under different vertical stresses. There is also the possibility of minor experimental errors during the testing.

To sum up, the influence of temperature on the interface shear behavior of BSM/smooth HDPE is relatively limited. However, the samples cured in the oven are sheared under room temperature in this research, which means that the HDPE properties are constant and this is different from real landfill conditions.

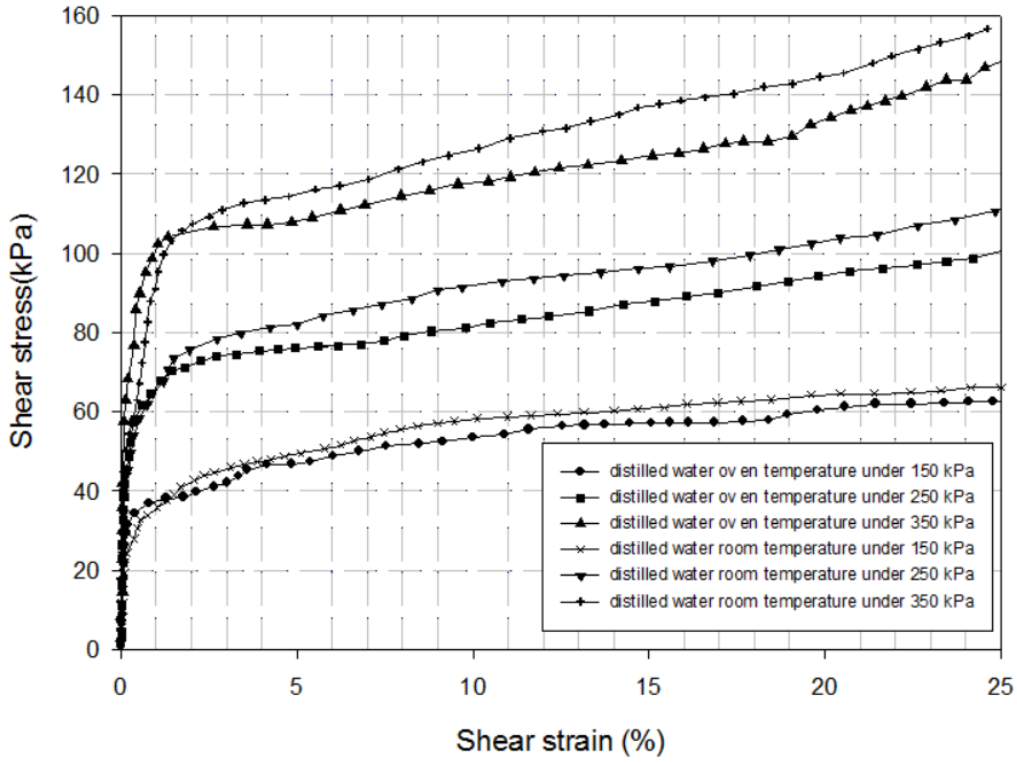

Figure 5.10 Influence of temperature on the stress-strain behavior of BSM/HDPE samples saturated with distilled water

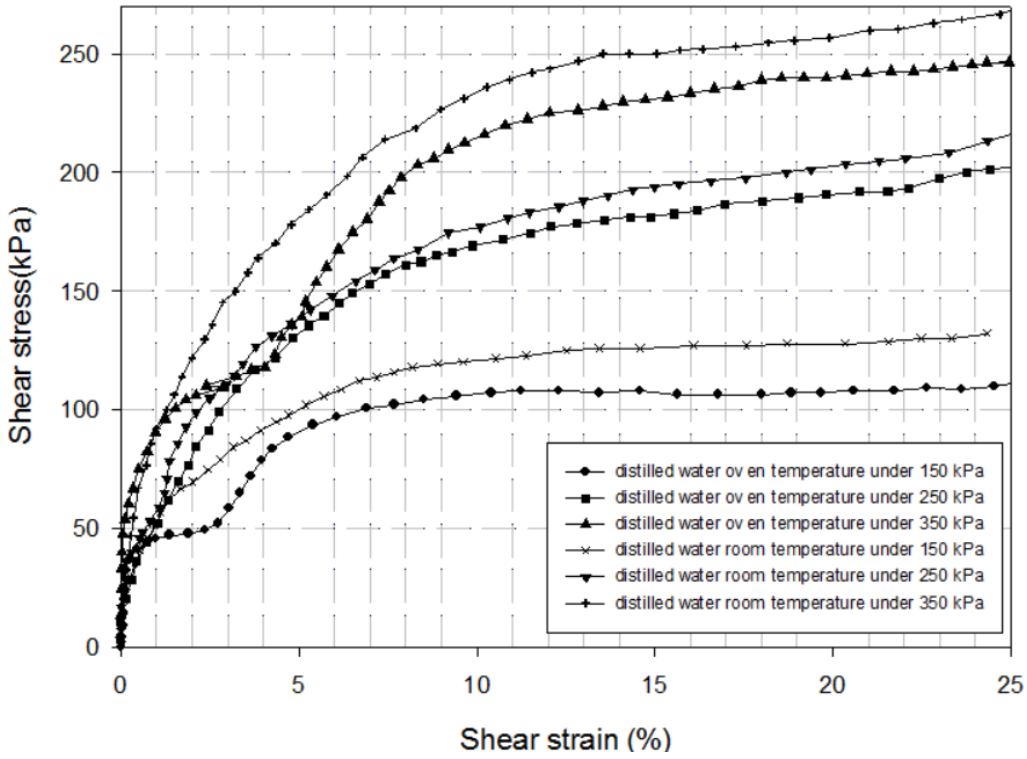

Figure 5.11 Influence of temperature on the stress-strain behavior of BSM samples saturated with distilled water

5.6.3 Influence of non-isothermal leachate on shear behavior

In order to compare the combined effects of the chemistry and temperature on the shear behavior of the BSM/geomembrane interface, the results of all the interface samples will be provided. These samples are cured under various temperatures and three different solutions are used, including distilled water, and potassium and calcium chloride solutions. Figures 5.12 to 5.14 show the shear stress versus strain curves of BSM/HDPE interface samples subjected to vertical loads of 150, 250 and 350 kPa, respectively. Figures 5.15 to 5.18 are used for comparison which illustrate the shear behavior of the BSM samples.

An analysis of Figures 5.5 to 5.7, 5.10 and 5.12 to 5.14 show that the combined effects of chemistry and temperature have no obvious impact on the shape of the stress-strain curves of the BSM/geomembrane interface compared with that influenced by individual chemistry or temperature changes. It can be seen that in the interface shear behaviors, the highest shear strengths are always obtained from the samples that were cured at room temperature, which were saturated with distilled water. The shear strengths of the rest of the samples have an

inconsistent order under different vertical stresses. All of the BSM/HDPE curves have relatively limited changes, which are hard to distinguish due to manual effects and experimental errors. The maximum shear strength change in the interface shear behavior is 11.5%, 8.5% and 9.5% when subjected to vertical stresses of 150, 250 and 350 kPa, respectively.

As a comparison, Figures 5.15 to 5.17 provide clarity on the shear strengths when influenced by the combined-effect of chemistry and heat. The highest shear strengths are all obtained from the samples that were saturated with distilled water and cured at room temperature. The maximum change in the shear strength from the combined effect of chemistry and heat is 13% 14.4% and 8.8% when subjected to a vertical stress of 150, 250 and 350 kPa, respectively. In terms of the shear behaviors of the BSM samples, those that were saturated with distilled water and cured in the oven, and those that used salinity solutions and cured at room temperature, usually obtain the second highest shear strengths. Samples that used the salinity solutions and cured at a high temperature always have the lowest shear strengths, but the difference is minimal.

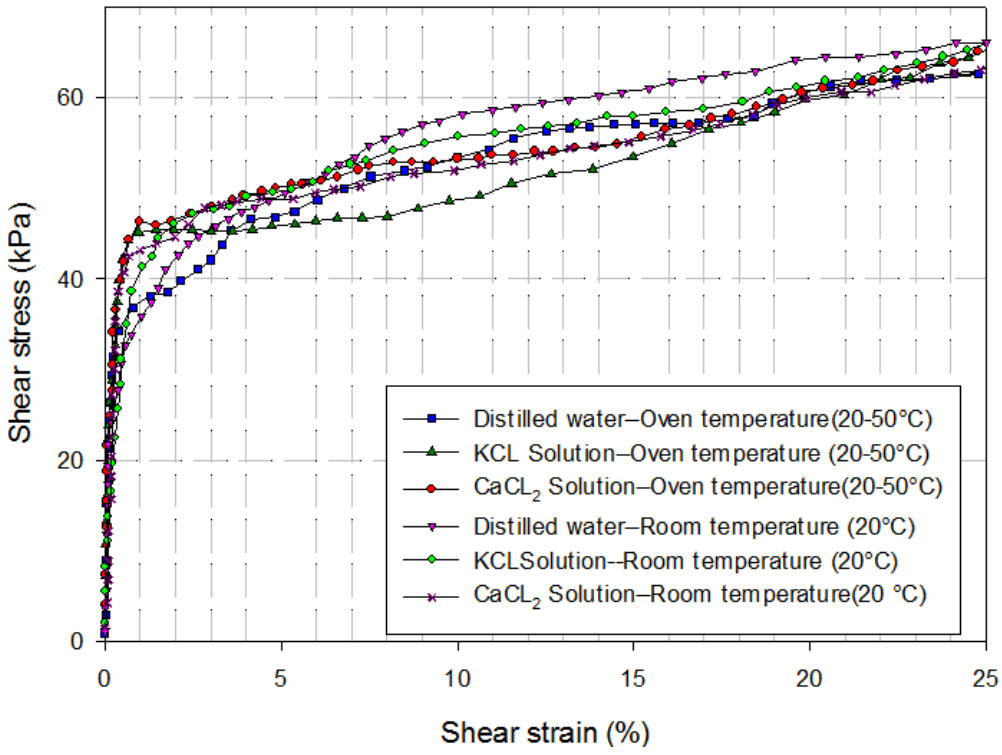

Figure 5.12 Thermo-chemical effect on the interface shear results for normal load of 150 kPa

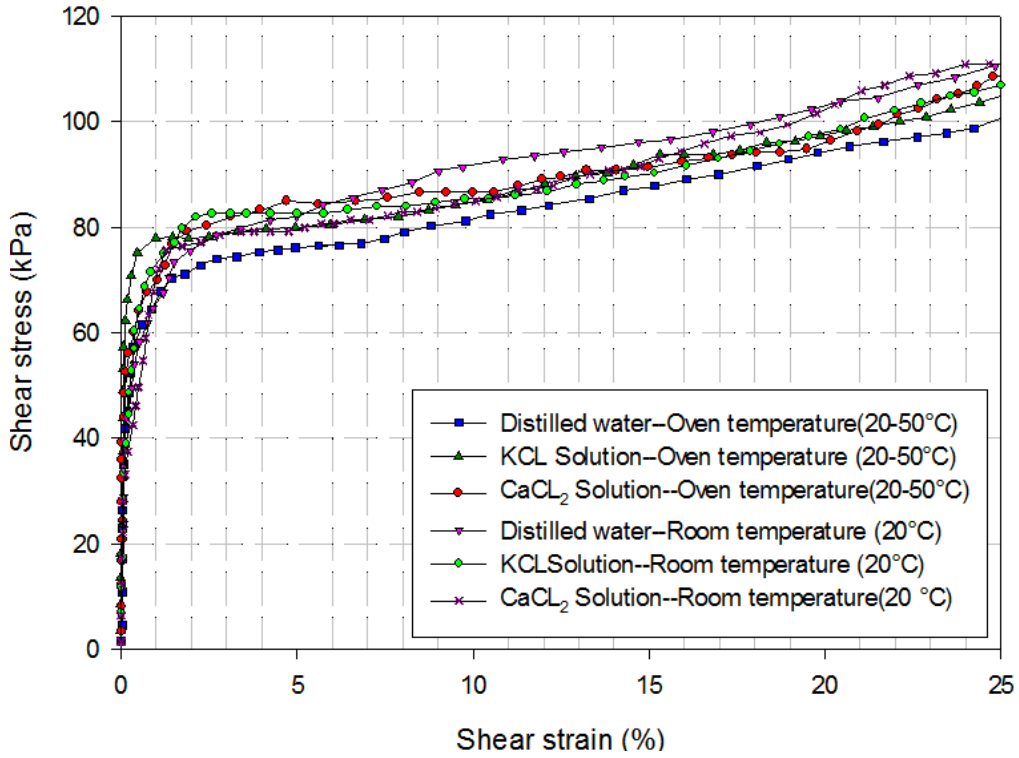

Figure 5.13 Thermo-chemical effect on the interface shear results for normal load of 250 kPa

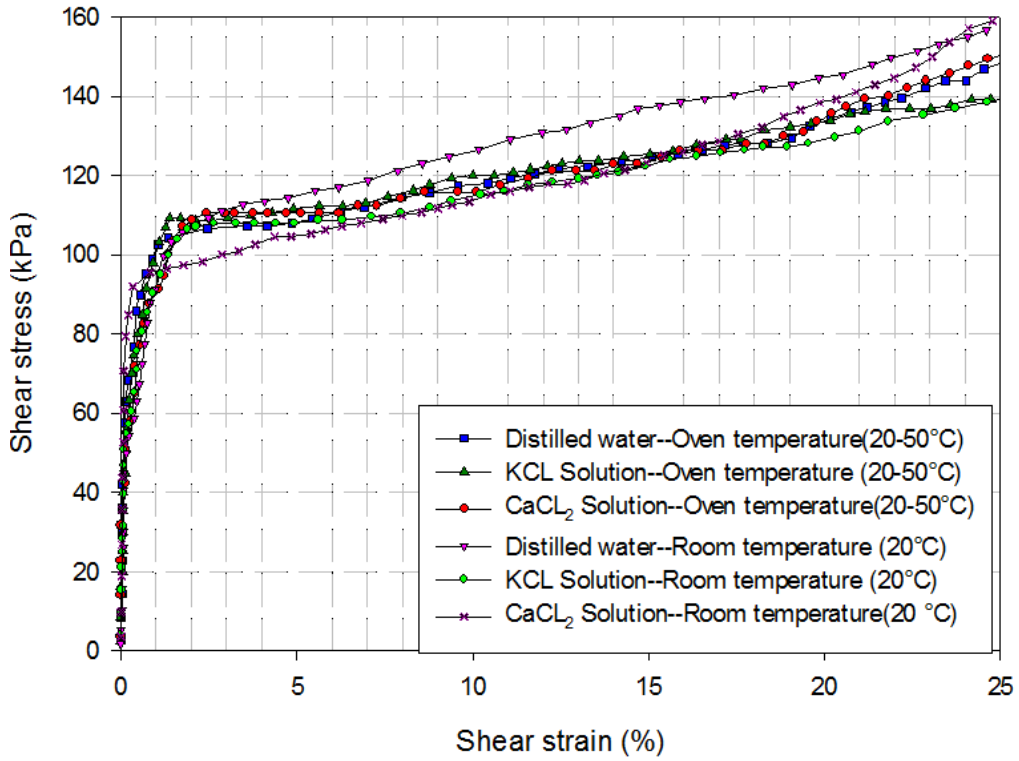

Figure 5.14 Thermo-chemical effect on the interface shear results for normal load of 350 kPa

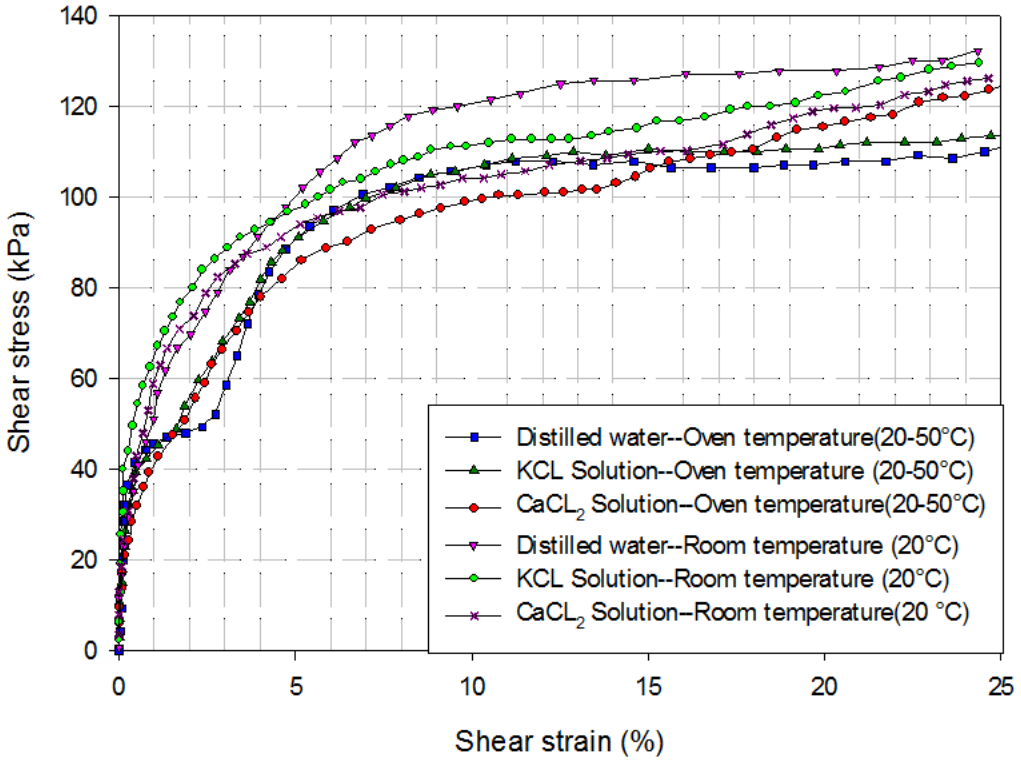

Figure 5.15 Thermo-chemical effect on the shear results of BSM for normal load of 150 kPa

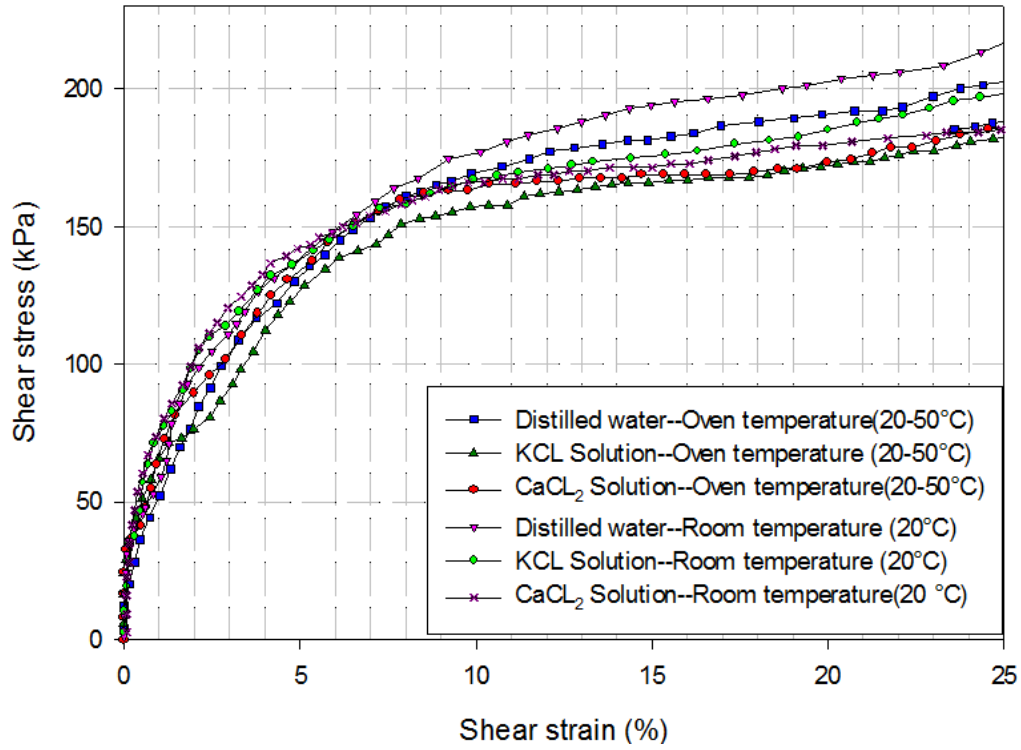

Figure 5.16 Thermo-chemical effect on the shear results of BSM for normal load of 250 kPa

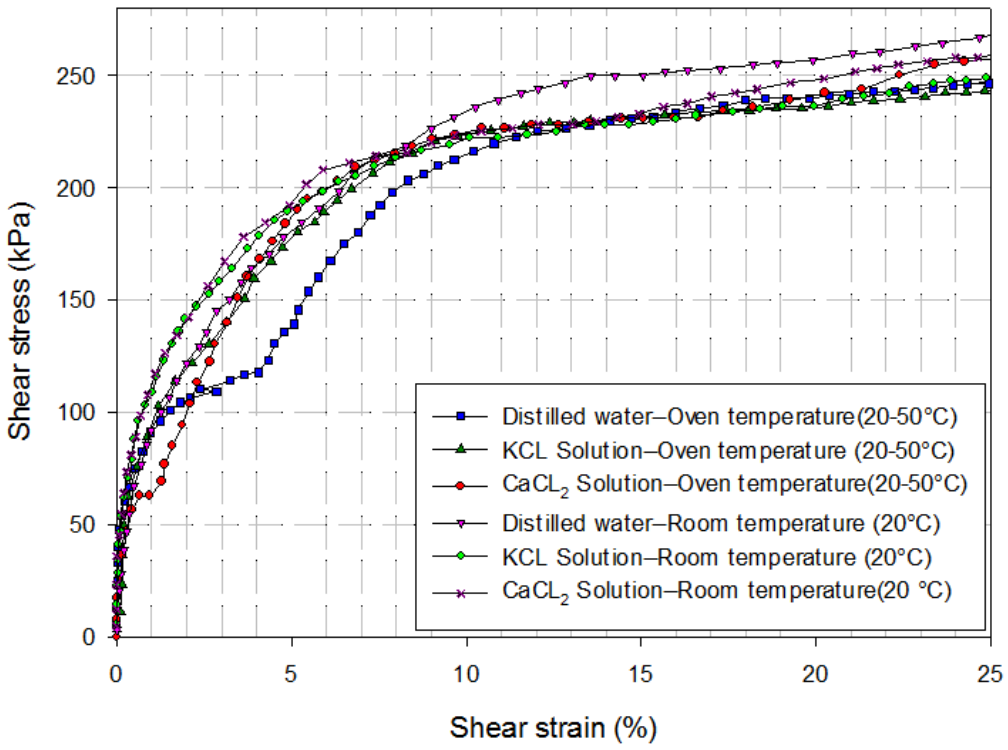

Figure 5.17 Thermo-chemical effects on the shear results of BSM for normal load of 350 kPa

This conclusion can be further confirmed by the friction angles. The friction angles of all the BSM/HDPE and BSM samples are presented in Table 5.3. Since the experiments were set for consolidated drained (CD) shear tests, the friction angle is the only parameter that needs to be considered to carry out the CD shear testing. Table 5.3 can be used to illustrate the changes of the shear resistance with the combined effect of cations and temperature for the two types of shear behaviors. The maximum friction angle of the BSM soil is 36.74°, which was measured from the samples cured at room temperature and saturated with distilled water. The friction angle decreases to a range from 34.4° to 33.8° when the samples were saturated in a saline solution, cured under high temperature or the sample were affected by the combined influence of salinity and temperature. The interface shear behavior of the samples that were cured at room temperature and saturated with distilled water have the highest friction angle as well, which is 21.30°. With changes in the thermal conditions or chemistry, or both, the friction angle is reduced to approximately 19.6° to 19.8°. The maximum interface friction angle change is 7.8%, which is low. Thus, the chemical and thermal effect on the interface shear behaviors is all limited.

Table 5.3 Interface friction angles and friction angles of all the samples

Condition	BSM/HDPE interface shear (degree)	BSM shear (degree)
Cured in oven and saturated with distilled water	19.62	34.43
Cured in oven and saturated with potassium chloride solution	19.80	33.87
Cured in oven and saturated with calcium chloride solution	19.76	33.81
Cured at room temperature and saturated with distilled water	21.30	36.74
Cured at room temperature and saturated with potassium chloride solution	19.64	34.21
Cured at room temperature and saturated with calcium chloride solution	19.82	34.14

5.6.4 XRD results of cured and saturated samples

The samples underwent X-ray diffraction (XRD) after curing and saturation. As the tested parts of the clay are separated from the cured and saturated BSM samples with a No.200 sieve, these clay components are not entirely the same as the original bentonite even though the samples are only saturated with distilled water. The XRD patterns which show the 2-theta and intensity relationships of BSM samples from Batches 1, 2, 3 and 4, are presented in Figures 5.18, 5.19, 5.20 and 5.21, respectively.

The XRD pattern of the BSM sample which was saturated with distilled water and cured in the oven for 40 days is presented in Figure 5.18. This figure indicates that the clay is primarily composed of sodium-smectite, which includes montmorillonite and beidellite. Beidellite is a clay mineral of the smectite family. The clay structure is slightly different from montomorillonite. The tetrahedrons in the beidellite structure have both Si and Al atoms, and the octahedrons have more charges than the tetrahedrons (Carlson, 2004). Thus, both montmorillonite and beidellite are commonly present in bentontie samples (Carlson, 2004).

Most of the characteristics of the clay minerals are represented by their basal reflections (the 001 peak). The characteristic features of the 001 reflection peak corresponding to a diffraction angle of 2θ is 7.57°, and the basal spacing (d001) is 11.68 Å. In general, the d-value of the 001 peak of the smectite group represents the thickness of the structural units, which is around 12 Å to 15 Å. When the thickness is around 12 Å, the major component is sodium cations and one layer of water molecules that is found in the interlayer. (Hubert et al., 2009) The exact value of the d001 collected from the XRD pattern is 11.68 Å. The small difference between the two values is because of measurement error and the difference in the cation hydration states (Carlson, 2004). The d (060) value can be used to determine the material type as well. In this pattern, the result of d060 is 1.4988 Å, which is in agreement with the range of the d060 of montmorillonite which is from 1.49 Å to 1.50 Å (Carlson, 2004).

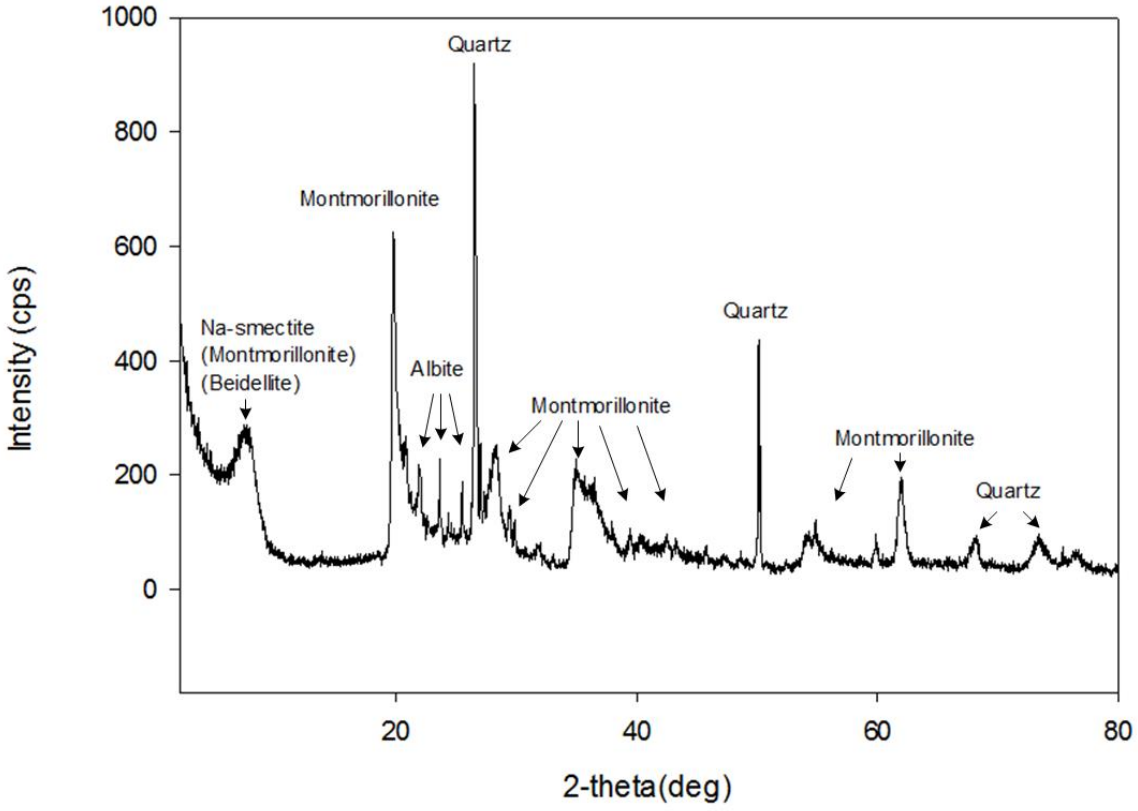

Figure 5.18 XRD pattern of BSM Batch 1

Figure 5.19 illustrates the XRD pattern of the BSM sample saturated with the potassium chloride solution and cured in the oven (Batch 2). The principal component of the clay is illite. The 001 reflection peak corresponding to 2θ is 8.35°, and the d-value of the 001 peak is 10.58 Å. Theoretically, illite has a d001 value equal to 10 Å, and the illite/smectite mixture has a d001 value that ranges from 10 Å to 14 Å (Schroeder & Irby, 1998). The ratio of the illite/smectite can be defined by the saddle/001 method, which measures the saddle height on the low-angle side of the 001 peak and the height of the 001 peak (Inoue et al., 1989). The intensity of the saddle is 170 cps, intensity of the 001 peak is 242 cps, and the base line intensity is 50 cps. As a result, this pattern indicates that the clay has more than 60% illite. In reference to the U.S. Geological Survey Open-file Report 01-041, the illite group d (060) reference value is 1.5 Å. In this pattern, d060 is equal to 1.50088 Å, which is further verified by the illite that dominates the clay component of the BSM sample.

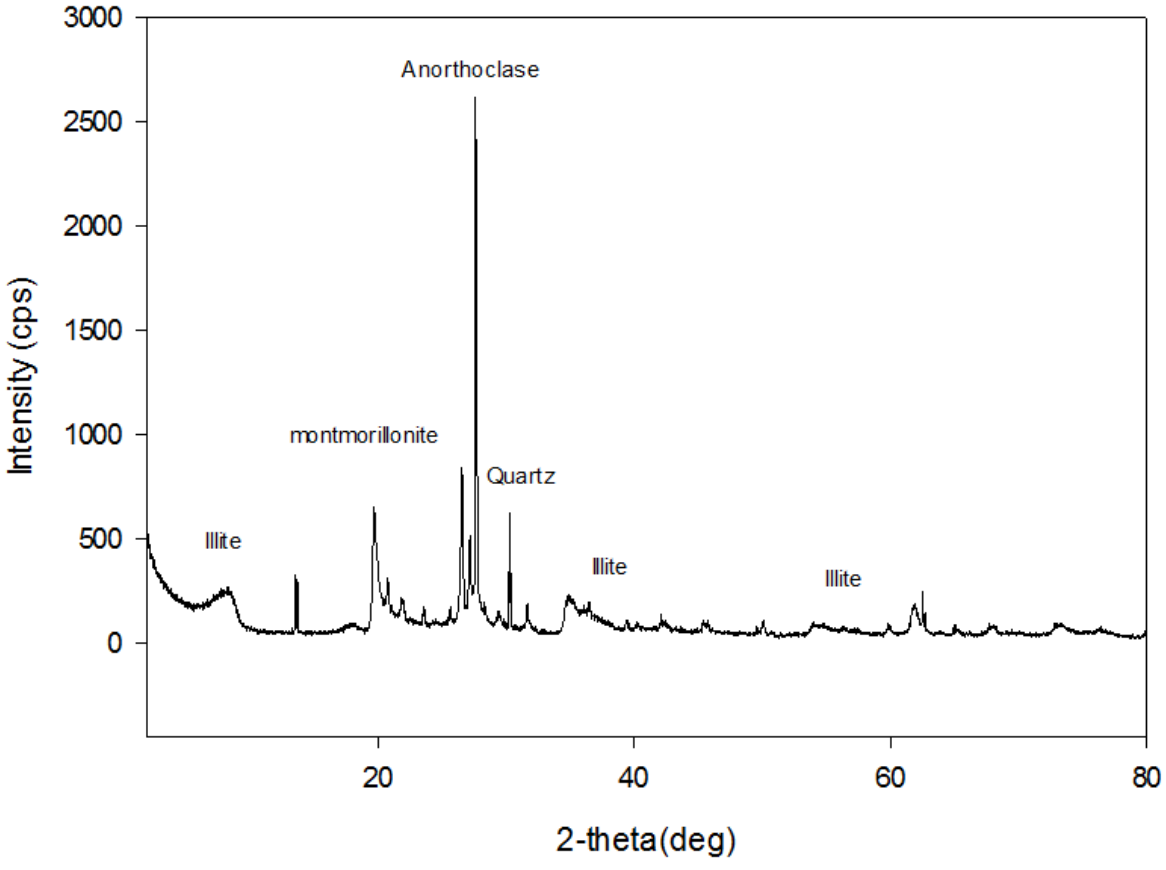

Figure 5.19 XRD pattern of BSM Batch 2

The XRD pattern of the BSM sample saturated with the calcium chloride solution and cured in the oven for 40 days (Batch 3) is presented in Figure 5.20. Figure 5.20 shows that the clay is primarily composed of montomorillonite which contains both sodium and calcium exchangeable cations. The diffraction angle 2θ of 001 reflection peak is 6.43°, and the basal space (d001) is 13.73 Å. Theoretically, the d-value of the 001 peak represents the thickness of the structural units of the smectite group. When the d001 value is greater than 14 Å, the montomorillonite contains divalent cations and two layers of water molecules (Carlson, 2004). In this XRD pattern, 13.73 Å is between 12 Å and 14 Å. Thus, the result confirms that there is a clay component of the BSM in the mix-layer of sodium bentonite and calcium bentonite. The d (060) value is 1.50076 Å which is close to the 1.50 Å of montomorillonite.

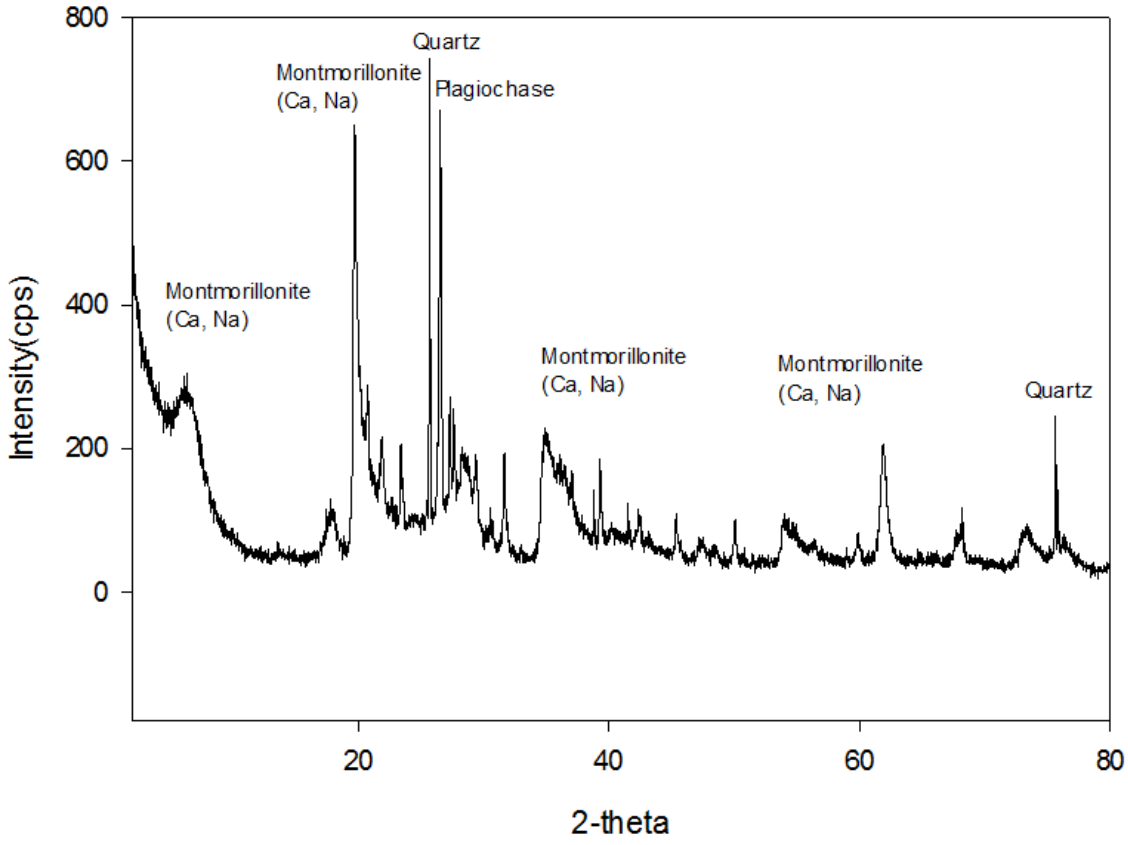

Figure 5.20 XRD pattern of BSM Batch 3

Figure 5.21 illustrates the XRD pattern of the BSM sample saturated with distilled water and cured at room temperature (Batch 4). The majority of the clay compoments are similar to those of Batch 1. Figure 5.21 indicates that the primary components of the clay component

are sodium-smectite as well. The clay component includes Na-montmorillonite and sodium beidellite. The 001 peak is important for examining the clay properties. (Hubert et al., 2009) In this XRD pattern, the 001 reflection peak is performed on the diffraction angle 2θ is 7.45°, and the basal space (d001) is equal to 11.85 Å. When compared with the main pattern in Figure 5.19, they are similar. However, the d001-value of the BSM sample cured in the oven and saturated with distilled water is slightly lower. This slightly different d-value represents the variation in the hydration of the cations. The variation also indicates that the increasing of the temperature can reduce the swelling capacity of bentonite.

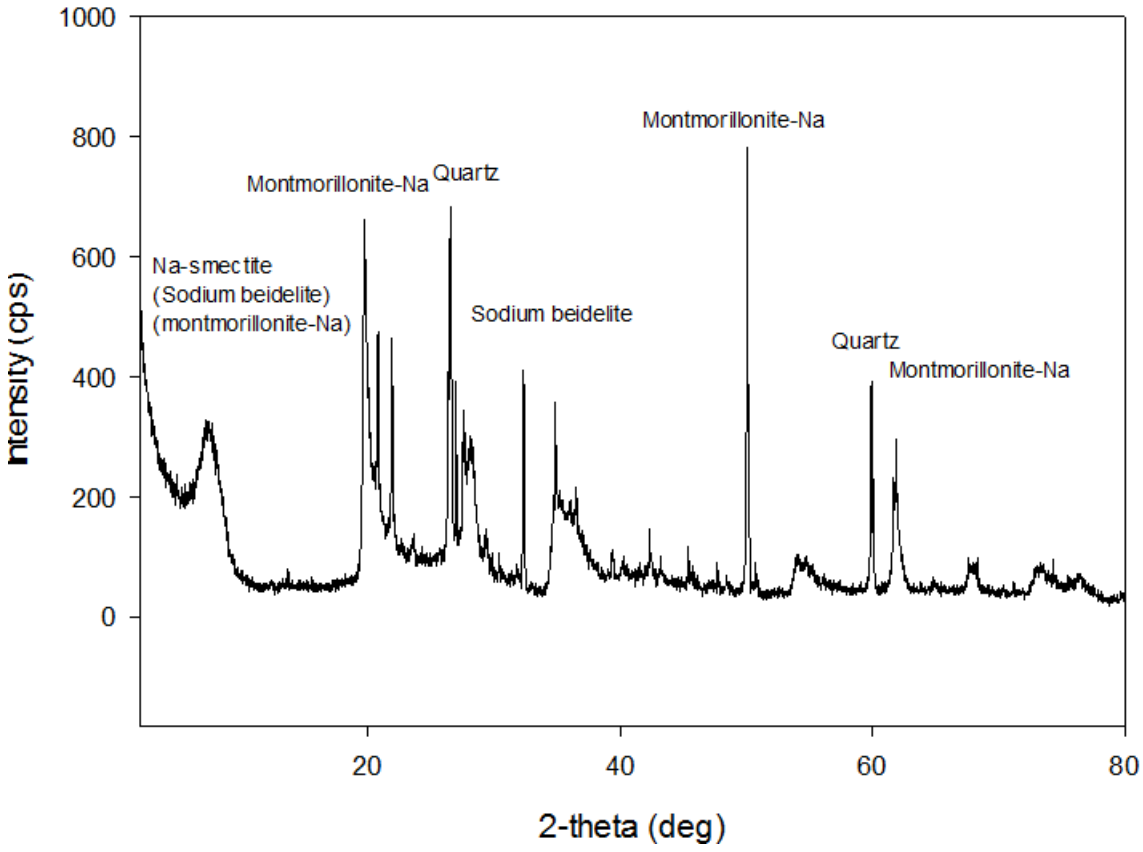

Figure 5.21 XRD pattern of BSM Batch 4

5.7 Conclusion

In this study, the influence of the non-isothermal effect of cations on the interface shear behavior of BSM/geomembrane is discussed. In addition, shear experiments on BSM soil samples are also evaluated for comparison purposes. The maximum shear strengths of the

BSM/smooth HDPE and BSM samples are found in the samples saturated with distilled water and cured at room temperature. The interface shear strengths are measured under vertical stresses of 150, 250 and 350 kPa, which are 61, 95 and 137 kPa, respectively. As well, the BSM soil samples saturated with distilled water and cured at room temperature have shear strengths of 126, 194 and 250 kPa, which are subjected to vertical stresses of 150, 250 and 350 kPa, respectively. The results show that all of the interface shear behaviors of BSM/smooth HDPE are slightly influenced by changes in temperature, the salinity solutions and the combined effects of both changes in temperature and salinity solutions. The XRD patterns illustrate the variations of the mineral components. Samples saturated with distilled water in different thermal conditions, show similar XRD patterns. The features of the 001 peak slightly change, the d001-value of the samples cured in the oven is slightly lower than that of the samples cured at room temperature. This result indicates that the hydration state of exchangeable cations has been affected by temperature. It confirms that the swelling capacity of BSM clay is partly reduced when cured in an oven at temperatures that range from 20^{o}C to 50^{o}C, the sand voids are filled with less hydrated clay, and the shear strength is slightly reduced. The mineral composition changes of the samples saturated with potassium and calcium chloride solutions and cured in the oven are also tested by using XRD. More than 60% of the sodium-smectite in the sample saturated with the potassium chloride solution transforms into illite. The thickness of the hydrated clay units is significantly reduced. The BSM samples saturated with the calcium chloride solution also show cation-exchange. The sodium-smectite transforms into calcium-rich montomorillonite. The thickness of the clay particle interlayer is reduced, and the hydration state is changed. The bentonite sand mixture ratio determined that the interface shear behaviour is dominated by sand. The mineral changes of clay parts caused by combined effect of temperature and leachate has limited influence on the interface shear behavior.

5.8 References

Ahonen, L., Korkeakoski, P., Tiljander, M., Kivikoski, H., & Laaksonen, R. (2008). Quality assurance of the bentonite material. Posiva Oy, Helsinki (Finland). URL： http://www.posiva.fi/files/526/WR_2008-33_web.pdf

Al-Douri, R. H., & Poulos, H. G. (1991). Static and cyclic direct shear tests on carbonate sands. Geotechnical Testing Journal, 15(2), 138-157.

Arifin, Y.F. (2008). Thermo-hydro-mechanical behavior of compacted bentonite-sand mixtures: An experimental study. Dissertation for doctor degree the Faculty of Civil Engineering, Bauhaus-University, Weimar. URL: http://e-pub.uni-weimar.de/opus4/files/852/Thermo_hydro_mechanical_behavior_of_compacted_bentonite_sand_mixture.pdf.

Bouazza, A., Jefferis, S., & Vangpaisal, T. (2007). Investigation of the effects and degree of calcium exchange on the Atterberg limits and swelling of geosynthetic clay liners when subjected to wet–dry cycles. Geotextiles and Geomembranes, 25(3), 170-185.

Carlson, L. (2004). Bentonite mineralogy. Part I: Methods of investigation – a literature review. Part II: Mineralogical research of selected bentonites. Working Report 2004-2, Posiva Oy, Olkiluoto, Finland.

Cho, W. J., Lee, J. O., & Chun, K. S. (1999). The temperature effects on hydraulic conductivity of compacted bentonite. Applied clay science, 14(1), 47-58

Cui, S. L., Zhang, H. Y. and Zhang, M. (2012). Swelling characteristics of compacted GMZ bentonite–sand mixtures as a buffer/backfill material in China. Engineering Geology, 141, 65–73

Dove, J. E., & Frost, J. D. (1996). A method for measuring geomembrane surface roughness. Geosynthetics International, 3(3), 369-392.

Egloffstein, T. A. (2001). Natural bentonites—influence of the ion exchange and partial desiccation on permeability and self-healing capacity of bentonites used in GCLs. Geotextiles and Geomembranes, 19(7), 427-444

Fall, M., & Nasir, O. (2010). Mechanical behavior of the interface between cemented tailings

backfill and retaining structures under shear loads. Geotechnical and Geological Engineering, 28(6), 779-790.

Fishman, K. L., & Pal, S. (1994). Further study of geomembrane/cohesive soil interface shear behavior. Geotextiles and Geomembranes, 13(9), 571-590.

Gueddouda, M. K., Lamara, M., Aboubaker, N., & Taibi, S. (2008). Hydraulic conductivity and shear strength of dune sand-bentonite mixtures. Electronic Journal of Geotechnical Engineering, 13, 1-15.

Geosynthetic Lining Systems (2015). GSE HD Smooth Geomembrane. Retrieved 11 March, 2015, from:http://www.gseworld.com/content/documents/datasheets/membranes/North_America/HD_Smooth_Geomem_METRIC_DS.pdf

Hubert, F., Caner, L., Meunier, A., & Lanson, B. (2009). Advances in characterization of soil clay mineralogy using X-ray diffraction: from decomposition to profile fitting. European Journal of Soil Science, 60(6), 1093-1105.

Inoue, A., Bouchet, A., Velde, B., & Meunier, A. (1989). Convenient technique for estimating smectite layer percentage in randomly interstratified illite/smectite minerals. Clays and Clay Minerals, 37(3), 227-234.

Jogi, M (2005). A method for measuring smooth geomembrane/soil interface shear behavior under unsaturated conditions. Thesis of Degree of Master's of Science, Department of Civil Engineering, University of Saskatchewan, Saskatoon, SK Canada. URI: http://hdl.handle.net/10388/etd-12122005-150824

Karnland, O., & Birgersson, M. (2006). Montmorillonite stability. With special respect to KBS-3 conditions. Swedish Nuclear Fuel and Waste Management Co., Stockholm (Sweden).

Kruse, K. (1994). Langfristiges emissionsgeschehen von siedlungsabfalldeponien, veröffentlichungen des instituts für stadtbauwessen. Technische Universität Braunschweig, Heft 54.

Kjeldsen, P., Barlaz, M., Rooker, A., Baun, A., Ledin, A., & Christensen, T. (2010). Present and Long-Term Composition of MSW Landfill Leachate: A Review. Critical Reviews in

Environmental Science and Technology, 297-336.

Lal, R., & Shukla, M. K. (2004). Principles of soil physics. CRC Press. United States.

Liu, J.S. and Neretnieks, I. (2006). Physical and chemical stability of the bentonite buffer. Technique Report of Chemical Engineering and Technology Royal Institute of Technolog, Swedish Nuclear Fuel and Waste Management Co.

Miller, G. A., & Hamid, T. B. (2007). Interface direct shear testing of unsaturated soil. Geotechnical Testing Journal, 30(3), 182.

Mitchell, J. K., (1993). Fundamentals of soil behavior. New York: Wiley.

Morkel, J., Kruger, S. J., & Vermaak, M. K. G. (2006). Characterization of clay mineral fractions in tuffisitic kimberlite breccias by X-ray diffraction. Journal-South African Institute of Mining and Metallurgy, 106(6), P397.

Murthy, V. N. S. (2002). Geotechnical engineering: principles and practices of soil mechanics and foundation engineering. Chapter 8. CRC Press. United States.

Nasir, O., Fall, M. (2008). Shear behavior of cemented pastefill-rock interfaces. Engineering Geology 101(3-4), 146-143.

Schroeder, P. A., & Irby, R. (1998). Detailed X-ray diffraction characterization of illite-smectite from an Ordovician K-bentonite, Walker County, Georgia, USA.Clay Minerals, 33(4), 671-674.

Simoni, A., & Houlsby, G. T. (2006). The direct shear strength and dilatancy of sand–gravel mixtures. Geotechnical & Geological Engineering, 24(3), 523-549.

Taylor, R., & Allen, A. (2006). Waste disposal and landfill: information needs. Protecting Groundwater for Health: Managing the Quality of Drinking-water Sources. IWA: London. URI: http://discovery.ucl.ac.uk/id/eprint/40075

Taha, A.M (2010) Interface Shear Behavior of Sensitive Marine Clays -Leda Clay Dissertation for Master Degree, University of Ottawa

Taha, A., Fall, M., (2013). Shear behavior of the sensitive marine clay – concrete interface. ASCE Journal of Geotechnical and Engineering Geology 139(4), 644-650.

Taha, A., Fall, M., (2014). Shear behavior of the sensitive marine clay – steel interface. Acta Geotechnica 9, 969–980.

USGS. (2015). Geological survey open-file report 01-041: A Laboratory Manual for X-Ray Powder Diffraction. Illite Group. Accessed June 6, 2015, from http://pubs.usgs.gov/of/2001/of01-041/htmldocs/clays/illite.htm.

Villar, M. V., Gomez-Espina, R., & Lloret Morancho, A. (2010). Experimental investigation into temperature effect on hydro-mechanical behaviors of bentonite.

Villar M.V., Lloret A. (2004) Influence of temperature on the hydro-mechanical behavior of a compacted bentonite, Applied Clay Science, Elsevier. 26, 337-350.

Ye, W.M., Huang, W., Chen, B., Yu, C. and Wang, J. (2009). Diffuse double layer theory and volume change behavior of densely compacted Gaomiaozi bentonite. Rock and Soil Mechanics, 30(7), 1900-1904

Chapter 6 Summary and Conclusion

6.1 Summary

The main objective of this research is to investigate the effect of different numbers of F-T cycles and the combined-effect of leachate with a high cation concentration and landfill temperature on the interface shear behavior and resistance of landfill composite liners. In order to attain an optimum landfill design in cold regions, specifically in Ontario, compacted Leda clay and BSM are chosen as the CCL materials for testing. Therefore, a series of experiments have been performed accordingly.

First, in order to evaluate the performance of composite liners that are affected by F-T cycles, compacted Leda clay / HDPE and BSM/HDPE samples are subjected to different numbers of F-T cycles (i.e. 0, 1, 2, 3, 5 and 10 cycles). The soil shear behavior of Leda clay and BSM are tested for comparison purposes. Due to the simplicity and suitability of DSTs, a direct shear testing machine is used to investigate the interface shear behaviors. CD DSTs are conducted under a low shear rate. The interface tests reveal that the interface shear strength decreases as the number of F-T cycles increase regardless of the normal stress applied to both remolded Leda clay / HDPE and BSM/HDPE samples. The friction angles decrease with increasing number of F-T cycles.

Second, in order to provide a better understanding of the combined chemical-thermal effect on the interface shear behavior of composite liners, a series of experiments have been conducted. Tests on the non-isothermal effect of potassium chloride and calcium chloride solutions on the interface shear behavior of BSM/smooth HDPE are performed. The BSM samples are tested for comparison. All of the samples are saturated with three different solutions: (i) distilled water; (ii) 1750 mg/l of a potassium cation solution; and (iii) 2300 mg/l of a calcium cation solution. All of the samples are cured for 40 days under two different conditions: (1) in the oven where the temperature is increased from 20°C to 30°C, then 40°C and finally 50°C; and (2) at room temperature which is kept constant at 20°C. Aside from the DSTs, XRD is conducted to examine the mineral changes in the clay component of the BSM. The BSM/HDPE shear behaviors are changed by both the cation solutions and the temperature.

6.2 Conclusions

The following conclusions can be made from this study.

1. The experimental results reveal that the F-T phenomenon has impacts on the interface shear behavior for both compacted Leda clay / HDPE and BSM/HDPE samples. Thus, the reduction in the interface shear and strength parameters due to the F-T cycles should be considered for landfill safety.

2. The samples which did not undergo an F-T cycle always obtain the highest shear strength regardless whether the CCL material is remolded Leda clay or BSM, and the interface shear strength decreases as the number of F-T cycles increases regardless of the vertical stress applied for both the Leda clay / HDPE and BSM/HDPE samples.

3. For the studied interface, the Leda clay with a geomembrane has weak shear resistance since the particle diameter is very small. On the contrary, the BSM has a matrix soil structure. The diameter of the sand particles is much larger than that of the clay particles. The sand particles penetrate the geomembrane surface. The depth of the penetration is related to the level of the normal load.

4. The shear stress versus strain curves of two different interface shear samples demonstrate different trends. On the one hand, the interface shear behavior of Leda clay/smooth HDPE can obtain a peak value of shear stress during shearing, and the shear stress becomes stable at around 25% horizontal displacement. The shear stress in the stable state is the residual shear strength. On the other hand, the BSM/HDPE samples have softer increasing curves, where the shear stresses at a 15% horizontal displacement are used as the shear strengths. The reason that there is no peak value in the curves can be attributed to the particle diameter and shear mechanisms.

5. For the Leda clay material, in both the interface shear and soil shear behavior tests, the first three F-T cycles have significant impacts on the friction angles which are reduced in this process, and after 3 F-T cycles, the changes are minimal. On the contrary, the influence of F-T cycles on the BSM samples is gradually decreased. In the first 5 cycles, the impacts on the friction angles are relatively obvious. After 5 cycles of F-T, there are still visible changes in the friction angles until the 10th F-T cycle. However, the effect from any further F-T cycles on the shear behavior is limited, which can be observed from the shape of the slopes in terms of the friction angle changes.

6. In terms of the experiments which examined the influence of high temperature, the shear strengths of the BSM/smooth HDPE and BSM samples which are cured at room temperature are slight higher than those of samples cured in the oven. This is because the bentonite hydration states are affected by high temperature conditions. Thus, the swelling capacity of bentonite and the percentage of hydrated clay that filled the sand voids change as well.

7. At room temperature, the distilled water saturated BSM/HDPE samples always have slightly higher shear strengths than the samples saturated with other salinity solutions, and this is also true for the shear behavior of the BSM samples. This is due to the changes in the swelling behavior of the clay in the sand voids.

8. Under the combined influence of cations and temperature, the maximum shear strengths of BSM/smooth HDPE and BSM samples are obtained by the samples which are saturated with distilled water and cured at room temperature. However, the combined effect of cation and temperature is limited.

The samples saturated with the potassium cation solution and cured in the oven can transform 60% of the smectite into illite. The samples saturated with the calcium cation solution and cured in the oven can transform the majority of the sodium-smectite into calcium-rich montmorillonite. However, the mineral change of the clay parts within BSM which is caused by the combined influence of temperature and cation does not have significant influence on the interface shear behavior of composite liner system.

6.3 Future Research Recommendations

The following recommendations are suggested.

1. In-situ Leda clay can be considered for direct compaction and the interface shear behavior tested with smooth HDPE, which are influenced by the F-T phenomenon.

2. Due to the limitations of the CCL materials in this study, different kinds of clay should be considered and tested in future studies.

3. In order to further understand the reason why shear strength decreases as the number of F-T cycles increase, different F-T cycles should be fully tested, and the samples should undergo 4, 6, 7, 8, 9 and even more F-T cycles.

4. This research uses a ratio of 10:1 sand-bentonite. Other ratios of BSM should be tested in future work. Other types of sand and bentonite can be considered as testing materials

to investigate the influence of the combined effects of F-T cycles and leachate with heat on the interface shear behavior.

5. Large scale shear box can be used and the interface shear of BSM/HDPE should be tested under a system that controls the temperature, which allows the shear behavior to take place under high temperatures. It is helpful to obtain insights on how the temperature influences BSM and HDPE at the same time, and it is more similar to real landfill conditions.

6. Landfill leachate comprises different components, and other ions and organics that are high in concentration should also be considered in examining their influence on the interface shear behavior of BSM/HDPE.

Chapter 7 Appendix

Consolidated- drained direct shear testing

In geotechnical research, a direct shear apparatus is commonly used to test the shear strength parameters. The friction angle and cohesion are mainly the examined factors for cohesive soil.

$$\tau_f = \sigma \tan \Phi + c$$

where, τf: shear strength of the soil

σ: applied normal stress

However, in considering the long-term stability issues of landfill liners, there is the need to look at the consolidation and drainage of saturated clay. This requires a long period of time. Typically, a standard Mohr Coulomb failure envelope for the CD direct shear testing of saturated clay presents a zero cohesion value (see Figure A-1) (Taha, 2010).

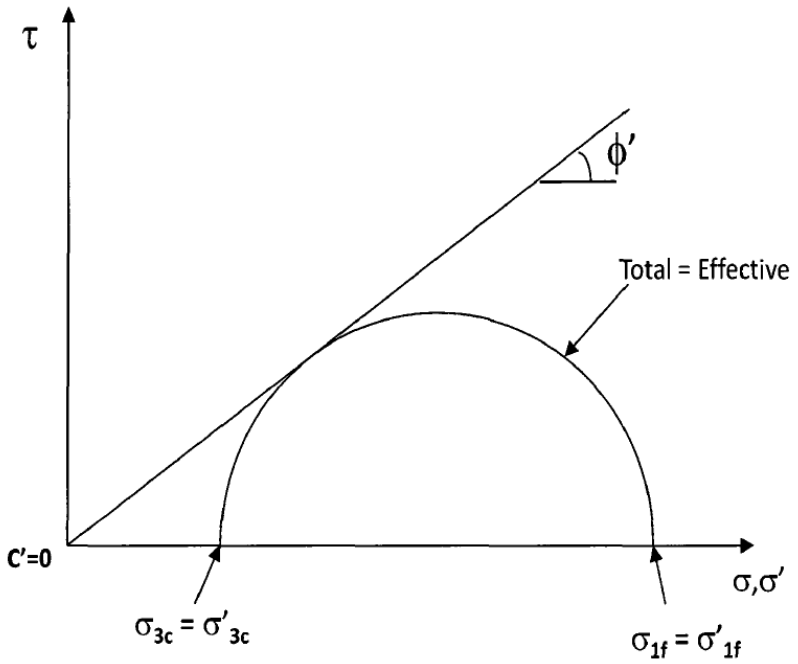

Figure 7.1 Mohr Coulomb failure envelope for consolidated drained direct shear testing of saturated clay

CD testing allows water drainage at both the consolidation and shearing stages. The consolidation stages are restricted by the consolidation testing, in accordance with the ASTM D2435 standard. The second stage of drainage, which requires very slow shear rate, is also affected by the consolidation results. Both ASTM D3080 and D5321 provide the shear rate which needs to be related to the consolidation results.

Consolidation and shear rate

Each consolidation increment is required to be added after the primary consolidation of the last increment is finished. This data can be obtained when the specimen reaches 90% consolidation. The shear rate of direct shear tests can be determined by the time required for the specimen to reach 50% consolidation under a current normal stress increment. Thus, the consolidation of remolded Leda clay and BSM are accordingly presented.

Following ASTM standard D2435, the time to reach 50% primary consolidation, $t_{50,}$ and the time to reach 100% consolidation, $t_{100,}$ can be obtained by each set of time versus vertical deformation curves by using the square root method. The detailed steps can be found in the standard. When the load was increased from 180 to 350 kPa, the t_{50} and t_{100} of BSM obtained in the time versus vertical deformation curve by using the square root method, which is presented as an example (Figure 7-2).

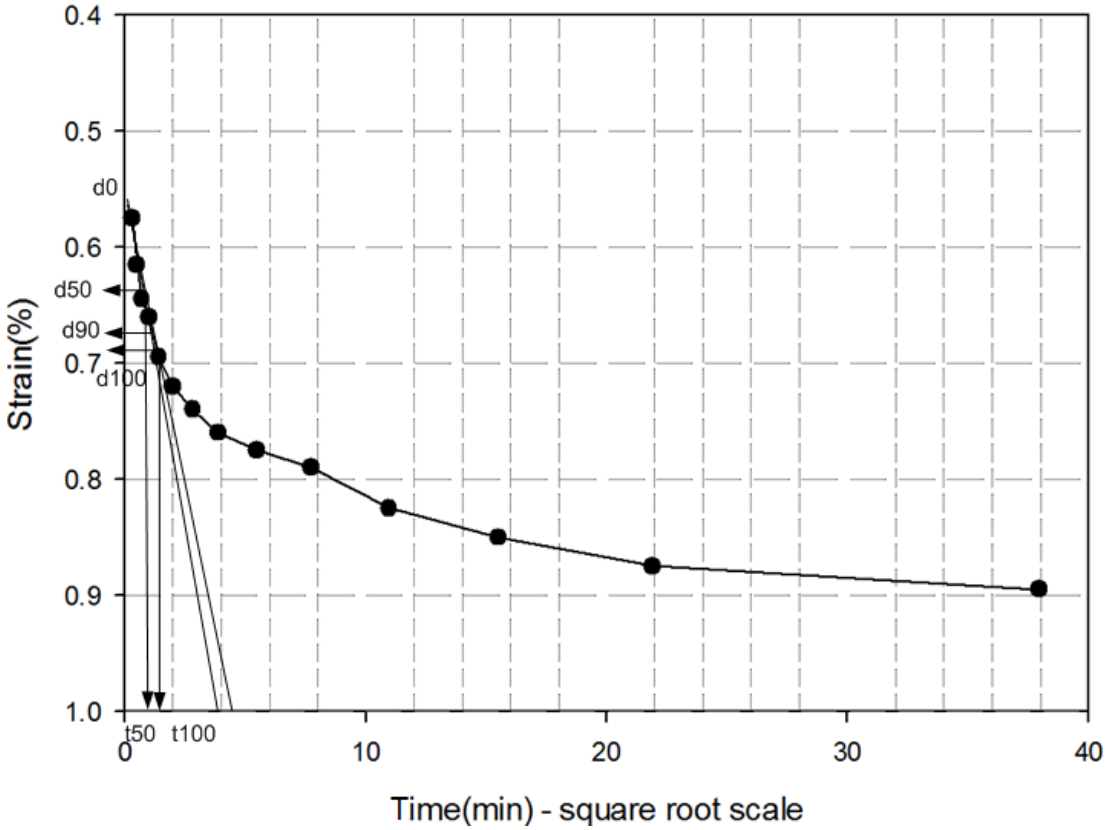

Figure 7.2 Time vs. deformation by using log method for BSM under 350 kPa

In Figure 7-2, the consolidation result of the BSM sample is presented. This sample is saturated with distilled water. The d_{50} is the 50% primary consolidation and the corresponding time is denoted as t_{50} which is equal to 0.64 min. The time for 100% primary consolidation, $t_{100,}$ is equal to 4 min.

The shear rate can be determined in accordance with ASTM standard D5321. The appropriate shear rate (R) of the drained shearing test can be determined with the following equation:

$$R = d_f/(50 * t_{50} * f)$$

where:

R = rate of shear displacement, mm/min,

d_f = estimated shear displacement at peak shear stress,

t_{50} = time required for specimen to reach 50 % consolidation under the current normal

stress increment.

f = factor to account for drainage conditions on the shear plane. According to ASTM standard D3080, the factor (f) that accounts for the drainage condition on the shear plane is 4.

Thus, $R = 10\ \text{mm}/(50 * 0.68\ \text{min} * 4)$=0.078 mm/min

The minimum shear rate of the interface shear behavior for remolded Leda clay and BSM material is 0.025 mm/min, and this shear rate is lower than the soil shear rate. In order to reduce the variability, a shear rate of 0.025 mm/min is used for all of the DSTs for both interface and soil shear behaviors in this research.

Figure 7.3 Grounding machine

Figure 7.4 Laboratory dynamic compactor

Figure 7.5 Static compaction

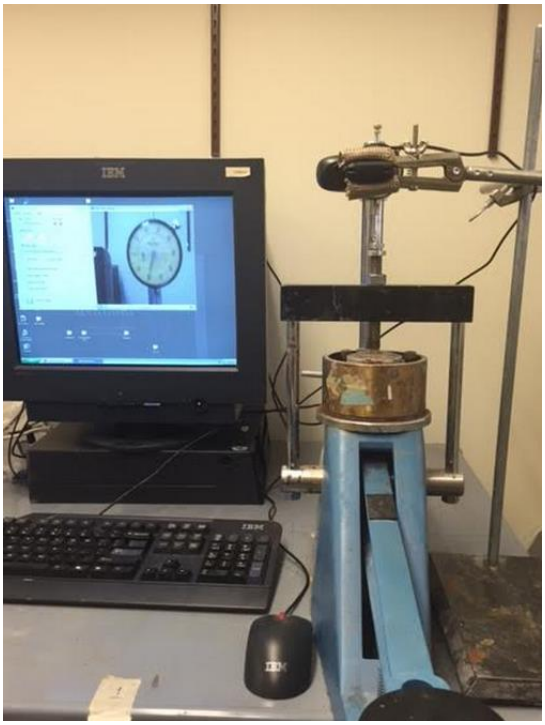

Figure 7.6 Consolidation apparatus

Figure 7.7 Thermal sensor and data acquisition system

Figure 7.9 Well-sealed container with strong vacuum resistance

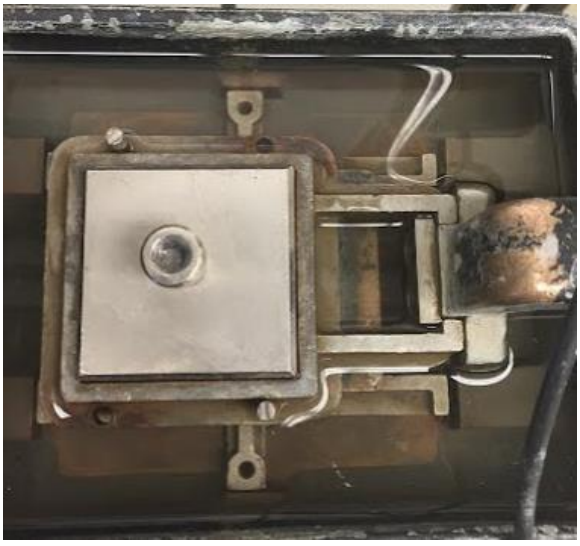

Figure 7.8 Shear box and the sink of direct shear apparatus

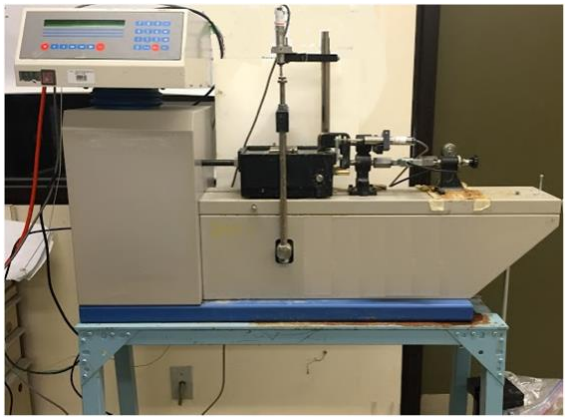

Figure 7.10 Direct shear apparatus